TOWARDS SPECIFIC INACTIVATORS OF *TRYPANOSOMA CRUZI* TRANS-SIALIDASE

by

Yuan Yao

B.Sc., Nanjing University, 2009

A THESIS SUBMITTED IN PARTIAL FULFILLMENT OF

THE REQUIREMENTS FOR THE DEGREE OF

MASTER OF SCIENCE

in

THE FACULTY OF GRADUATE STUDIES

(Chemistry)

THE UNIVERSITY OF BRITISH COLUMBIA

(Vancouver)

March 2013

Abstract

The *Trypanosoma cruzi* (*T. cruzi*) trans-sialidase is thought to be an essential enzyme for infection by *T. cruzi* since sialic acid is needed for its nutrition and pathogenesis yet *T. cruzi* cannot biosynthesize sialic acid. The overall goal of this project is to identify a tight binding and specific inactivator of the *T. cruzi* trans-sialidase (TcTS). A library of mechanism-based inactivators of TcTS was synthesized based upon the known inactivator 9-azido-3-fluorosialyl fluoride (parent inactivator) by click chemistry with a series of alkynes in yields of 40-81%. Kinetic parameters for the clicked inactivators and its parent were determined using 5-acetamido-3,5-dideoxy-2-(4-trifluoromethylumbelliferyl)-D-*glycero*-α-D-*galacto*-non-2-ulopyranosonic acid as substrate. Inactivation parameters for the clicked inactivators were generally inferior to those of parent compound 9-azido-3-fluorosialyl fluoride. The substrate binding pocket of TcTS prefers non-polar moieties near the 9-position, especially aliphatic rings. It was also found that TcTS can tolerate negative charges better than positive charges at this position. These results suggest that improved reagents might incorporate moieties attached to C-9 through an amide or an ether linker rather than through a triazole.
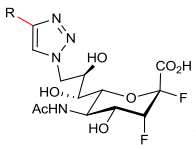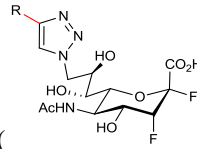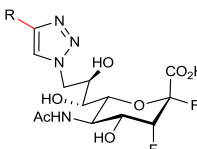
Table of Contents

List of Tables

List of Figures

List of Schemes

List of Abbreviations

Å	angstrom
Ac	acetyl
Asp	aspartate
BSA	bovine serum albumin
CMP	cytidine monophosphate
DCM	dichloromethane
DMF	dimethylformamide
DNA	deoxyribonucleic acid
EA	ethyl acetate
EDTA	ethylenediaminetetraacetic acid
GlcNAc	*N*-acetyl-D-glucosamine
Glu	glutamic acid
IC_{50}	half maximal inhibitory concentration
LB	lysogeny broth
ManNAc	*N*-acetyl-D-mannosamine
Me	methyl
MS	mass spectrometry
NMR	nuclear magnetic resonance
PCR	polymerase chain reaction
Pyr	pyruvate
RNA	ribonucleic acid
RT	room temperature
TLC	thin-layer chromatography
Tris-HCl	tris(hydroxymethyl)aminomethane hydrochloride
Trp	tryptophan
Try	tyrosine
UV	ultra violet

Acknowledgement

It is with the greatest sincerity that I express my gratitude to my supervisor, Professor Stephen G. Withers for all his support and encouragement throughout my time in his laboratory. His insights and enthusiasm were a constant source of inspiration for me.

Besides my supervisor, I would like to extend a warm, heartfelt thank you to all my fellow labmates, both past and present, for all their assistance and more importantly, their encouragement over the years.

To all my family and friends, especially my parents, my grandfather, thank you all for your love, support and unwavering belief in me.

"But seek first the kingdom of God and His righteousness
And all these things shall be added to you."

-Matthew 6:33

1 General Introduction

1.1   Sialic Acid

Sialic acid is a generic term which signifies a common member of a family of 9-carbon sugars bearing an acidic functionality. It also refers to *N*-acetylneuraminic acid (Neu5Ac or NANA, Figure 1.1), the most widespread member of this family. Interestingly, sialic acids are mainly found in "higher" animals (starfish to human) as well as a few pathogenic bacteria.[1] Sialic acids exist mostly as terminal constituents of oligosaccharide chains attached to the outer or inner cell membranes.[2]
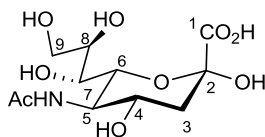
Figure 1.1 α-*N*-Acetylneuraminic acid and the numbering scheme employed.

Sialic acids play various important roles physiologically, for instance:[1-5]

1) At physiological pH (7.3-7.4), sialic acid ($pK_a = 2.6$) normally bears a negative charge, which renders cell membranes anionic and in addition mediates cell adhesion;

2) Sialic acids act to mask receptor sugars, such as galactose. This can modulate the clearance of glycoproteins from circulation, and avoid cell recognition by the innate immune system;

3) Sialic acids can also be receptors: they serve as targets for pathogenic infections and possible regulators in the central nervous system;

4) Some bacteria can utilize sialic acids to build in the cell wall as nutrients or as carbon and nitrogen sources.

In vivo, sialic acids are rarely available as monosaccharides. Free sialic acids come from two pathways. One is the aldolase-catalyzed condensation between *N*-acetyl-D-mannosamine (ManNAc) or *N*-acetyl-D-mannosamine-6-phosphate (ManNAc-6-P) and pyruvate or phosphoenol pyruvate, as shown for pyruvate in Figure 1.2.[5] The other is through the action of sialidases.
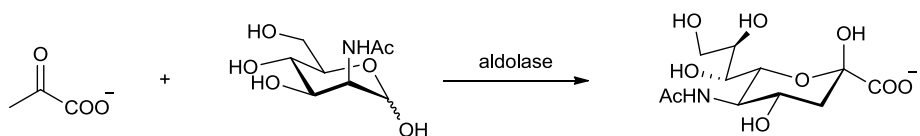
Figure 1.2 The reaction normally catalyzed by Neu5Ac aldolase to form *N*-acetylneuraminic acid.

Sialidases are a superfamily of glycoside hydrolases which hydrolyse sialic acids from various sialoglycoconjugates. In some cases, they are also involved in trans-sialylation. Sialidases can hydrolyze sialylated conjugates to release free sialic acid (Figure 1.3).[1]
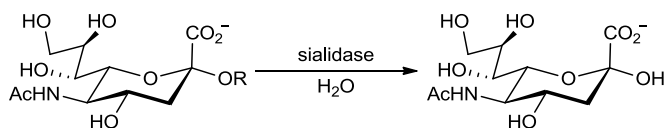
Figure 1.3 The reaction normally catalyzed by a sialidase to release α-*N*-acetylneuraminic acid.

In vivo, free sialic acid is converted to CMP-sialic acid by CMP-sialic acid synthetase (Figure 1.4). [1]
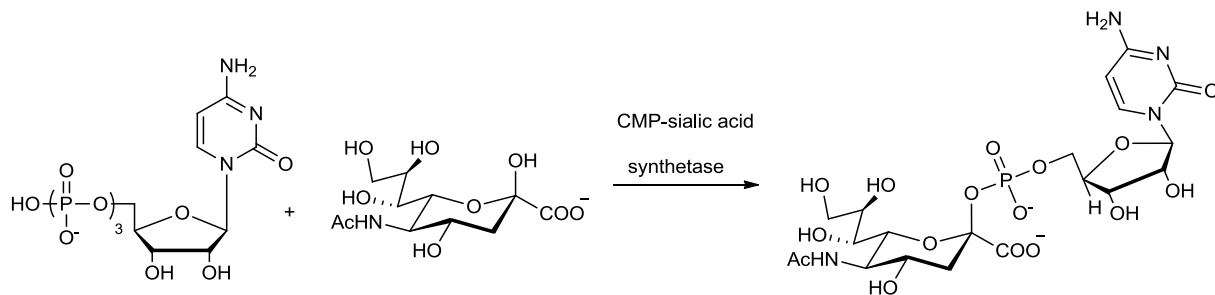
Figure 1.4 The reaction normally catalyzed by a CMP-sialic acid synthetase to form CMP-β-*N*-acetylneuraminylpyranose**.**

CMP-sialic acids are then used by sialyltransferases to modify various moieties, such as glycoproteins (Figure 1.5).[1]
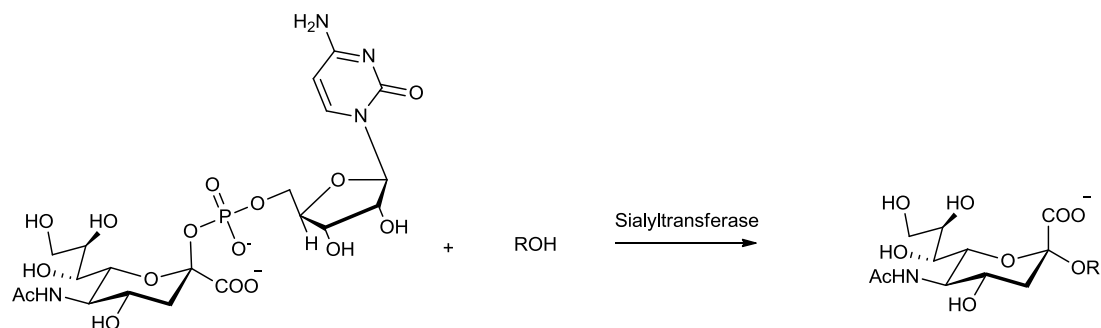
Figure 1.5 The reaction catalyzed by a sialyltransferase to transfer sialic acid from a CMP- Neu5Ac to an acceptor, ROH.

In 1983, an unusual enzyme which transfered sialic acids from sialosides to β-galactosyl residues was discovered (Figure 1.6), and was aptly named "trans-sialidase". This enzyme belongs to the sialidase family.[6]

sialic acid donor   sialic acid acceptor   sialoglycoconjugate
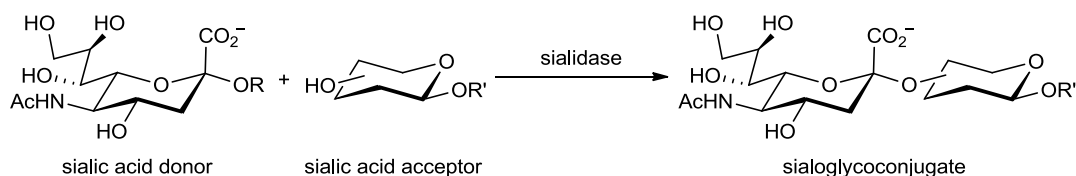
Figure 1.6 Transglycosylation of sialosides. (R=glycoside or aglycone; R'=glycoside)

1.1.1 Classification of Sialidases

There are two distinct classes of sialidases. Exo-sialidases (EC 3.2.1.18) cleave α-(2, 3) (Figure 1.7a), α-(2, 6) (Figure 1.7b), α-(2, 8) (Figure 1.7c) and/or α-(2, 9) (Figure 1.7d) terminal sialic acids from sialoglycoconjugates. Endo-sialidases (EC 3.2.1.129) hydrolyze endo α-(2, 8) bonds in oligo or polysialic acids (Figure 1.7).[6-8] The Carbohydrate-Active Enzymes (CAZy) database (http://www.cazy.org/) and the associated Wiki-CAZypedia (http://www.cazypedia.org/) provide genomic, structural and biochemical information on carbohydrate related enzymes and proteins. Five groups of such proteins are designated: glycoside hydrolases (GHs), glycosyltransferases (GTs), polysaccharide lyases (PLs), carbohydrate esterases (CEs) and

carbohydrate-binding modules (CBMs). These families have been assembled on the basis of sequence similarities. However, based on the structural similarities, some of those assigned families (131 sequence-based families) in GHs are clustered into 14 clans. At this point, exo-sialidases are found only in GH-33, GH-34 and GH-83, and all belong to Clan E (6-fold β-propeller fold). In addition, endo-sialidases are found in GH-58. Although the overall amino acid sequence homologies among those three exo-sialidase families are very low, the catalytic centers are well conserved with six unique residues and a six-bladed β sheet fold.[7]
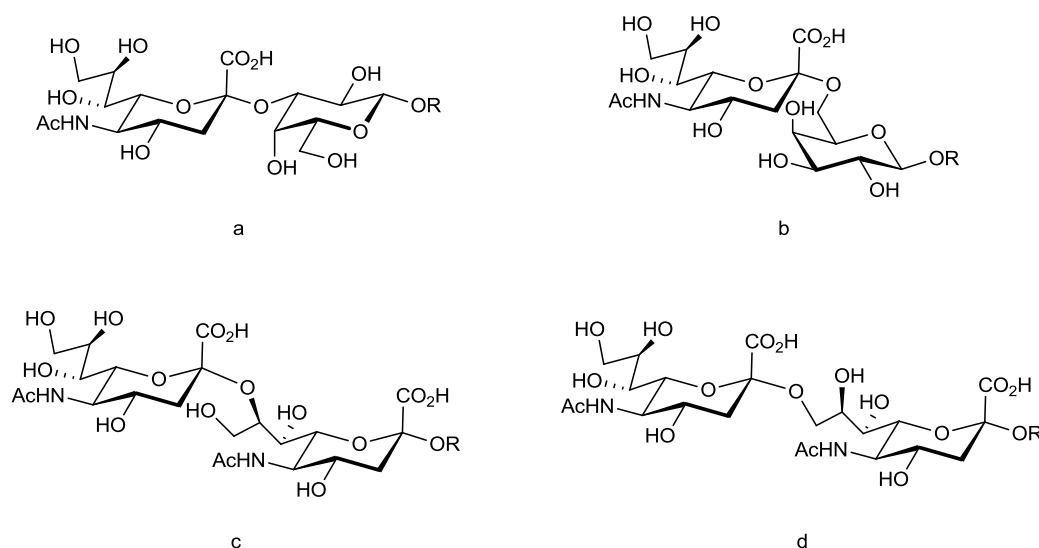
Figure 1.7 Different sialyl-linkage types of sialoglycoconjugates: a. α-(2, 3); b. α-(2, 6); c. α-(2, 8); d. α-(2, 9). (R=glycoside)

1.1.2 Catalytic Mechanism of Sialidases

According to the difference of stereochemistry at anomeric centers of the substrate and the product, retaining and inverting enzymes are classified. In 1995, it was discovered that exo-sialidases from both viruses and bacteria are retaining enzymes.[9] Subsequent research showed that sialidases from higher animals and trans-sialidases also hydrolyze or transfer sialic acid with retention of configuration at the anomeric center.[10,11] Recently, more detailed structural and mechanistic studies have revealed that exo-sialidases generally follow a double displacement

4

mechanism.[10,12-14] In the substrate binding pocket, three polar amino acids, tyrosine, glutamic acid and aspartic acid, are conserved.[12,15-18] With the aid of a nearby glutamic acid, the tyrosine serves as catalytic nucleophile while the acid/base catalyst is an aspartic acid. Another glutamic acid assists to stabilize an arginine triad which interacts with and stabilizes the negative charge of the carboxylate group of sialic acid.
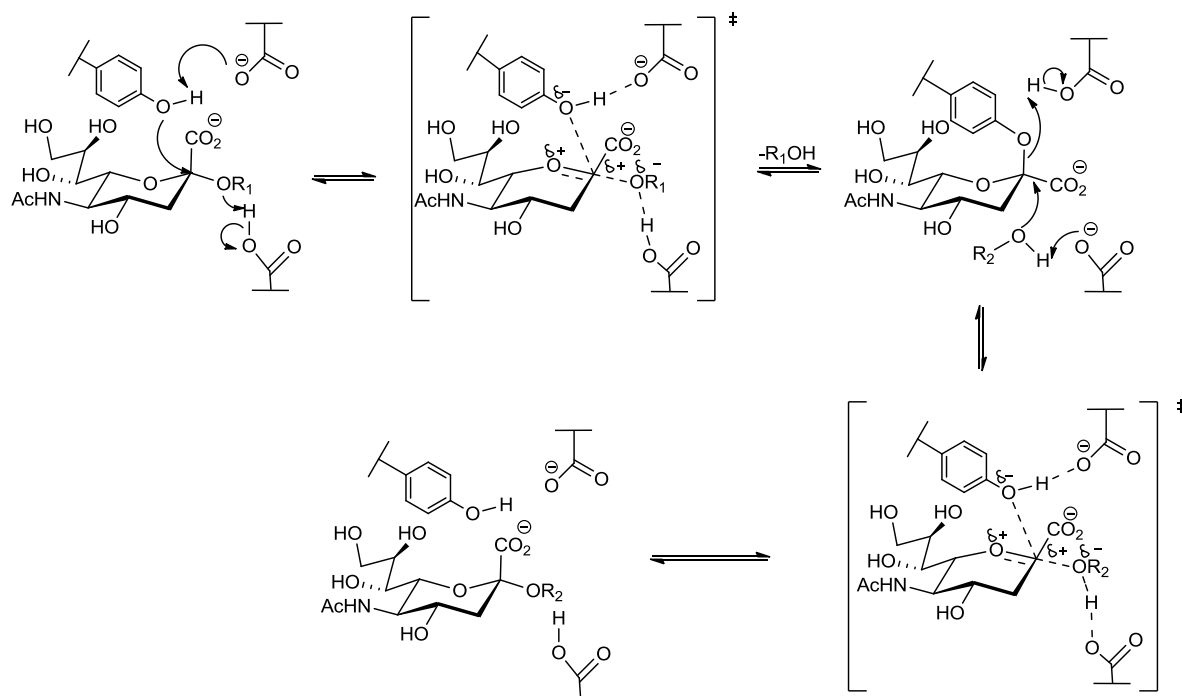
Scheme 1.1 The proposed mechanism for retaining exo-α-sialidases.

(R_1=glycoside or aglycone; R_2=glycoside or aglycone or H)[12,15-18]

The catalytic nucleophile (tyrosine) attacks the anomeric center of sialic acid to form a covalent sialyl-enzyme intermediate, while the catalytic acid (aspartic acid) protonates the R_1O^- leaving group to form R_1OH. Then, either a water molecule or a carbohydrate (in the case of trans-sialylation) is deprotonated by the catalytic base (aspartate) in order to attack the anomeric center and displace the nucleophile tyrosine, regenerating the free enzyme (Scheme 1.1). Reaction occurs via oxocarbenium ion-like transition states.

Ordinarily, mutation of either of the two active site catalytic residues of a glycosidase results in extremely low activity mutants.[19] Interestingly, it was found that some mutants of the nucleophilic residue *of M. viridifaciens* sialidase (originally a retaining exo-sialidase) were not inactive. Instead, the mutants still catalyze hydrolysis, but by an alternative mechanism.[20] Different amino acid substitutions of the nucleophilic tyrosine resulted in three different catalytic mechanisms: S_N1 with net inversion, S_N1 with net retention and S_N2 with net retention. If the substituted amino acid had nucleophilic tendency, hydrolysis could follow an S_N2-like retention mechanism. If not, the reaction operates through either S_N1 inversion or S_N1 retention, depending on whether enough space existed between the enzyme and substrate for a water molecule. Despite the similar features shared by all the exo-sialidases, they differ in their substrate preference and affinity and reaction rates.[1,21]

In 2009, a new mechanism for GH-58 endo-sialidases was proposed by Morley *et al.*[8] Sialidases from family GH-58 are the only class of endo-sialidases that require a minimum sialoside trimer glycoside as substrate. The main differences from exo-sialidases are that the tyrosine nucleophile residue, one of the two acid/base residues and one of the three arginine residues are missing from the endo-sialidase active site. Based on X-ray crystallographic data, kinetic and mutagenesis studies, it was suggested that endo-sialidases use a glutamic acid as the general acid, and the carboxylate from sialic acid as the general base (Scheme 1.2). Thus, endo-sialidases lack a catalytic nucleophile and are inverting enzymes. The proposed mechanisms provide scientists better insights to design inhibitors of sialidases.
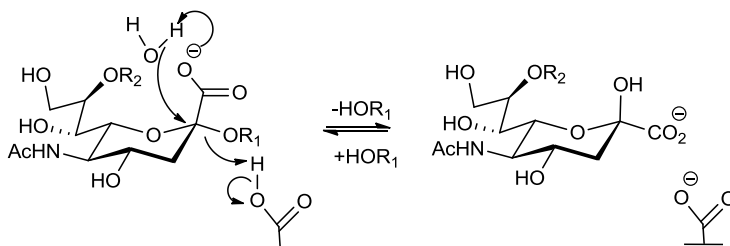
Scheme 1.2 The proposed catalytic mechanism of endo-sialidases. (R_1=glycoside; R_2=glycoside or aglycone)[8]

1.1.3 Inhibitors of Exo-sialidases

It is known that influenza sialidases cleave sialic acid from host's cells in order to release progeny viruses from the infected cells. Exo-sialidase inhibitors can serve as anti-viral and anti-bacterial drugs.[22] The majority of research in this field has focused on investigating therapies for viral infections, especially influenza viruses. Exo-sialidase inhibitors fall into two main groups: non-covalent (reversible) inhibitors and covalent inhibitors, the latter class will be further discussed in the next section. The exo-sialidase inhibitors reported are mostly non-covalent inhibitors, which usually mimic the substrate or the oxocarbenium ion-like transition state, especially the planar geometry and/or positive charge. The first inhibitor of interest is Neu5Ac2en (DANA), a general inhibitor for most exo-sialidases (Figure 1.8b), which mimics the planar geometry of the transition state.[23,24] It has been found that DANA can be naturally synthesized in organisms, which indicates that DANA might be an inhibitor to moderate activities of sialidases in nature.[25-27] Substitution of the hydroxyl group at C-4 on DANA by a positively charged guanidino group causes the large increase of affinity between the inhibitor molecular and the influenza sialidases by interacting with both Glu119 and Glu227.[28] Consequently, zanamivir (Figure 1.8c) was synthesized and commercialized as Relenza®, a treatment of flu. Similarly, oseltamivir—another derivative of DANA (Figure 1.8d) was designed as a prodrug and commercialized as Tamiflu®, which conserves the acetamide, positive-charged moiety at C-4 and planar geometry features.[28,29] In addition, the acidic character is also preserved since oseltamivir can be hydrolyzed into the active form by esterases in human liver. X-ray crystallographic studies revealed that the C-7 hydroxyl group does not interact with influenza sialidases, so it has been replaced by more hydrophobic groups in order to increase the hydrophobic interactions and specificity for influenza sialidases over human sialidases.[28,29]

Figure 1.8 a. The sialidase glycosylation transition state; non-covalent exo-sialidase inhibitors and transition state mimics: b. DANA; c. zanamivir; d. oseltamivir.

1.1.3.1 Mechanism-based Covalent Fluoro-sugar Inactivators
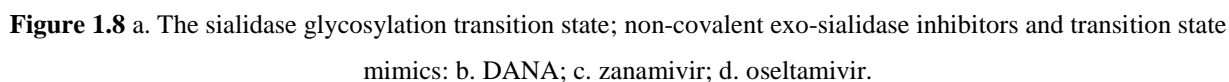
A covalent inactivator, as its name suggests, can react with an enzyme and form a covalent linkage within the active site, blocking the active site and thus inactivating the enzyme's activity. These inactivators are normally substrate analogues. For mechanism-based covalent inactivators, the following kinetic scheme applies.

$$\text{E} \ + \ \text{I} \ \underset{k_{-1}}{\overset{k_1}{\rightleftharpoons}} \ \text{EI} \ \overset{k_i}{\longrightarrow} \ \text{E-I} \ (\ K_i = k_{-1}/k_1 \ )$$

Scheme 1.3 Simplified scheme for mechanism-based inactivators of retaining sialidases.

In 1987, the Withers group showed that activated 2-deoxy-2-fluoroglycosides can serve as covalent inactivators of retaining β-glycosidases.[30] Similarly, 3-fluorosialyl fluoride was suggested as a potential inactivator of exo-sialidases (Figure 1.9).[17,18] By taking advantage of the

oxocarbenium ion-like transition state, an electron-withdrawing group at C-3 of sialic acid increases the activation energy for both chemical steps due to the cationic nature of the two transition states; in concert, a good leaving group at C-2 lowers the activation energy for only glycosylation. Thus, the sialidase is trapped in its covalent sialyl-enzyme intermediate and thereby prohibited from participating in further catalytic cycles. To this end, fluoride was chosen as both the electron-withdrawing group and the good leaving group due to its characteristics, such as small atom size, large electronegativity and similar bond length with carbon compared to a hydroxyl group. Modifications at different positions on 3-fluorosialyl fluoride were installed to obtain better binding and increase specificity for different types of exo-sialidases.[31,32]
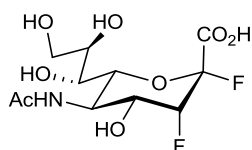
Figure 1.9 Covalent inactivator of exo-sialidases: 3-fluorosialyl fluoride.

1.2   Chagas Disease

Chagas disease is an endemic disease in Latin America. The latest survey shows that there are approximately 17 million people infected all over the world and this number is increasing by thousands of people per year.[33] Brazilian physician Carlos Chagas first found that this disease is caused by the parasite *Trypanosoma cruzi (T. cruzi)* a century ago.[34] Primarily, *T. cruzi* is transmitted across species by the feces of blood-sucking insect vectors from the Reduviidae family, such as *Rhodnius prolixus* (also known as "kissing bugs").[35] As Figure 1.10 shows, *T. cruzi* passes through four stages of development in its life cycle: epimastigote (E), metacyclic trypomastigote (M), trypomastigote (T) and amastigote (A). The epimastigote and amastigote are the reproducing forms in insects and mammals, respectively. Epimastigotes transform to the infective metacyclic trypomastigotes in bugs' hindguts, and are released with bugs' feces. Once metacyclic trypomastigotes penetrate mammalian cells, they transform to amastigotes and replicate in cells. After replication, amastigotes transform to the highly infective trypomastigotes, which rupture the

cells and are released to infect more host cells.[36] Because *T. cruzi* can access human bodies through broken skin or mucous cell membranes, infections usually occur after being bitten by an infected insect or eating contaminated food.[37]
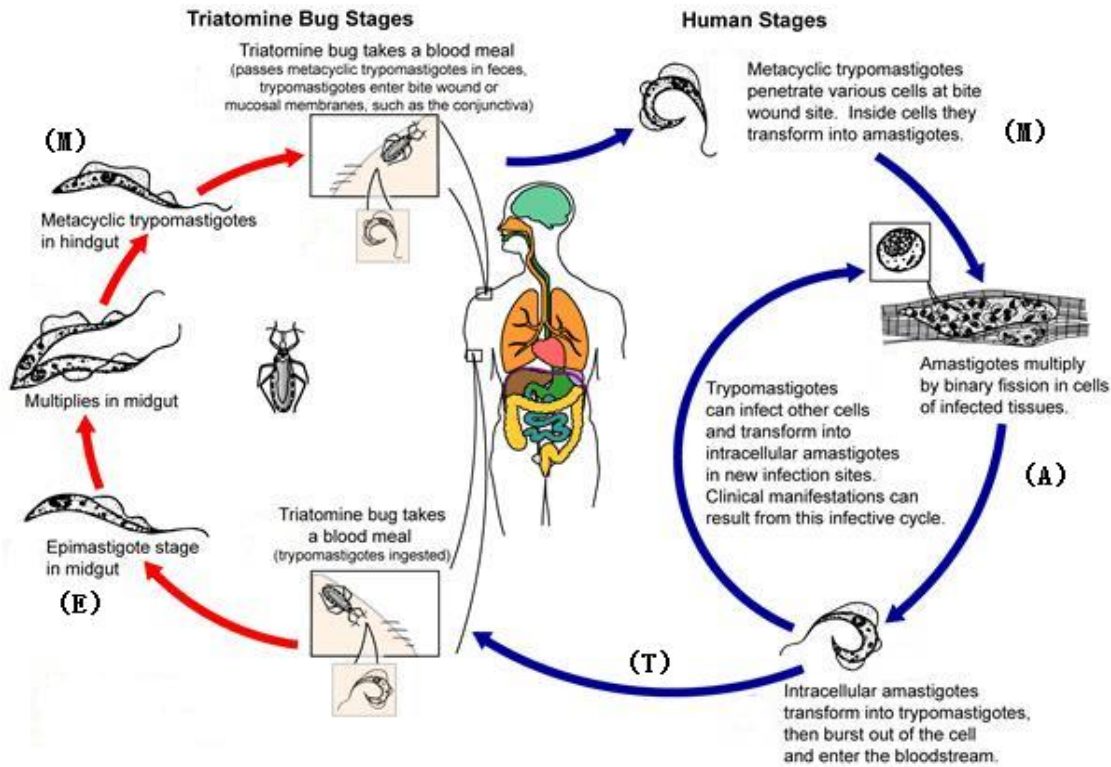
Figure 1.10 Life cycle of *T. cruzi* (modified figure taken from Ref 36).[36]

Chagas disease has become a global issue (Figure 1.11) partially due to the travel and migration of the infected population, increasing the spread of the parasite through blood transfusion, organ transplantation and mother-to-child pathways.[38] Also, the spread of Chagas disease is difficult to control due to the fact that the mild and non-specific symptoms (such as low fever, flu-like symptoms, rashes and swollen eyelids) of the acute phase are not attributed to Chagas disease in most cases. Infected patients enter the intermediate phase with almost no symptoms after 4-8 weeks of infection, which further increases the difficulty of Chagas disease diagnosis.[39] In the chronic phase, the symptoms differ depending on individuals and regions. Statistical data shows that 70-80% of individuals are unaware of the infection for their entire lives as a consequence of

mild or no symptoms and the remaining 20-30% of patients discover the infection from serious heart-related or digestive-related complications, sometimes after decades of infection.[40] Although the majority of chronic patients do not suffer from serious chronic phase symptoms, there are approximately 50000 people that die each year due to Chagas disease.[33] Diagnosis of Chagas disease, such as through serum antibodies and PCR reactions, is complicated and expensive, which is another factor restricting the effective control of the disease spread.[41] The current treatment of Chagas disease focuses on relief of symptoms and parasite clearance. Anti-parasitic therapies will be discussed in the next section.
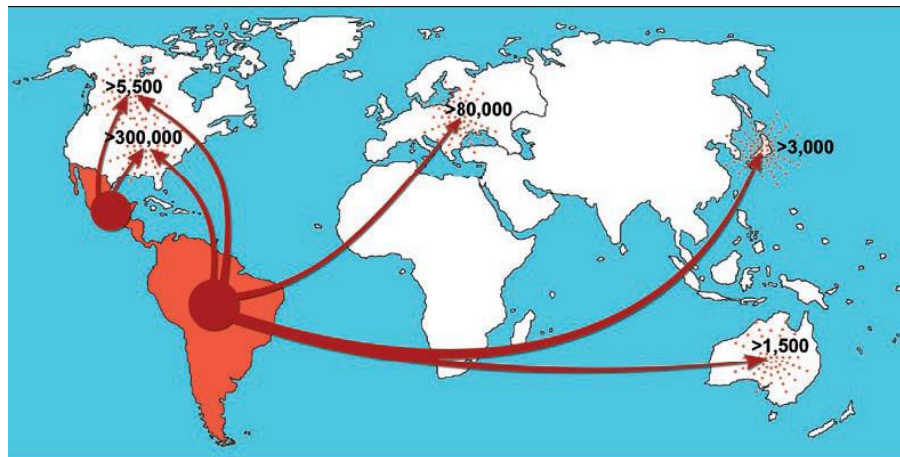
Figure 1.11 Population migration routes from Latin America and estimation of the total number of infected individuals in non-endemic countries (figure taken from Ref 38).[38]

1.2.1 Therapies for Chagas Disease

Chagas disease has always lacked attention and efforts from pharmaceutical companies due to economic considerations.[42] Fortunately, academic institutions and global health organizations, such as the World Health Organization (WHO), have continued to contribute to the development of treatments for Chagas disease.

Currently, there are only two commercially available drugs for Chagas disease: benznidazole (BNZ) (Figure 1.12a) and nifurtimox(Figure 1.12b).[43] However, these are plagued with poor tolerance, serious side effects and uncertain efficacy.
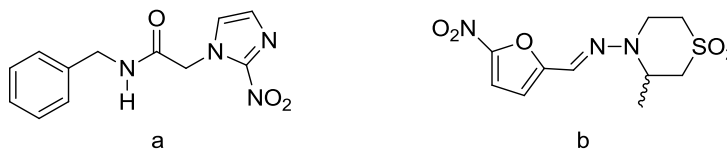
Figure 1.12 Current therapies for Chagas disease: a. benznidazole (BNZ); b. nifurtimox.

BNZ functions by inhibition of RNA synthesis, which introduces dermatological adverse effects.[44,45] This treatment option, offered since 1978, is still the drug of choice because it is better tolerated compared to nifurtimox.[46] Nifurtimox treatment is based on the fact that accumulation of free radicals and superoxide is toxic for parasite DNA (Figure 1.13).[45]

$$NAD(P)H \ + \ H^+ \ + \ 2ArNO_2 \longrightarrow 2Ar\overset{\bullet}{N}O_2^- \ + \ NAD(P)^+ \ + \ 2H^+$$

$$Ar\overset{\bullet}{N}O_2^- \ + \ O_2 \longrightarrow ArNO_2 \ + \ \overset{\bullet}{O}_2^-$$

$$\overset{\bullet}{O}_2^- \ + \ \overset{\bullet}{O}_2^- \ + \ 2H^+ \longrightarrow H_2O_2 \ + \ O_2$$

$$\overset{\bullet}{O}_2^- \ + \ H_2O_2 \longrightarrow O_2 \ + \ \overset{\bullet}{O}H \ + \ \overline{O}H$$
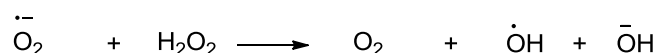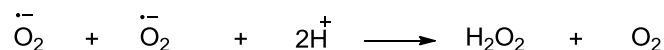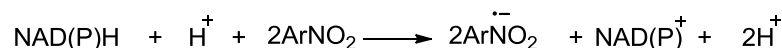
Figure 1.13 Chemical reactions of nitrofuran derivatives occur in epimastigotes.

Moreover, both of the drugs can cause neurological side-effects and nifurtimox can cause digestive problems.[46] Although those drugs are 50% effective in an acute phase and more effective in children, they have low efficacy for chronic Chagas disease.[47] The reason for this has not yet been elucidated.

In attempts to develop more promising therapies, research is moving in two directions. First, new therapeutic strategies, such as drug combinations and novel delivery systems, are under investigation. Because of the severe side effects, adult patients can only continuously take BNZ for 2 months or nifurtimox for 3 months. Switching between these two drugs is considered

12

as one of the strategies, and combinations of anti-parasitic drugs and immunomodulatory drugs have been suggested for evaluation as well.[45] In the chronic phase, improving the delivery systems may improve their efficacies, which are believed to be low as a result of the inability to penetrate into cells of deeper tissue where the parasites exist.[46] Second, inhibitors of various drug targets, which are essential for infection and/or survival of the parasite, are being widely explored as new chemotherapeutics.[48,49] For instance, posaconazole (Figure 1.14) was evaluated as an inhibitor of sterol 14 α-demethylase, which leads to 14 α-methylsterol accumulation and thus damages membrane-bound enzyme systems. In a murine model, posaconazole showed similar effectiveness to BNZ.[50,51]
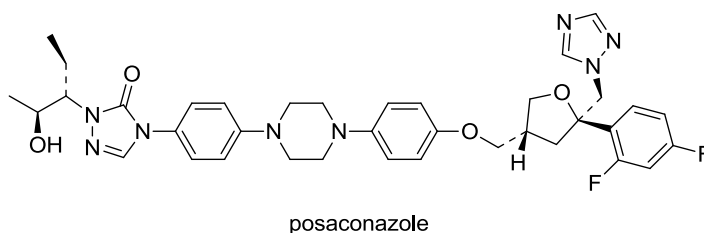
posaconazole

Figure 1.14 An ergosterol biosynthesis inhibitor, posaconazole.

Another enzyme which is widely investigated as a drug target is the trans-sialidase of *T. cruzi*.

1.2.2 *Trypanosoma cruzi* Trans-sialidase (TcTS)

TcTS was first identified in the 1980's by Pereira and coworkers.[52] Several years later, it was found that trans-sialidases were not unique to *T. cruzi*; other protozoic species also express trans-sialidase, for example, African *Trypanosoma brucei*, which causes sleeping sickness.[53,54]

T. cruzi expresses TcTS, which is located on the parasite's membrane surface through a GPI anchor (a glycolipid commonly attached to the C terminal of a protein) or in the host's blood stream.[55-58] TcTS is a retaining exo-sialidase that belongs to GH family 33 (http://www.cazy.org/) and has a similar topography and conserved residues to other members of the sialidase superfamily.[15] TcTS preferentially transfers a terminal α-(2, 3)-linked sialic acid from a donor β-

galactopyranosyl (β-Gal)moiety of oligosaccharides to a β-Gal acceptor residue and has a neutral optimum pH (the optimum pH for sialidases is typically <7).[55] In 1992, Vandekerckhove and colleagues studied the substrate specificity of TcTS and concluded that the substrate transfer is restricted to α-(2, 3) linkages between sialic acids and terminal β-Gal.[59] β-Gal-(1-4)-GlcNAc and β-Gal-(1-6)-GlcNAc act as better acceptors than β-Gal-(1-3)-GlcNAc, regardless of the length and structure of the vicinal sugar chains. As donors, β-Gal-(1-4) is preferred over β-Gal-(1-3).[59] Substituents at C-2, C-3 and C-4 diminish the transfer ability, but substitutions at the C-6 position of β-Gal can maintain acceptor capability, even when the substituent is as large as a glucose moiety.[60] Additionally, TcTS is tolerant of modifications at C-9 of sialic acid, but intolerant of modifications at C-4, C-7 and C-8.[59] TcTS follows the proposed mechanism shown in Scheme 1.1; in the absence of acceptors, TcTS can also act as a sialidase, however, with a lower rate of hydrolysis. According to the crystal structures of both TcTS alone and TcTS with sugar ligands, the different enzymatic behavior of TcTS can be attributed to its narrower and more hydrophobic active site and the significant conformational change that is induced by ligand binding.[61] The conformational change is believed to restrict water attack at the active site by reducing the flexibility and opening of the active site cleft (Figure 1.15).[62] In addition, it shortens the distance between the tyrosine catalytic nucleophile (Tyr342) and C-2 of sialic acid and assists in the formation of an acceptor binding site.[15,61] In this process, Trp312 has been suggested to assist Tyr119 in completing the conformational change. The role of Tyr119 is suggested to be in assisting in substrate orientation and arrangement.[15,63]
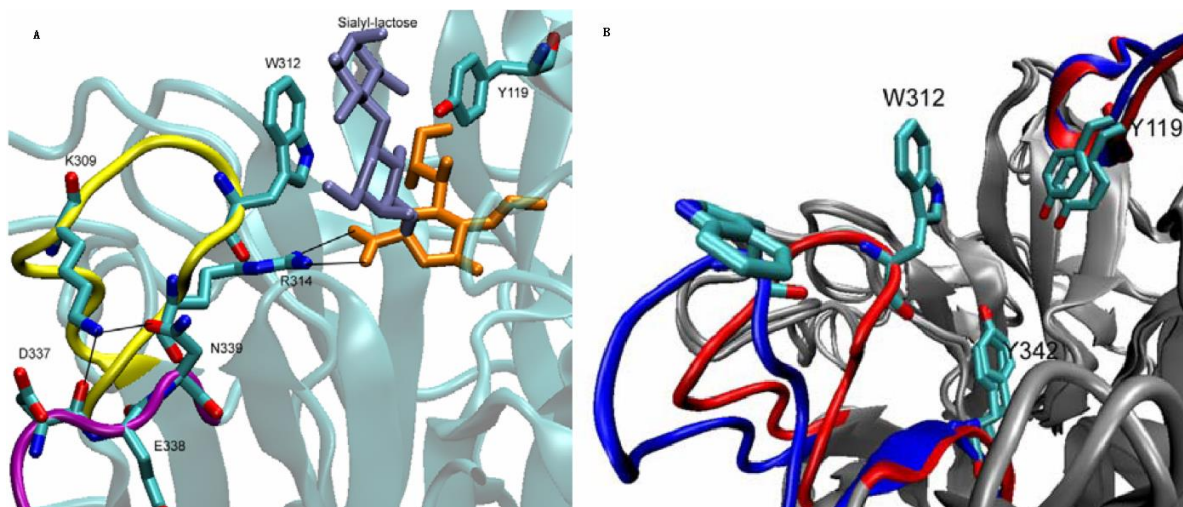
Figure 1.15 Sialic acid binding site of TcTS: A. TcTS binding to sialyl-lactose; B. conformational change between apo form (blue) and holo form (red) of TcTS active site.[62]

Investigations have revealed that TcTS is essential for the invasion of hosts' cells and survival of *T. cruzi* in the host.[64] The *T. cruzi* genome contains 1430 trans-sialidase genes and expresses differing trans-sialidases in various amounts in different forms of its life cycle,[64,65] indicating that TcTS plays a crucial role in the parasite's development. Epimastigotes have low TcTS activities, which are raised in metacyclic trypomastigotes; amastigotes have zero TcTS activity, but activity is restored in trypomastigotes, which have the highest TcTS activities.[64] Another reason why TcTS is so significant is that TcTS can influence the hosts' immune system to a large extent. *T. cruzi* cannot synthesize sialic acids *de novo*, but TcTS can remove sialic acids from host cell surfaces to transfer onto its own cell surfaces. This process would lead to several consequences:

1) The sialylated *T. cruzi* can escape the detection of the host's immune system due to its negatively charged cell membrane;

2) *T. cruzi* is able to use TcTS not only as an efficient trans-sialidase but as a tool to assist binding between parasites and host cells as well by FLY domain (the conserved motif VTVXNVXLYNR);[66]

3)   TcTS may affect Ca^{2+} concentrations in both parasites and host cells by regulating the locations of sialic acids; increased $[Ca^{2+}]$ was suggested to be necessary during invasion;[67]

4)   Removal of sialic acids from cells such as platelets dramatically decreases the half-lives of these cells;[68]

5)   TcTS can desialylate the parasite's own sialic acids in order to increase invasion efficiency, which is supported by the evidence that TcTS-pretreated metacyclic trypomastigotes have higher infectivity;[69]

6)   Active TcTS can induce apoptosis of immune cells, while inactive TcTS cannot.[70]

7)   In addition, the negative charge provided by sialic acid on the parasite's cell surface can help invasion and break down of the hosts' cells, which is necessary for releasing trypomastigotes after duplication of amastigotes in hosts' cells.[64]

Inhibition of TcTS may have a significant impact on the viability of *T. cruzi* inside the human host, and can be used as a potential therapy for Chagas disease.

1.2.2.1   Inhibitors of TcTS

TcTS is mildly inhibited by the classic sialidase inhibitor DANA with a K_i value of 12.29 mM (Figure 1.8a).[71,72] Developments toward better inhibitors of TcTS occur in four general directions. The first is natural product screening, which is an extensively used method to explore inhibitors of various enzymes. In 2010, Arioka and colleagues screened a natural product library and identified flavonoid and anthraquinone derivatives as specific and non-competitive inhibitors of TcTS. The two compounds shown in Figure 1.16 are candidates with the highest efficacy and specificity within those two derivative series, respectively.[73]

a   b
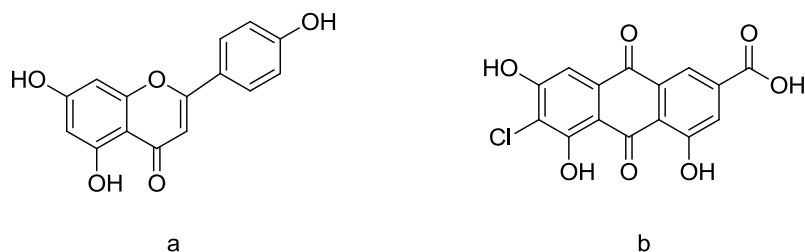
Figure 1.16 "Winner" inhibitors from natural product screening: a. flavonoid derivative (IC_{50}=78 µM, specificity to human sialidase Neu2=7.3); b. anthraquinone derivative (IC_{50}=0.58 µM, specificity to human sialidase Neu2>170).

Due to the development of molecular docking, quantum mechanical/molecular mechanical (QM/MM) and molecular dynamics (MD) simulations, design of inhibitors could be achieved from a new perspective.[74] By evaluating a library of commercially available compounds through this strategy, a promising compound (Figure 1.17) was identified as either a non-competitive or a mixed inhibitor, which seems to bind at both the active site and other regions of TcTS.[72]
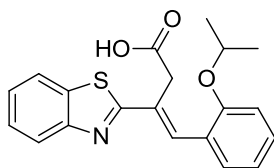
Figure 1.17 Inhibitor selected by computational methods (IC_{50}=150 µM).

It has also been found that there are some antibodies which can directly inhibit TcTS with great specificity and efficiency, such as the recently identified neutralizing mouse monoclonal antibody (mAb 13G9).[75] The proposed mechanism is that it interacts with and blocks the movement of Tyr119 (Figure 1.18), which is a residue essential for trans-sialylation activity, as previously shown.[75]

17
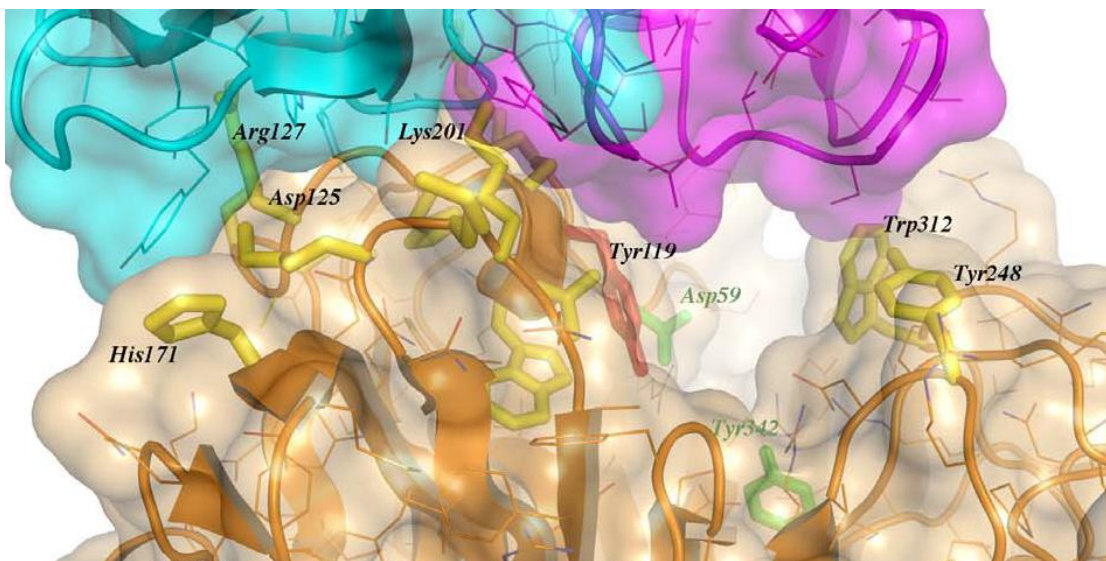
Figure 1.18 Close-up of the TcTS/antibody interface: TcTS is shown in orange and the antibody complex is shown in magenta (light chain) and cyan (heavy chain), the catalytic nucleophile Tyr342 and acid/base Asp59 are highlighted in green.[75]

Another approach to develop inhibitors of TcTS is substrate modification, including both donor and acceptor modification. In 2004, it was suggested that the trans-sialidase lactose binding site may be a good inhibition target, since lactitol (Figure 1.20a) can inhibit the transfer of sialic acid to *N*-acetyllactosamine efficiently.[76] In 2010, Carvalho and colleagues synthesized and evaluated a library of C-1 or C-6 modified 1,2,3-triazole-substituted galactose derivatives and recommended *N*-benzyl-*N*-methyl-1-[1-(methyl 6-deoxy-β-D-galactopyranosid-6-yl)-1*H*-1,2,3-triazol-4-yl]-methylamine (Figure 1.20b) as a potential drug candidate.[77] In the same period, investigation indicated that lactitol derivatives with polyethylene glycol (PEG) modifications improved their stability in blood and retained similar inhibition parameters as lactitol.[78]

Various sialic acid derivatives – "donor mimics" – are potential inhibitor candidates as well. 3-fluorosialyl fluoride derivatives (Figure 1.20c) are the first class of interest, which inactivate TcTS through a covalently linked sialyl-enzyme complex as discussed earlier.[17] Moreover, the extra space around C-9 in the binding pocket allows a bulky group to be attached to C-9 and provides various possibilities to improve the specificity since human sialidases have less space here and TcTS might develop new interactions.[32] Buchini suggested that modifications at C-9 of 3-

18

fluorosialyl fluoride with aryl groups (Figure 1.20c) increased the affinity and reduced the reactivation rate in the presence of lactose (without lactose, no reactivation was observed).[32] The compound she investigated with the highest inactivation constant was 5-acetamido-9-[7-hydroxycoumarin-3-carboxamido]-3,5,9-trideoxy-3-fluoro-D-*erythro*-β-L-*manno*-non-2-ulopyranosonate fluoride (Figure 1.19). This compound was a better-binding and a more specific inactivator compared to the 3-fluorosialyl fluoride, with inactivation parameters of k_i/K_i 14×10^{-3} $min^{-1}mM^{-1}$ and $(k_i/K_D)^{lactose}$ 0.3×10^{-3} $min^{-1}mM^{-1}$. In comparison, 3-fluorosialyl fluoride has a k_i/K_i of 8×10^{-3} $min^{-1}mM^{-1}$ and a $(k_i/K_D)^{lactose}$ of 1330×10^{-3} $min^{-1}mM^{-1}$, indicating that this compound reactivated more slowly.
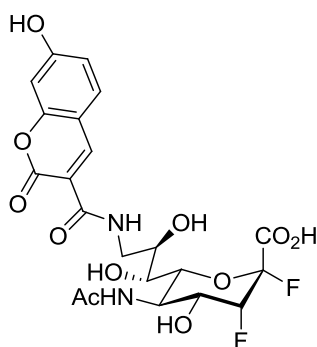
Figure 1.19 The best inactivator developed by Buchini.[32]

In 2010, Carvalho suggested the use of 2-difluoromethyl-4-nitrophenyl-3,5-dideoxy-D-glycero-α-D-galacto-2-nonulopyranosid acid (NeuNAcFNP) as a substrate of TcTS, which results in inactivation through the reactive fluorinated quinone methide generated upon cleavage (Figure 1.20d).[79] However, this is highly likely to be toxic since the quinone methide can diffuse and react elsewhere. Last year, Meinke *et al.* developed a series of aromatic C-sialosides which inhibited TcTS through the interaction between the aryl group and Tyr119 and/or Trp312 side chains. The K_D value of the most efficient compound among them was 0.16 mM (Figure 1.20e).[80] Last year, five compounds that could occupy both the acceptor binding site and the donor binding site were identified, with a lowest reported IC_{50} of 260 μM (Figure 1.20f).[81] Additionally, research indicated that the sialic acid precursors with elongated N-acyl side-chain can reduce the infection of *T. cruzi* (Figure 1.20g).[82] However, none of them have shown any high affinities, which are sufficient as drug candidates.

19
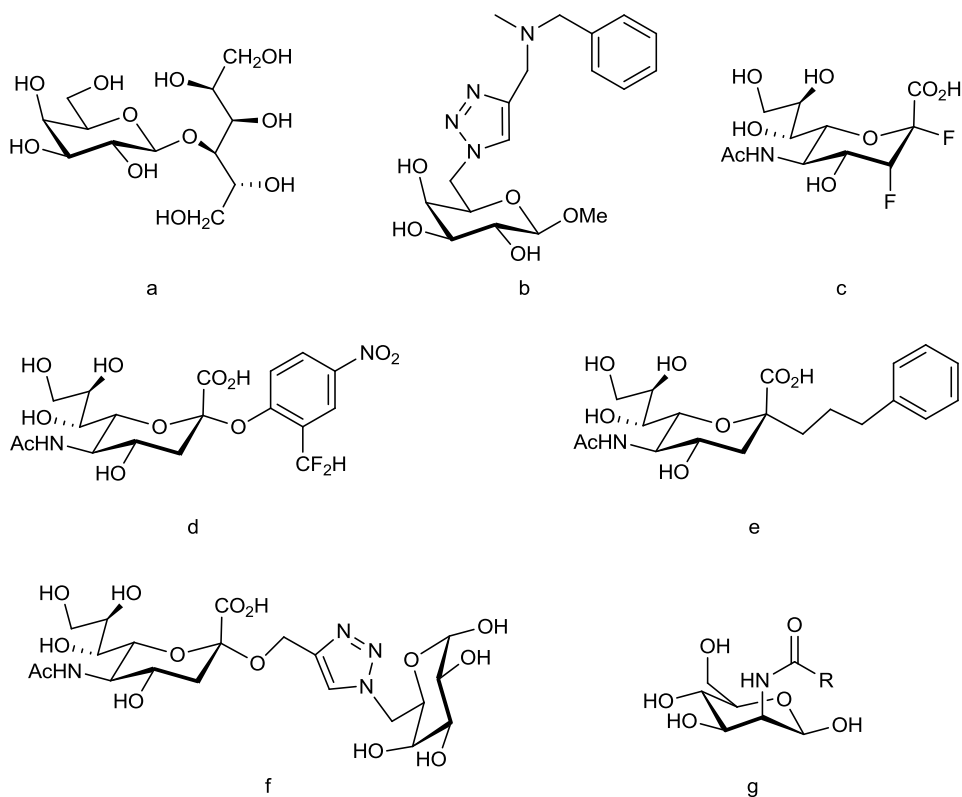
Figure 1.20 Outstanding inhibitors selected based on substrate modification. (R=short alkyl group)

1.3   Aims of This Thesis

As mentioned previously, 3-fluorosialyl fluoride has been shown to act as an inactivator of TcTS.[15] It has also been shown that an aromatic modification at C-9 of 3-fluorosialyl fluoride will increase the specificity since Neu2 (typical human sialidase used in sialidase-inhibitor-drug development) has a smaller substrate binding pocket compared to TcTS, which may tolerate a bulky group at the C-9 position.[32] An aromatic group was shown to reduce the rate of reactivation of 3-fluorosialyl TcTS by lactose due to the additional hydrophobic interaction between the aromatic ring and the Tyr 119 side chain. The goal of this work is to develop tight-binding and specific inactivators of TcTS, which can serve as potential drug candidates. There are two aims of this thesis towards that goal.

The first aim is to assemble a library of C-9 modified potential mechanism-based inactivators of TcTS. This will be achieved by click chemistry using a series of alkynes and 9-azido-3-fluorosialyl fluoride (Figure 1.21). The second aim is to evaluate these compounds as inactivators of TcTS and Neu2. The ideal drug candidate will have high specificity towards the protozoan TcTS and low specificity towards human Neu2.
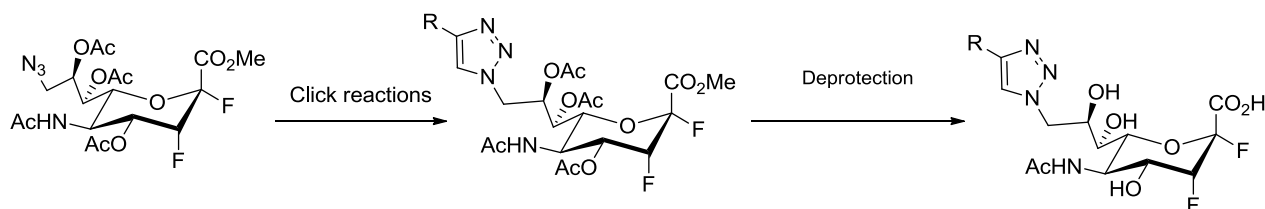
Figure 1.21 Scheme of the approach to build the inactivator library.

Before the start of Chapter 2, a general introduction of click chemistry will be provided.

1.3.1 Click Chemistry

In 2002, click chemistry was originally described as the chemistry of Copper-Catalyzed Azide Alkyne Cycloaddition (CuAAC), which was first developed by Sharpless *et al.* (Figure 1.22a).[83,84] Nowadays, the term click chemistry is extended to include other metal catalyzed reactions, such as Ruthenium-Catalyzed Azide Alkyne Cycloaddition (RuAAC), established in 2005 and produces 1,5-disubstituted triazole, compared to the 1,4-disubstituted triazole product of CuAAC (Figure 1.22b).[85]
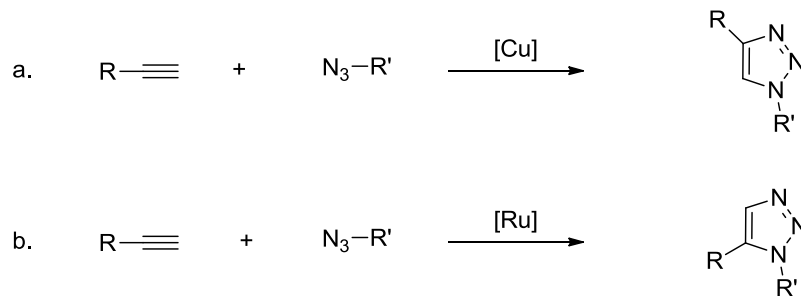
Figure 1.22 Click reactions: a. [Cu] catalyzed 1,4-disubstituted triazole; b. [Ru] catalyzed 1,5-disubstituted triazole.

Due to the high stability of 1,2,3-triazoles, click chemistry is widely applied in the biomolecular modification field with its advantages of being a generally fast reaction with high yields.[84]

The mechanism of click chemistry is still under investigation due to the complexity and variability of the reactions. In 2010, Fokin *et al.* presented their mechanistic insights, reproduced in Figure 1.23.[84] First, copper(I) acetylide is formed through π-coordination (A); then, N-1 of the azide acts as a π-donor in most cases and interacts with Cu^I, where the azide is activated (B); in the end, the triazole ring is formed and the Cu^I catalyst is released (C). During process C, side products could form in the presence of oxidizing agents (D).
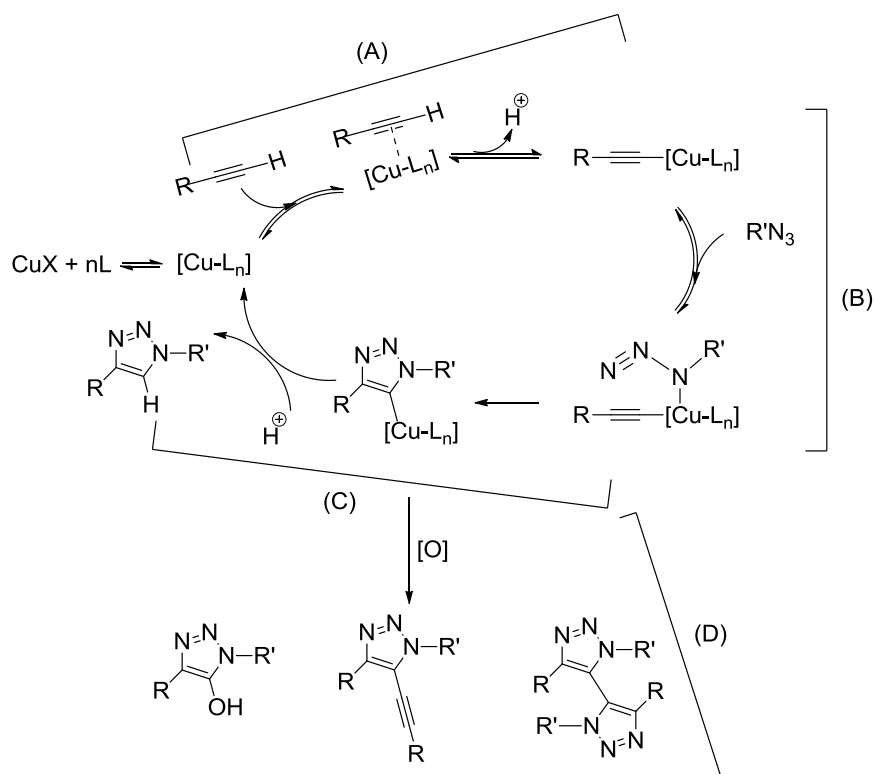
Figure 1.23 Proposed mechanism for click chemistry.[84] (L=ligand; R and R'= alkyl or aryl groups)

In addition, the absence of azide causes the copper (I) acetylide to form poly-aggregates, which cannot be reactivated once formed. Thus, effective ligands of Cu^I are necessary in order to prevent polymer formation without preventing the copper (I) acetylide from interacting with the azide. Various ligands, such as tris(benzyltriazolyl) methyl amine ligand (TBTA, in Figure 1.24)[86],

have been developed in an attempt to improve the adaptability of the click reaction and the stability of the Cu^{I} species, which are easily oxidized in the presence of O_2.
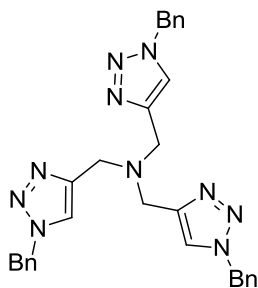
Figure 1.24 Structure of TBTA.

2 Synthesis of 5-Acetamido-9-azido-3,5,9-trideoxy-3-fluoro-D-*erythro*-β-L-*manno*-non-2-ulopyranosonate Fluoride and Derivatives as Inactivators of *T. cruzi* Trans-sialidase

2.1 Synthesis

5-Acetamido-9-azido-3,5,9-trideoxy-3-fluoro-D-*erythro*-β-L-*manno*-non-2-ulopyranosonate
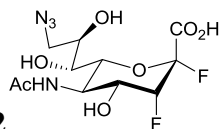
fluoride (**2.12**) is not found in nature and acts as a "donor mimic" inactivator for TcTS. We chose this as a parent compound in an attempt to build a screening library since this library could be expanded by click chemistry. From the nature of "donor mimic" inactivator development, there were two possible approaches to build the screening library and to assess inactivation activities of the designed compounds for TcTS. One possible approach was to build a synthetic substrate library with an appropriate leaving group (chromophore) at C-2, which could be quantitatively monitored by modern analytical techniques. Hence, the most promising compounds could be identified as better binding substrates and the corresponding inactivators could be synthesized and their inactivation probed. The other possible approach was to directly synthesize a series of inactivators and assess their inactivation activities by enzyme kinetics study. Comparing the two alternatives, the first method involves much simpler chemistry. However, there are some disadvantages: it was necessary but difficult to introduce the azido group into sialic acid selectively through a chemical pathway; the choice of leaving group was complicated by the need to balance reactivity and stability to the click chemistry conditions. For the second method, the fluorides should be stable under the click chemistry reaction conditions. However, the main difficulty of this method was the synthesis of the parent compound on larger scales since both fluorines had to be inserted with desired regio- and stereo-selectivity, which reduced the yields. After several test

reactions, the second approach in which the inactivators are directly synthesized was chosen for this thesis.

2.1.1 Synthesis of 5-Acetamido-9-azido-3,5,9-trideoxy-3-fluoro-D-*erythro*-β-L-*manno*-non-2-ulopyranosonate Fluoride

There are two options for installing two vicinal fluorine atoms on the sialic acid sugar ring: a chemical route via DANA or an enzymatic route via *N*-acetylneuraminic acid (Neu5Ac) aldolase using ManNAc and β-fluoropyruvate. However, the direct addition of two fluorines to DANA doesn't lead to the desired compound since the trans product is preferred. In 2002, Beliczey *et al.* explored the enzymatic synthesis of 3-fluorosialic acid using β-fluoropyruvate and successfully optimized the experimental conditions for the new substrate.[87] In 2004, Withers *et al.* suggested that ^{19}F NMR could be used to monitor this reaction in a general route to synthesize 5-acetamido-2,3,5-trideoxy-3-fluoro-D-*erythro*-β-L-*manno*-non-2-ulopyranosonate fluoride in high yields.[88] A modified synthesis, which used 6-azido-ManNAc, instead of ManNAc, adapted from this route was published in 2008 by Buchini *et al.* (Scheme 2.1).[32]

For the sections of this thesis that describe synthesis, a reproduction of Buchini's work, the focus will be on steps where difficulties were encountered and adjustments were made in order to increase the yields of the desired targets.
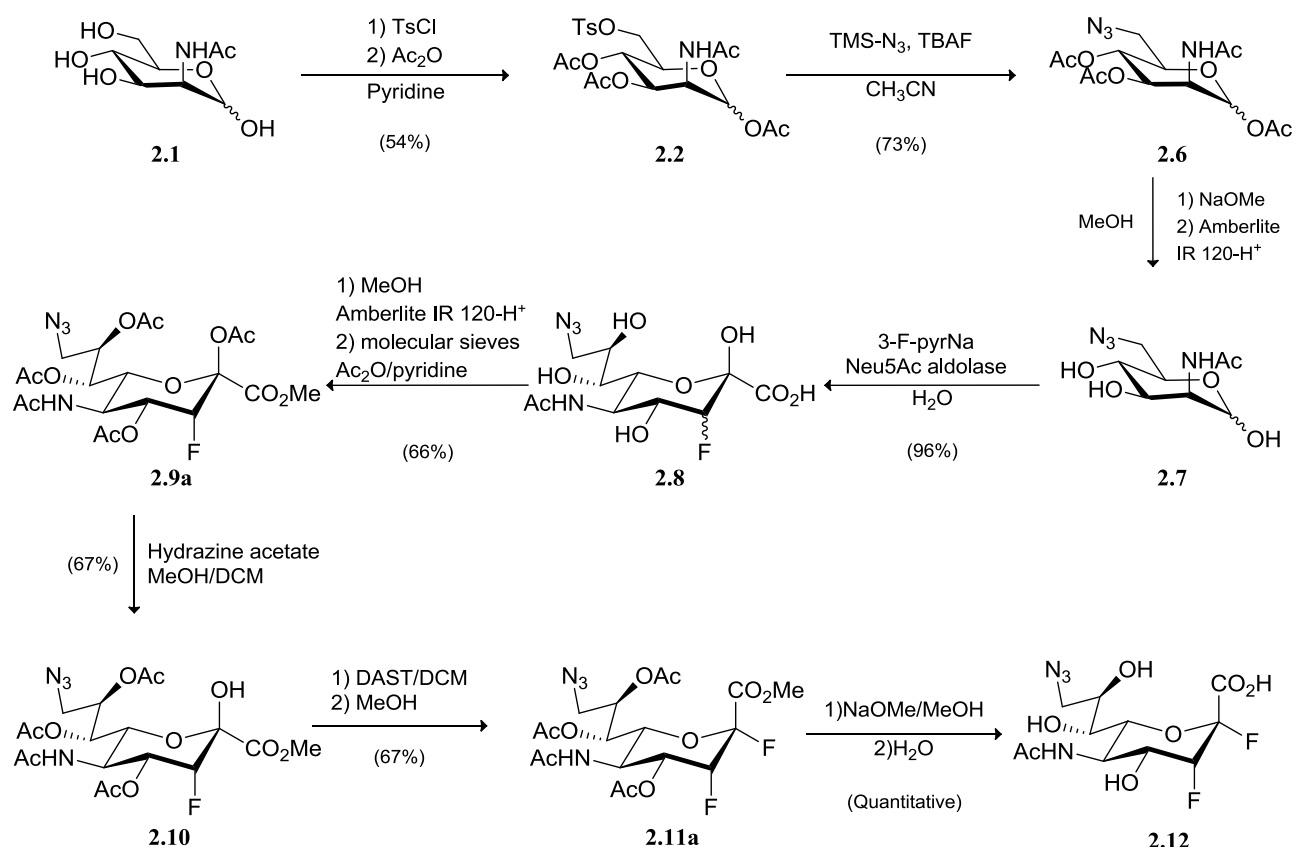
Scheme 2.1 Synthetic route to afford 3-fluorosialyl fluoride.[32]

Buchini's published protocol started with ManNAc. After tosyl chloride (TsCl) selectively reacted with the primary alcohol at 0°C, acetylation was achieved in one pot. As the very first reagent in a nine-step routine, a large quantity of **2.2** was required. A 53.4% yield was obtained for this reaction, similar to that in literature procedures. The main side products were di-tosyl substituted compounds, as confirmed by mass spectrometry (Figure 2.1). Due to the moisture-sensitivity of TsCl, the commercially available TsCl is usually a mixture of both species. For initial reaction optimization, recrystallized TsCl was used to increase the yield. The recrystallization was performed by dissolving commercial TsCl in CHCl$_3$ and adding petroleum ether (40-60%) to precipitate impurities. After filtration, the residue was concentrated to obtain white TsCl crystals (whereas the commercial material is off yellow). [89] Using recrystallized TsCl, the yield of the first step was improved to 77%.
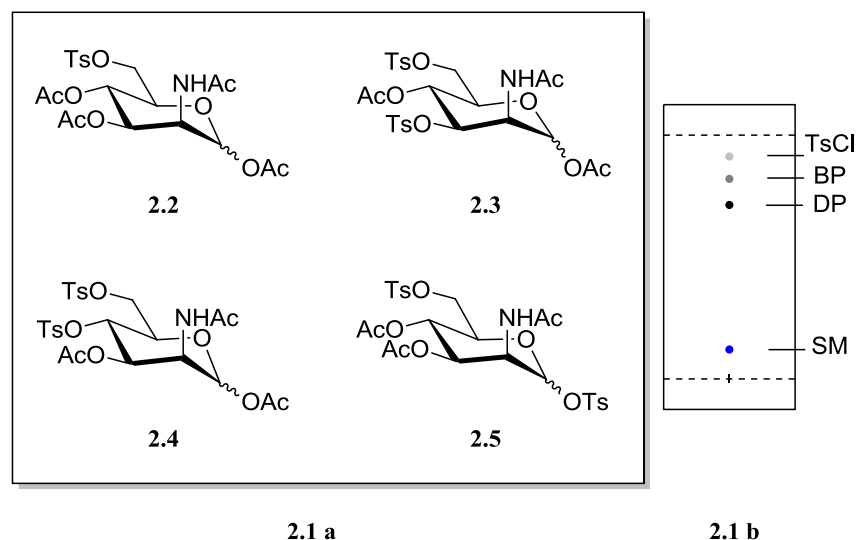
Figure 2.1 a. Target compound **2.2** and possible side products; b. representation of a TLC plate obtained from the tosyl substitution reaction with the eluent (EA: Hexanes = 3:1): SM = starting material, DP = desired compound (major product), BP = byproduct (minor product).

In Buchini's paper, a yield of 73% for the synthesis of **2.6** was achieved by refluxing **2.2** with trimethylsilyl azide (TMS-N_3) and *tetra-N*-butylammonium fluoride (TBAF) in dry CH_3CN. When reproducing this reaction, only a 57.5% yield was obtained. I found that the dryness of TBAF was crucial since this is a moisture-sensitive reaction. Due to the strong affinity to water of TBAF, anhydrous TBAF is hydrated readily during storage. In addition, TBAF will decompose according to the reactions outlined in Figure 2.2 during the removal of water[90,91] An exploration of an alternative method for the introduction of the azido group was needed.

$$(n\text{-}C_4H_9)_4\overset{\oplus\,\ominus}{N}F \cdot 3H_2O \xrightarrow{\Delta} (n\text{-}C_4H_9)_4\overset{\oplus\,\ominus}{N}F + 3H_2O$$

$$2(n\text{-}C_4H_9)_4\overset{\oplus\,\ominus}{N}F \xrightarrow{\Delta} (n\text{-}C_4H_9)_4\overset{\oplus\,\ominus}{N}FHF + (n\text{-}C_4H_9)_3N + CH_3CH_2CH{=}CH_2$$
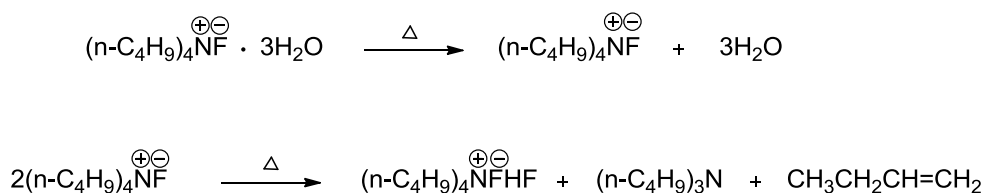
Figure 2.2 TBAF decomposes during the drying process.[90]

The common approach of treating a tosylated compound with sodium azide at 80 °C in anhydrous DMF was tried and the yield dropped to 34%, compared to 91% in the literature.[92] Increasing the reaction temperature to 100°C dramatically raised the amount of byproduct. In 1996,

27

Ercegovic *et al.* reported that treating the methyl ester of 9-tosyl sialoside with sodium azide in the presence of 18-crown-6 at 60 °C in DMF for 20 h generated the methyl ester of 9-azido sialoside successfully with a 83% yield (Scheme 2.2).[93]
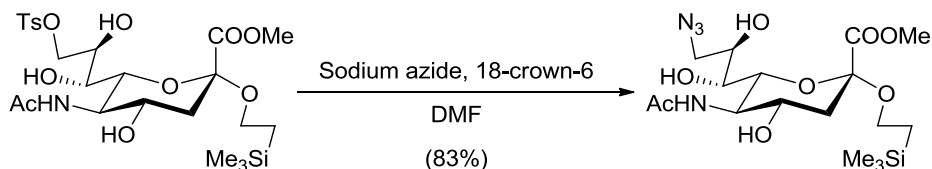
Scheme 2.2 Azide substitution method presented in Ref 93.[93]

This strategy was applied and after reacting for 24 h, a yield of 76% was obtained. The tosylated compound used was fully protected by acetyl groups, thus, the polarity difference between the sodium azide and the targeted tosylated compound seemed to be the reason why the sodium azide could not displace the tosyl group on the C-6 position of per-*O*-acetylated ManNAc. 18-Crown-6 was used as a phase-transfer catalyst. $Na^+N_3^-$ is solvated by 18-crown-6, and the nucleophilic attack from N_3^- onto the tosylated protected sugar was much more efficient (Figure 2.3). According to procedures provided by literature[32], deprotection was conducted and producing 6-azido-ManNAc.
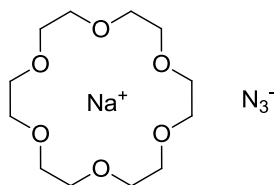
Figure 2.3 Sodium azide carried by 18-crown-6.

Neu5Ac aldolase catalyzes the aldol condensation between ManNAc and β-fluoropyruvate to form a mixture of axial and equatorial diastereomers (Scheme 2.3). The most challenging part of this overall synthetic routine was the enzymatic reaction, for two reasons. First, the product of the enzymatic reaction (3-fluorosialic acid) is an inactivator of Neu5Ac aldolase with a K_i of 2.5 mM.[94] Second, using 6-azido-ManNAc, instead of the natural substrate, induces difficulties in two respects: axial/equatorial fluorine ratio and reaction rate. As mentioned previously, in 2002, Beliczey *et al.* published a synthetic pathway to furnish the 3-fluorosialic acid in high axial/equatorial ratio using

the following conditions: 50 mM β-fluoropyruvate, 300-400 mM ManNAc with 20-500 U/mL

Neu5Ac aldolase at pH = 7.5 and 25 °C.[87] In addition, they emphasized that a large excess of

ManNAc is crucial for the axial diastereometic preference. However, it is not practical to use a

large excess of 6-azido-ManNAc, since a number of steps of reactions were needed to make it. In

addition, 6-azido-ManNAc reacts more slowly than ManNAc.
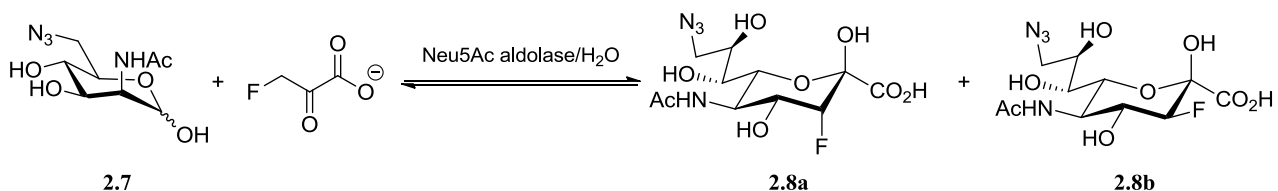
Scheme 2.3 Neu5Ac aldolase catalyzes condensation between 6-azido-ManNAc and β-fluoropyruvate.

Buchini *et al.* developed a method to add 0.3 eq. of β-fluoropyruvate four times. Each

aliquot was added after the previous addition of β-fluoropyruvate was fully consumed, thereby

providing an excess of 6-azido-ManNAc during the majority of the reaction period. In this way, an

efficient use of 6-azido-ManNAc was attained due to the total excess of β-fluoropyruvate (1.2

eq.).[32] However, the axial/equatorial ratio obtained in my hands was only 2:1 compared to 7:1 from

Buchini's paper. Several key factors influencing the ratio were addressed by optimization reactions.

First, the second aliquot addition of β-fluoropyruvate should be added no later than 0.5 h after full

consumption of the first aliquot. The ratio decreased from 5:1 to 2:1 when the second addition was

after 2 h. As the kinetic product, the axial-F product formed faster and was then converted into the

more thermodynamically stable equatorial-F product without need for additional β-fluoropyruvate.

Second, addition of 1/3 of the initial amount of Neu5Ac aldolase in conjunction with the third

aliquot of β-fluoropyruvate increases the ratio and reduces the reaction period at the same time.

During the 3-4 days to reach complete consumption of 6-azido ManNAc (monitored by TLC and

^{19}F NMR), the aldolase lost its activity due to the long period of time required. This approach was

better than adding more aldolase at the very beginning, since large amounts of aldolase would

increase the possibility of axial/equatorial conversion. In addition, the freshness of the aldolase was

crucial to the ratio. In the first attempts at this reaction, an old batch of enzyme was used and the

highest ratio obtained was 5:1.Under the same condition, a ratio of 7:1 was obtained by using a new

batch of enzyme. The ratio of axial/equatorial and the consumption of β-fluoropyruvate were determined by ^{19}F NMR. The chemical shifts for β-fluoropyruvate, axial and equatorial 3-fluorosialic acid products were 220 (t), 209 (dd) and 200 (dd) ppm, respectively.

Another modification was in the installation of the fluorine at C-2, which involved the nucleophilic substitution of the anomeric hydroxyl group by F using diethylaminosulfur trifluoride (DAST). Buchini reported a 67% yield of **2.11a.** By following the same procedure, a combined 50% yield of both **2.11a** and its equatorial anomer was obtained. Due to the fact that no starting material was seen on TLC before quenching the reaction, the assumption was made that the reaction was left too long and that excess fluoride caused some equilibration. Buchini conducted the reaction at -30°C for 30 minutes. By monitoring the reaction by TLC every 5 minutes, it was observed that reaction was complete after 15 min. Following this reaction time, a yield of 65.2% for **2.11a** was obtained.

Throughout the whole synthetic process, from **2.1** to **2.12**, the separations between diastereomers were consistently inefficient. At each step, the flash columns had to be run twice in order to obtain the presented purity and yield. Various eluents were explored; however, the gradient mixture suggested by Buchini (EA/hexane mixture) provided the best results.

2.1.2 Synthesis of Alkyne-coupled Triazole Derivatives

Based on Buchini's previous work, we decided to create a library of inactivators bearing aryl groups installed through click chemistry (Figure 2.4).
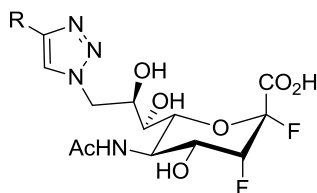
Figure 2.4 Inactivator library structure. (R=Alkyl or Aryl group)

2.1.2.1   Click Condition Optimization

Based on a previous study concerning the optimization of click chemistry conditions by the Withers group, compound **2.12** was chosen as the key intermediate for click chemistry and *m*-tolylacetylene as the alkyne for the optimization of conditions, since the product can be visualized by both UV light and molybdate stain on TLC. The conditions reported were the following: stirring with 40 mol% sodium ascorbate (NaAsc), 10 mol% CuSO$_4$ and 1 mol% TBTA (mol% regarding the azide) in wet methanol at room temperature overnight. These conditions were tested with 6-azido-ManNAc as a less "valuable" model compound, a yield of 72% was obtained. However, no conversion of compound **2.12** was observed after 4 days with 3 times the amount of added alkyne, CuSO$_4$/ NaAsc and TBTA. Thus, an exploration of conditions using compound **2.12** was necessary. CuSO$_4$/ NaAsc was used as the Cu^I source in all test reactions shown in Table 2.1 (Scheme 2.4).
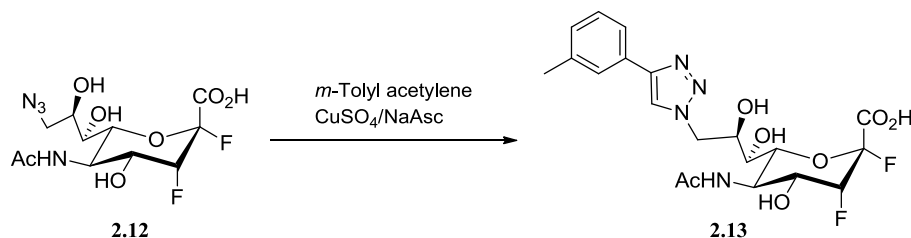
Scheme 2.4 General scheme for the first set of click reactions.

The variables taken into consideration were solvent, amount of reactants and ligands. Temperature was not varied, since **2.12** is not stable at high temperature. At the same time, the newly synthesized ligand 2-[4-{(bis[(1-tert-butyl-1*H*-1,2,3-triazol-4-yl)methyl]amino)-methyl}-1*H*-1,2,3-triazol-1-yl]ethyl hydrogen sulfate (BTTES), which was suggested by Besanceney-Webler *et al.* due to its higher efficacy for bioorthogonal click reaction (Figure 2.5),[95] was also tested during condition optimization.
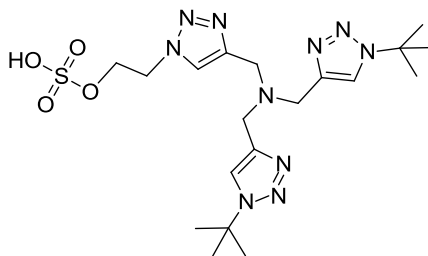
Figure 2.5 Structure of BTTES.

For all small scale reactions, sonication was applied to ensure efficient mixing and conversion was monitored by TLC. The outcomes of several click reactions are summarized in Table 2.1.

Table 2.1 Optimizing conditions for click chemistry (Reactions carried out at RT, CuSO$_4$/NaAsc (2 eq./3 eq.) as source of Cu^I, modified free sugar as azide).

m-Tolyl acetylene	Solvent	Time	Ligand	Product[a]
3 eq.	Wet methanol	36 h	-	No conversion
			TBTA	≈ 25% conversion
			BTTES	Trace
3 eq.	H$_2$O	36 h	-	No conversion
			BTTES	Trace
1.5 eq.	H$_2$O/^{t}BuOH/ DCM 1:2:1	24 h	BTTES	100% conversion
			TBTA	≈ 75% conversion

[a] Based on TLC analysis.

Wet methanol and water as solvent resulted in poor yields. During 36 h, 1.3 eq. of *m*-tolyl acetylene, 0.01 eq. of CuSO$_4$ and 1.2 eq. of NaAsc were added initially, then increased to 3 eq., 2 eq. and 3 eq., respectively. The reaction conducted in wet MeOH using TBTA as the ligand reached approximately 25% conversion after 12 hours but with no further conversion even after 36 h. In

2009, Weïwer *et al.* reported that click chemistry of azido-substituted sialic acids proceeded in high yields using $H_2O/^tBuOH/DCM$ (1:2:1) as solvent.[96] This solvent mixture was tested and approximately 90% conversion was obtained after reacting overnight. Additionally, it was found that under this condition, BTTES was a better ligand than TBTA. TLC analysis at 5 time points (5 min, 15 min, 30 min, 45 min and 60 min) during the reaction showed that the azide disappeared after 5 min; however, the conversion to product was not complete. A polar complex was formed, which slowly converted to the product. Unfortunately, for a large scale reaction using the same conditions, only approximately 30% conversion was obtained. For large scale reactions, sonication may not have been sufficient to ensure good mixing. A dark yellow precipitate appeared after reacting for 10 min, possibly due to formation of an inactive species of Cu, as was also observed by Fokin *et al.*[84] Since $H_2O/^tBuOH/DCM$ (1:2:1) is a delicate solvent mixture whose homogeneity is easily disrupted, mixing was not optimal, even with vigorous stirring. New solvent systems were explored. Yan Lu *et al.* reported that $H_2O/^tBuOH$ (1:1) produced a range of alkynes in 69-87% yield from per-*O*-acetylated 4-azido-DANA methyl ester.[97] A series of test reactions were therefore conducted using the per-*O*-acetylated 4-azido-2,3-difluoro sialic acid methyl ester (**2.14**) as a less valuable model compound to seek a better synthetic pathway with higher yields (Scheme 2.5).
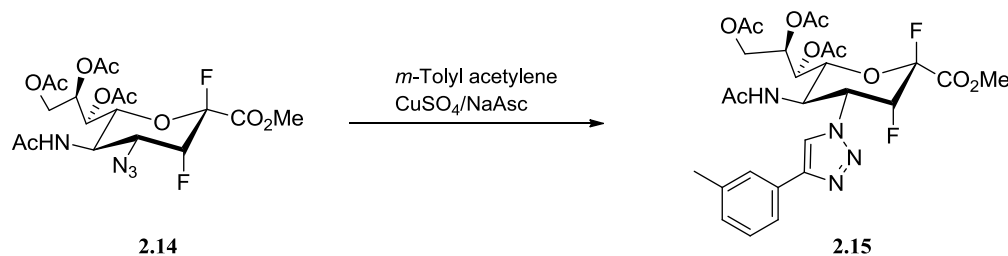
Scheme 2.5 General scheme for the second set of test click reactions.

To initiate the reaction, 1.2 eq. alkyne, 1 mol% BTTES and 7 mol% $CuSO_4$/36 mol% NaAsc were added. After overnight reaction, half of the starting material was consumed and another 1 mol% BTTES and 36 mol% NaAsc were added. Both of the reactions with BTTES as ligand proceeded with 100% conversion after 36 h, based on TLC; furthermore, there was less byproduct formation using $H_2O/^tBuOH$ 1:1 as solvent. Consequently, a higher yield was obtained. In addition, increasing the reagent amounts to 4 mol% BTTES and 9 mol% $CuSO_4$/1.2 eq. NaAsc

reduced the reaction time to 24 h without affecting yield (Table 2.2). Control reactions that lacked ligand yielded only trace amounts of product.

Table 2.2 Optimizing condition for click chemistry (Reported yields are after purification).

m-Tolyl acetylene	Cu^I source	Solvent	Time	Ligand	Product[a]
1.2 eq.	CuSO$_4$/NaAsc 0.07/0.72 eq.	Wet methanol	36 h	-	No conversion
				BTTES (0.02eq.)	100% conversion (60% yield)
1.2 eq.	CuSO$_4$/NaAsc 0.07/0.72 eq.	H$_2$O/^{t}BuOH 1:1	36 h	-	Trace
				BTTES (0.02eq.)	100% conversion (75% yield)
1.2 eq.	CuSO$_4$/NaAsc 0.09/1.2 eq.	H$_2$O/^{t}BuOH 1:1	24 h	BTTES (0.04eq.)	100% conversion (76% yield)

[a] The conversion percentage was based on TLC analysis while the yields were obtained after flash column purification.

In order to determine whether the fully deprotected azide was able to react in H$_2$O/^{t}BuOH (1:1) as the solvent system, the compound 4-azido-3-fluorosialyl fluoride (**2.16**) was tested (Scheme 2.6). By TLC, 100% conversion was observed; however, there were more side products compared to the fully protected compound **2.14**. Consequently, the protected compound (**2.11a**) and a H$_2$O/^{t}BuOH (1:1) solvent system were used for further reactions.

2.16 *m*-Tolyl acetylene CuSO$_4$/NaAsc **2.17**
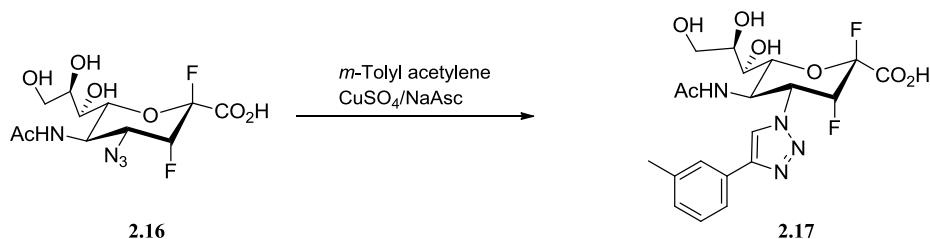
Scheme 2.6 General scheme for the third set of click reactions.

To further prove the validity of these conditions, compound **2.11b** was reacted and 100% conversion was observed after 48 h. Compound **2.11a** also fully reacted after 12 hours. After 3 flash chromatography columns using different eluents, the product was not pure, having an approximate

yield of 80%. It was found that after 3 columns the product could be used for the next step, since the impuries did not react during deprotection process.

2.1.2.2   Selection of Alkynes for Click Reactions

Attention was then focused on the creation of a small library of **2.11a** derivatives through click chemistry using these optimized conditions (Scheme 2.7). The outcome of small scale testing reactions with 19 alkynes is summarized in Table 2.3. The optimal conditions determined in Section 2.1.2.1 were used: BTTES (4 mol%), $H_2O/^tBuOH$ (1:1), $CuSO_4$ (9 mol%)/NaAsc (1.2 eq.) at room temperature. The reaction time and the amount of alkynes were varied from case to case in order to push the reactions to completion. In all cases, 1.2 equivalents of alkyne were initially added, and then more was added if necessary, according to TLC analysis and mass spectrometry.
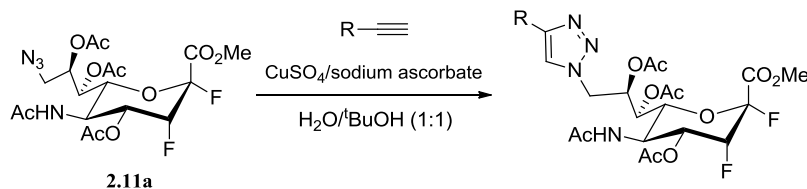
Scheme 2.7 General scheme for small scale reactions with alkynes.

The reaction time for most of the reactions with approximately 80% or higher conversion was approximately 12 h, except for amine substituted compounds, where reaction was complete around 4 h. Those with less than 80% conversion were left for 3 days with additional alkyne and Cu^I additions twice a day. It was noticed that 3-diethylamino-1-propyne and 1-dimethylamino-2-propyne reacted with **2.11a** with 100% conversion, however, 3-(di-*n*-butylamino)-1-propyne did not react at all. This might be related to the steric hindrance induced by the *n*-butyl group. In addition, the amine substituted triazole products were not as stable as the non-amine substituted ones.

Table 2.3 Small scale reactions with different alkynes.

Alkyne	TLC [a]	MS [b]
Ethoxyacetylene (50% solution in hexane)	≈ 20% conversion	SM&P
Cyclopentylacetylene	≈ 80% conversion	SM&P
4-*tert*-Butylphenylacetylene	≈ 50% conversion	SM&P
5-Phenyl-1-pentyne	≈ 80% conversion	SM&P
Cyclopropylacetylene	≈ 80% conversion	SM&P
3,3-Dimethyl-1-butyne	≈ 75% conversion	SM&P
1-Dimethylamino-2-propyne	100% conversion	P
2-Ethynylpyridine	≈ 20% conversion	SM&P
5-Hexyn-1-ol	≈ 80% conversion	SM&P
Phenylacetylene	100% conversion	P
2-Methyl-3-butyn-2-ol	≈ 80% conversion	SM&P
3-(Di-*n*-butylamino)-1-propyne	No conversion	SM
3-Diethylamino-1-propyne	100% conversion	P
1-Ethynylcyclohexanol	No conversion	SM
2-Ethynyl-benzaldehyde	No conversion	SM
3-Aminophenylacetylene	No conversion	SM
Propiolic acid	No conversion	SM
Sodium 4-ethynylbenzoate	No conversion	SM
17-α-Ethynyl estoadiol	No conversion	SM

[a] Based on TLC analysis. [b] SM and P mean that there are starting material and product signal present in the MS, respectively.

Accordingly, the following alkynes were chosen to conduct large scale (preparative) click chemistry reactions: cyclopentylacetylene, 5-phenyl-1-pentyne, cyclopropylacetylene, 3,3-dimethyl-1-butyne, 1-dimethylamino-2-propyne, 5-hexyn-1-ol, phenylacetylene, 2-methyl-3-butyn-2-ol (Scheme 2.8).
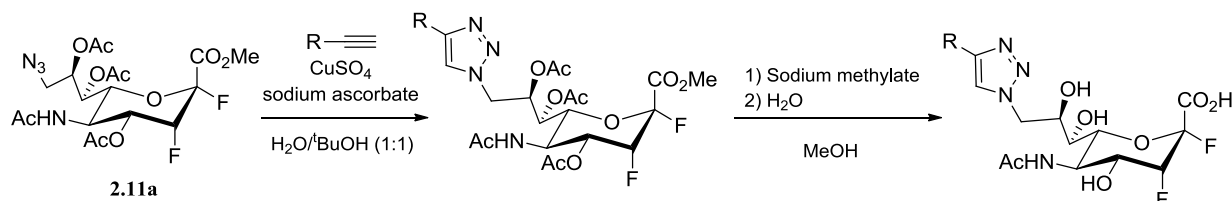
Scheme 2.8 General scheme for triazole inactivator synthesis

Average to good yields were obtained for all alkynes mentioned (Table 2.4), except for 1-dimethylamino-2-propyne, which will be discussed in Section 2.1.2.3.

All of the clicked per-*O*-acetylated 2,3-difluoro sialic acid methyl esters in the library were purified through flash chromatography with an increasing gradient eluent (DCM to 5% MeOH in DCM). The acetyl protecting groups were removed using sodium methylate (1.3 eq.) in dry MeOH at $0°$C. After deacetylation, distilled water (0.1 mL) was added to initiate the saponification reaction. Purification was by flash chromatography and the eluent was varied according to the polarity of the moiety attached to the triazole ring, from EA/MeOH/H_2O (10/2/1) to EA/MeOH/H_2O (17/2/1). Further purification by reverse phase chromatography (Sep-Pak C18) was used to remove impurities and any possible silica gel.
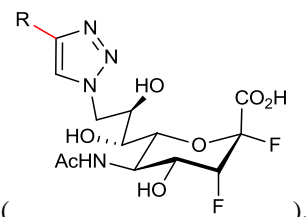
Table 2.4 First generation of synthesized inactivators, reactions were left overnight ( ).

Alkyne	Amount of alkyne	Product (R—)	Yield (after 2 steps)
m-Tolylacetylene	1.24 eq.	**2.18**	53%
5-Phenyl-1-pentyne	1.30 eq.	**2.19**	56%
Cyclopentylacetylene	1.44 eq.	**2.20**	76%
Cyclopropylacetylene	1.29 eq.	**2.21**	56%
5-Hexyne-1-ol	1.28 eq.	**2.22**	40%
Phenylacetylene	1.27 eq.	**2.23**	75%
2-Methyl-3-butyn-2-ol	1.27 eq.	**2.24**	54%
3,3-Dimethyl-1-butyne	1.30 eq.	**2.25**	60%

2.1.2.3   Synthesis of Additional Derivatives

Based on the kinetic analysis of the inactivation of TcTS by the compounds shown in Table 2.4, which will be discussed later with other kinetic data, more inactivators were synthesized in order to develop a better understanding of the binding pocket of TcTS. The synthesis of 3 compounds was attempted: compound **2.26**, which bears a negative charge at the optimal pH for TcTS; compound **2.29**, which bears a positive charge at optimal pH for TcTS (compound **2.28**, the intermediate in synthesis of **2.29**, was also tested as inactivator); and compound **2.27** with a six membered cycloalkyl moiety, for comparison with the phenyl acetylene and cyclopentyl acetylene derivatives (Table 2.5).
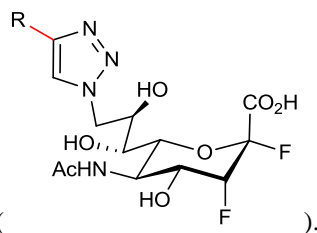
Table 2.5 Second generation of inactivators synthesized (   ).

Alkyne	Amount of alkyne	Reaction time	Product (R—)	Yield (after 2 steps)
Methyl propiolate	1.50 eq.	24 h	HOOC **2.26**	69%
Cyclohexylacetylene	1.30 eq.	Overnight	**2.27**	70%
tert-Butyl prop-2-ynylcarbamate	1.30 eq.	Overnight	**2.28**	81%

As mentioned in Section 2.1.2.2, the product obtained from 1-dimethylamino-2-propyne and 2.11a was unstable. The starting material was fully consumed after 5 h and purification by flash

chromatography was attempted. An eluent containing triethylamine (1%) was used to minimize binding between the positively charged amine product and negatively charged silica gel. Finally, methanol was used to wash the column to ensure that no products were left on the silica gel. However, no product was observed by TLC and MS in any fractions. On the assumption that the positive charge on the triazole compound allowed the compounds to decompose easily on silica gel, propargyl amine was protected using di-*tert*-butyl dicarbonate to form *tert*-butyl prop-2-ynylcarbamate, which was used in the click reaction. All of the purifications, deacetylation and saponification were conducted as mentioned in Section 2.1.2.2. A yield of 81% for compound **2.28** was obtained. Deprotection of the amine using neat trifluoroacetic acid (TFA) was carried out at room temperature and no side product was observed by TLC (Scheme 2.9). After evaporation *in vacuo*, the remaining residue was precipitated with methanol/diethyl ether and filtered. Since ^{19}F NMR showed the signal of TFA, lyophilisation was conducted. However, a ^{19}F NMR peak corresponding to TFA still remained due to the formation of salt between TFA and the free amine of **2.29**. Since previous kinetics studies had showed that TFA is not an inactivator of TcTS, the TFA•**2.29** salt was used in the inactivation study without further purification.
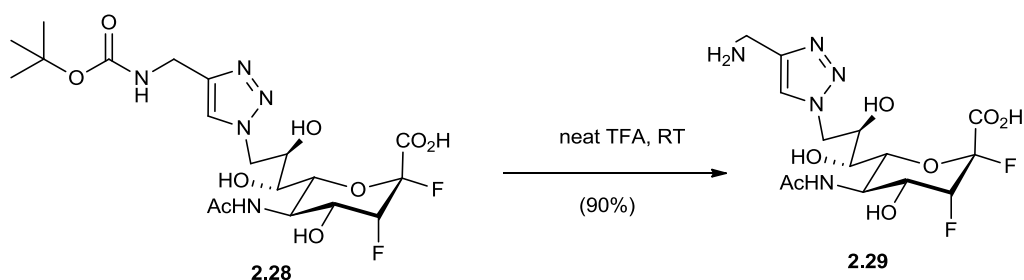
Scheme 2.9 Deprotection reaction of carbamate.

As shown in Table 2.3, propiolic acid did not react with **2.11a** under these conditions. The negative charge of the propiolic acid in the aqueous environment may have hindered the click reaction. Based on this assumption, methyl propiolate was used and a 69% yield was obtained, albeit requiring longer reaction times. During deacetylation and saponification, it was observed that one methoxyl group was more easily removed, even before the addition of water (it was not known which methoxyl group was removed first). However, the removal of the second methoxyl group

needed harsher conditions which were realized by the addition of 0.1 M sodium hydroxide (0.2 mL) and longer reaction time (overnight).

The reactions with cyclohexyl acetylene were similar to those of the other alkynes shown in Table 2.4. The results for all the above reactions are presented in Table 2.5. For all the compounds mentioned above in both Table 2.4 and Table 2.5, NMR pure compounds (TFA complex for **2.29**) were obtained. The copper absorbing resin, Cuprisorb, was used to remove any extra copper species. Since accurate weighing was difficult, concentrations of all inactivators in inactivation studies were determined by quantitative ^{19}FNMR (q^{19}FNMR) as described below.

2.1.2.4   Quantitative ^{19}F NMR (q^{19}F NMR)

Due to the limited amount of each synthesized inactivator, each compound (1-2 mg) was weighed and dissolved in distilled water as a stock solution. A q^{19}F NMR technique was used to measure an accurate concentration for each. In 2006, He *et al.* reported a method to use ^{19}F NMR in an attempt to quantitatively analyze the ratio of different fluorinated compounds in aqueous solutions.[98] They suggested that the integration ratio of each signal should be equal to the ratio of fluorine atom amounts in each compound once the parameter delay time (d1) was set to more than 5 times the longest relaxation time (T1) among those fluorine atoms in different chemical environments. In addition, they also measured the standard deviation of this method, which was less than 2.0% with a 1 mM detection limit for sixty-four scans on a Varian Mercury 400 NMR spectrometer. Based on this, we developed a method to apply q^{19}F NMR to measure the actual concentrations of stock solutions of inactivators. The idea was to make a 1:1 (concentration ratio) mixed sample with an internal standard stock solution of precisely known concentration and the desired compound stock solution based on weight. The concentration of the internal standard stock solution was accurate due to weighing of a large amount. If the d1 was set to greater than 5 times the T1 of both the fluorine from the internal standard and the fluorine from the desired compound, and the ^{19}F NMR was measured, as long as the signal to noise ratio was high enough, the desired compound stock solution concentration could be calculated. Comparing the structures and ^{19}F NMR data for compound **2.12** and various triazole derivatives (from **2.18** to **2.29**), the chemical shifts of F-2 and F-3 of different compounds were, not surprisingly very similar, since structural differences

occurred only at C-9, relatively far from F-2 and F-3. Thus, it was assumed that the T1 values of F-2 and F-3 were similar enough to be considered as constant in different compounds. UBC NMR technicians measured the T1 values for compound **2.12** as 0.5 s for both F-2 and F-3. They then set d1 as 5 s for compound **2.12** in the q^{19}F NMR measurement. As an internal standard, the following criteria should be satisfied: 1) the compound should be stable (no tautomerization or hydrolysis) and not toxic; 2) the compound must not react with the inactivators; 3) its water solubility should be good since the inactivators were dissolved in water; 4) the chemical shift difference between F of the internal standard and F in the inactivators should be between 2 ppm and 70 ppm, or it won't be quantitative; 5) the fluorine signal of the internal standard should not be split into a big multiplet; 6) if there is more than one fluorine atom in the standard, it is better to have fluorine atoms only in one chemical environment. In this particular case, it would be ideal if the chemical shift of the internal standard is between the chemical shifts of both F atoms in the inactivators. Based on the above criteria, difluoro acetic acid (DFA, T1=1.2 s) was chosen as the internal standard since its chemical shift is 3 ppm higher than F-2 and the inactivators are tolerant to slightly acidic conditions. A stock solution of compound **2.12** (11 mg) was used to test the effectiveness of this method, since its weight measurement was considered to be accurate. A sample of 1 mM **2.12** with internal standard (1 mM DFA) was measured in order to prove the validity of this q^{19}F NMR method and the corresponding parameters setting (acquisition time of 4 h and d1 of 8 s). As shown in Figure 2.6, the integration ratio of F-2: DFA: F-3 is 1.02:1.99:0.98 (theoretical value is 1:2:1). In q^{19}F NMR experiment, if the error is less than 5%, the result is considered as quantitative. Figure 2.6 clearly shows that proposed q^{19}F NMR method and the set conditions can be used to measure the actual concentrations of fluorinated inactivators synthesized.
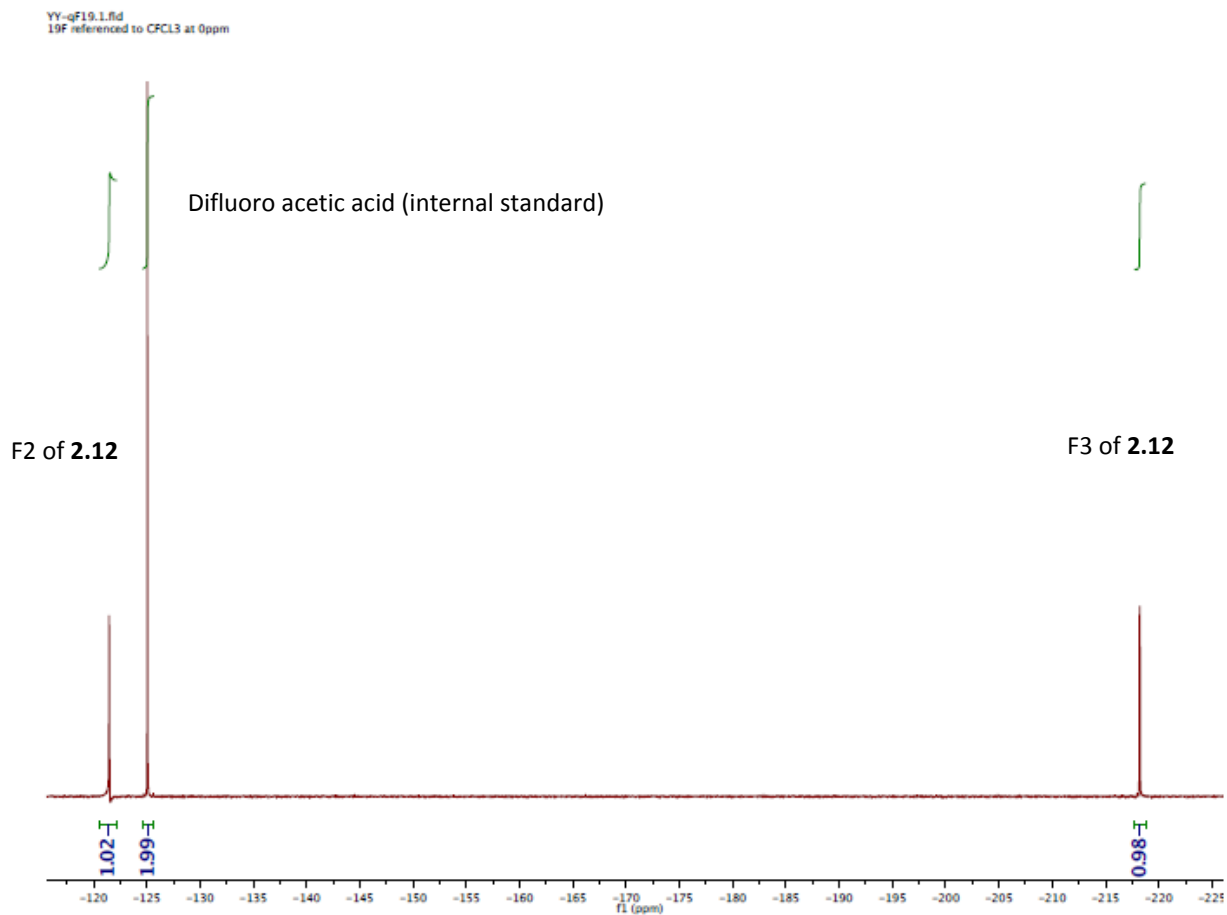
Figure 2.6 q^{19}F NMR of 1:1 difluoro acetic acid and compound **2.12**.

For the triazole inactivators, the same settings were used, except for a longer data acquisition time of 6 h in order to increase the signal to noise ratio. The results are presented in Table 2.6.

Table 2.6 Concentration correction results determined by q^{19}FNMR.

Compound	Predicted concentration (mM)	Actual concentration (mM)
2.18	1	0.82
2.19	1	0.83
2.20	1	0.94
2.21	1	0.87
2.22	1	0.72
2.23	1	0.83
2.24	1	0.86
2.25	1	0.77
2.26	1	0.61
2.27	1	0.65
2.28	1	0.68
2.29	1	0.60

2.2 Kinetic Analysis of TcTS

TcTS was expressed following previously published procedures.[99] After French press, purification of the enzyme was attempted through HisTrapFF chromatography. In an attempt to confirm the purity and activity of TcTS, an SDS-PAGE protein gel was run (an approximately 70 kD molecular weight was obtained, comparable to the molecular weight of wild-type TcTS, which is 70.6 kD) and the Michaelis-Menten parameters for hydrolysis were determined ($K_M = 0.07$ mM, $k_{cat} = 2.2$ s^{-1}).[16]

For all kinetics studies, assays were conducted at 25 °C using 5-acetamido-3,5-dideoxy-2-(4-trifluoromethylumbelliferyl)-D-*glycero*-α-D-*galacto*-non-2-ulopyranosonic acid (TFMU-SA) as substrate and the release of TFMU was monitored by UV-Vis spectrophotometry at 385 nm. Due to the fact that TcTS catalyzes both hydrolysis and transglycosylation, two sets of experiments were conducted in order to measure both hydrolysis and transglycosylation as described in Damager's paper.[16] The K_M and k_{cat} values for hydrolysis were determined at varied donor substrate concentrations. Kinetic parameters for transfer were obtained by varying both lactose and TFMU-SA concentrations (Figure 2.7). All kinetic data were in accordance with previous results.[16]
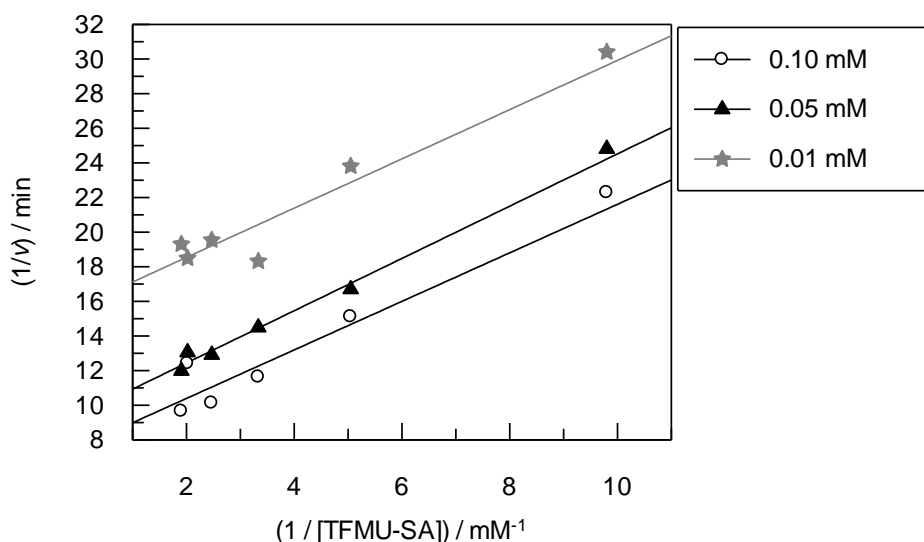
Figure 2.7 Lineweaver-Burk analysis for transglycosylation of TcTS in the presence of lactose. (Legend shows the concentrations of lactose)

Although the rough working pH optimum for TcTS has been measured previously,[100] a detailed pH profile to obtain pK_{a1} and pK_{a2} had never been established. I therefore measured such a profile to ensure that optimal conditions were employed. Prior to determining the pH profile, pH stability assay was conducted by incubating TcTS in different pH buffers and assaying aliquots of incubated enzyme mixture collected at different time intervals, with the concentration of TFMU-SA kept consistent. The results suggested that TcTS was stable between pH 4 and 9 (Figure 2.8). Therefore, we concluded that pH 4-9 was an appropriate range for the substrate depletion assay.
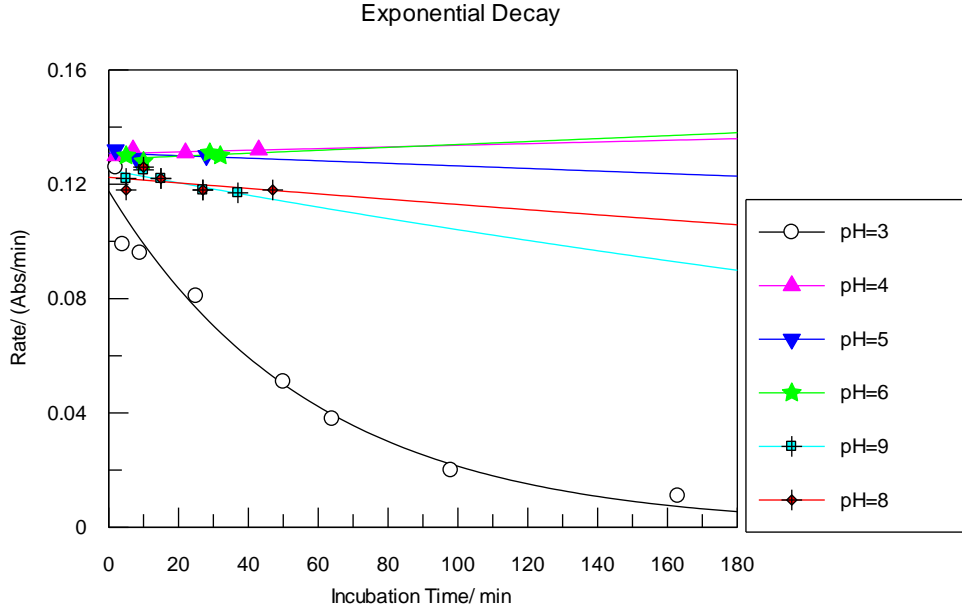
Figure 2.8 pH stability test for TcTS.

The substrate depletion assay was carried at low substrate concentration ([S] ≈ 0.1×K_M), as based on the Michaelis-Menten equation.

$$v = \frac{d[ES]}{dt} = -\frac{d[P]}{dt} = \frac{k_{cat}[E]_{total}[S]}{K_m + [S]}$$ **Equation 2.1**

Here, v stands for initial rate, k_{cat} is the turnover number, K_M is Michaelis constant, [S] stands for the substrate concentration and $[E]_{total}$ stands for the concentration of total enzyme.

When [S]<<K_M, the above equation becomes

$$v = \frac{k_{cat}[E]_{total}[S]}{K_m + [S]} \approx \frac{k_{cat}[E]_{total}[S]}{K_m} = \frac{k_{cat}}{K_m}[E]_{total}[S]$$ **Equation 2.2**

Also, since [S] is very small, $[E]_{total}$ can be considered as a constant, then

$$v = \frac{d[ES]}{dt} = -\frac{d[P]}{dt} = k_{app}[S] \ (k_{app} = \frac{k_{cat}}{K_m}[E]_{total})$$ **Equation 2.3**

The integration of Equation 2.3 yields the first order correlation between the product concentration increase and time. Hence, by fitting a reaction process curve to a first-order equation,

46

the value of k_{app} could be obtained. The $[E]_{total}$ was known, therefore, the values of k_{cat}/K_M at different pH values could be obtained.

The plot of k_{cat}/K_m *vs* pH is shown below (Figure 2.9a). Values of pK_{a1} and pK_{a2} for TcTS by fitting to a double bell equation using Grafit 5 is shown in the table (Figure 2.9b). These pK_a values correspond to essential ionizations in the free enzyme or free substrate.
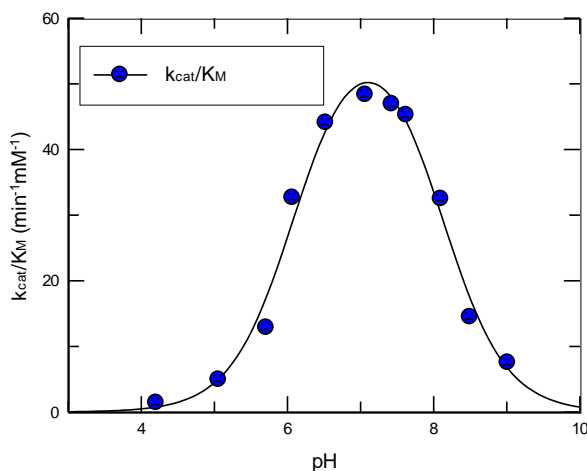
pK_{a1}	pK_{a2}
6.1±0.1	8.1±0.1

a   b

Figure 2.9 pH profile of TcTS: a. the double bell curve; b. pKa_1 and pKa_2. (fitted by Grafit 5)

Moreover, Figure 2.9 revealed that the optimum pH range for TcTS activity is between 6.9 and 7.5.

2.3   Inactivation Studies with TcTS

After the synthesis and characterization of the desired compounds, inactivation studies were performed at pH 7.48 in tris-HCl buffer (Tris-HCl buffer does not inhibit TcTS) with 20 mM NaCl at 25 °C. As briefly mentioned, the inactivation kinetics follows the scheme below (Scheme 2.10).

$$E + I \underset{k_{-1}}{\overset{k_1}{\rightleftharpoons}} EI \xrightarrow{k_i} E\text{-}I \xrightarrow{k_{reactivation}} E + P$$
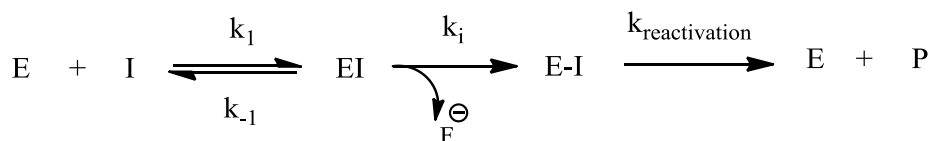
Scheme 2.10 General scheme for mechanism-based inactivators of retaining sialidases.

TcTS was pre-incubated at 25 °C with different concentrations of each inactivator (concentrations between 10 mM and 0.1 mM) and 1% BSA. Aliquots of the incubated TcTS mixtures were taken out at different time points and added to a 0.5 mM TFMU-SA solution, which had been pre-incubated at 25 °C for 10 min (Figure 2.10). Then, the rates were measured.

Substrate: TFMU-SA
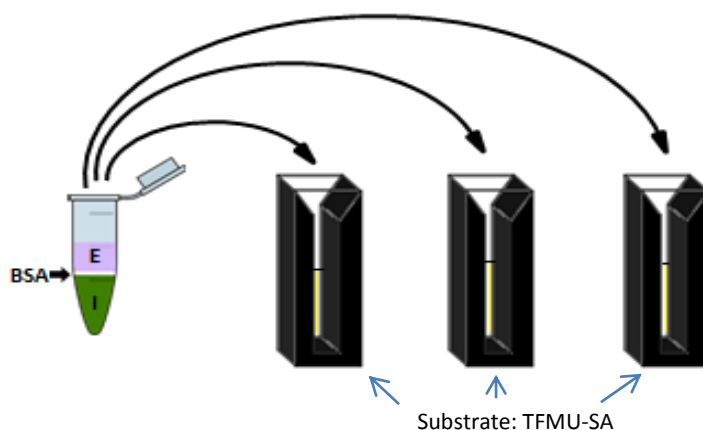
Figure 2.10 Inactivation assay demonstration picture

A control assay was conducted with no inactivator. The initial rates were measured by UV spectrometry, plotted as a function of time and fitted to an exponential decay with offset equation in Grafit 5 (Figure 2.11a shows the graph for **2.20** as a typical example). Time-dependent exponential decreases were observed and k_i and K_i values were determined from these by fitting to a Michaelis-Menten equation in Grafit 5 (a representative graph is shown in Figure 2.11b). Consequently, the k_i/K_i values were calculated for each compound and listed in Table 2.7 (The individual graphs are presented in the Appendix).

48
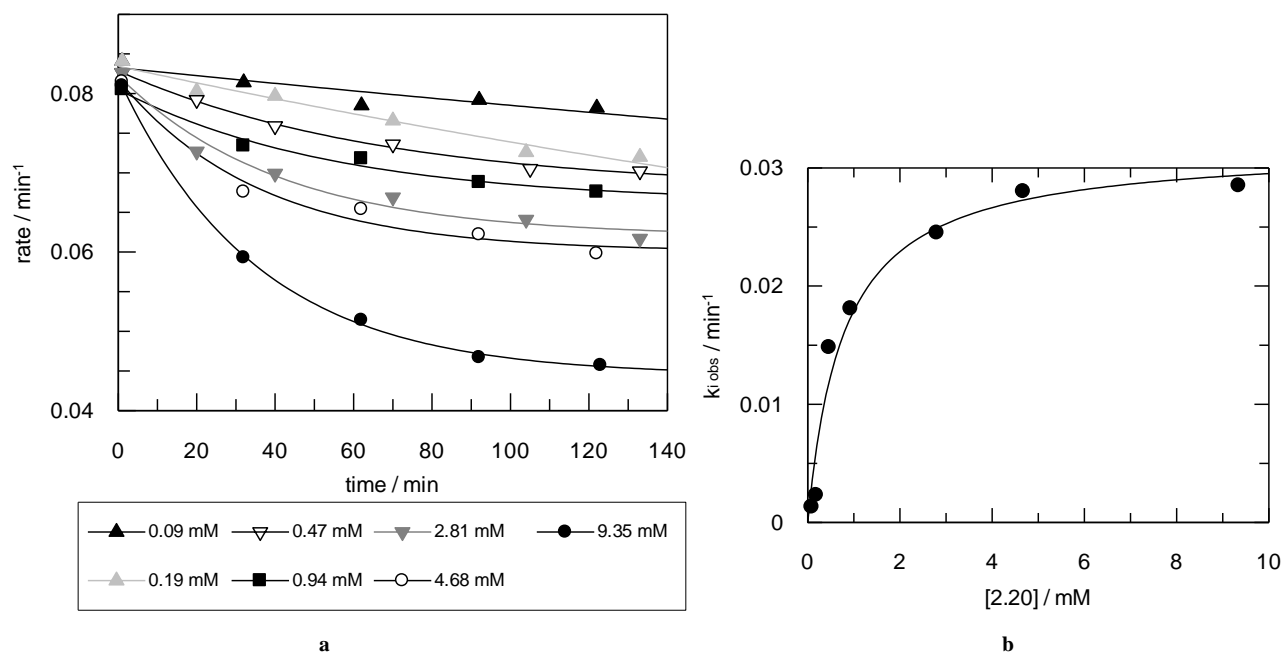
Figure 2.11 a. Time-dependent inactivation of TcTS by **2.20** (Legend shows the concentrations of **2.20**); b. replot of data for inactivation of TcTS by **2.20**.
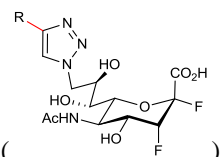
Table 2.7 Kinetic parameters for inactivation of TcTS by triazole derivatives of 3-fluorosialyl fluoride. ( ).

Compound	R—	k_i (min^{-1})	K_i (mM)	k_i/K_i ($\times 10^3$ min^{-1}mM^{-1})
2.18		0.036±0.008	7.54±2.48	4.8±1.9
2.19		0.017±0.002	4.81±1.20	3.5±0.9
2.20		0.032±0.002	0.78±0.21	41.0±11.3
2.21		0.017±0.001	1.59±0.24	10.7±1.7
2.22		0.011±0.003	3.65±2.06	3.0±1.9
2.23		0.016±0.001	2.31±0.48	6.9±1.5
2.24		0.057±0.010	5.86±1.75	9.7±3.4
2.25		0.025±0.004	2.01±0.79	12.4±5.3
2.26		0.030±0.002	1.46±0.32	20.5±4.7
2.27		0.021±0.003	1.04±0.47	20.2±9.6
2.28		0.020±0.003	1.96±0.73	10.2±4.1
2.29		0.044±0.007	8.43±1.86	5.2±1.4

From Buchini's paper in 2008, the second-order rate constant k_i/K_i of compound **2.12**
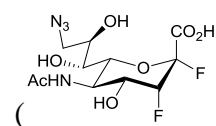
( ) was determined to be 1.4×10^{-2} $min^{-1}mM^{-1}$.[32] My measurement gave a value of 5.09×10^{-2} $min^{-1}mM^{-1}$. The difference may be due to the lower concentration of BSA (5% in Buchini's paper). I used 1% BSA instead of 5% BSA due to formation of bubbles during mixing. For high concentrations of compound **2.12** (Figure 2.12a), inactivation was too fast to be measured accurately. Thus, the second-order constant k_i/K_i was calculated from the slope of the plot shown in Figure 2.12b.
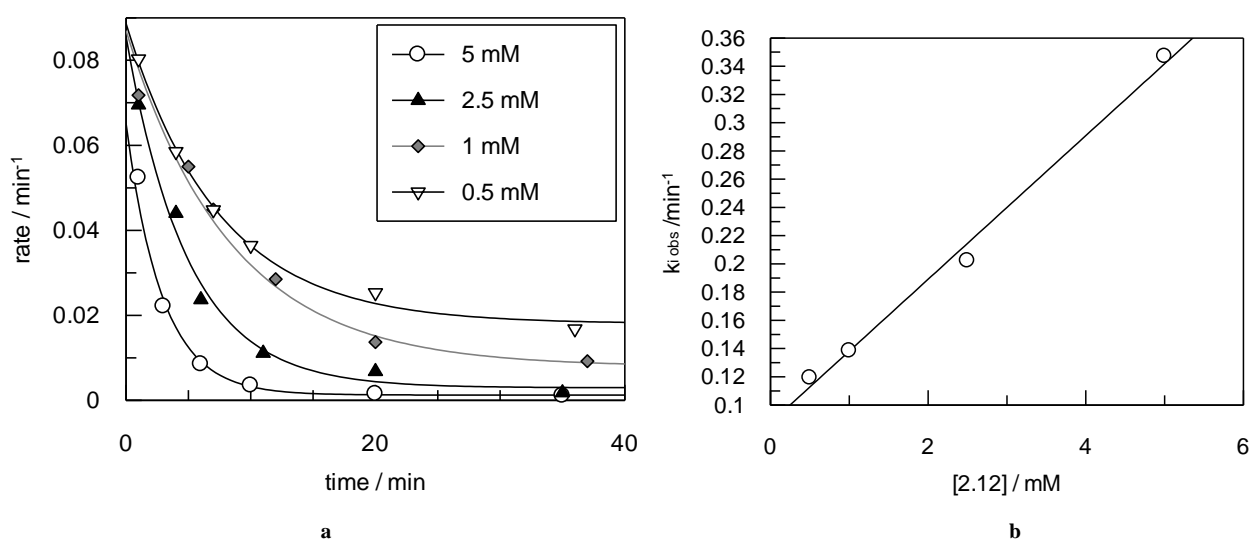
Figure 2.12 a. Time-dependent inactivation of TcTS by reference compound **2.12** (Legend shows the concentrations of **2.12**); b. replot of data for inactivation of TcTS by compound **2.12**.

In my studies, I used a constant BSA concentration, thus internal comparison of k_i/K_i values is reasonable. Table 2.7 shows that the k_i/K_i values for all the desired compounds varies, but over a small range with **2.20** being the best inactivator among all the triazole inactivators.
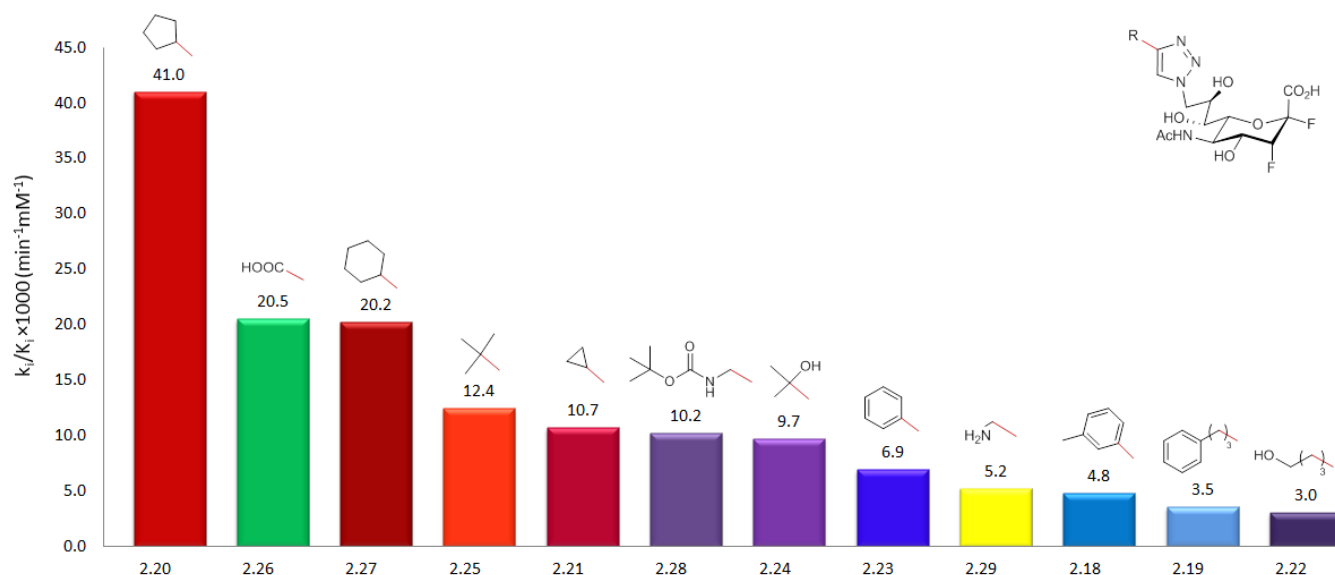
Chart 2.1 Inactivation data comparing specific constant-k_i/K_i (Red labels: aliphatic series; blue labels: aromatic series; purple labels: polar series; green label: acid; yellow label: base).

With the exception of **2.26** (R=carboxyl), non-polar derivatives were generally better inactivators than polar derivatives, which indicated that hydrophobic interaction might be the main source of affinity between TcTS and the R— group of inactivators in the library. Compound **2.20** (R=cyclopentyl) was the best among all the triazole derivatives and **2.27** (R=cyclohexyl) was tied for second best. In each series, increasing the size of the R— group generally decreased the k_i/K_i value, which indicated that the space of substrate binding pocket of TcTS is limited. For instance, **2.23** (R=phenyl) was 1.5-fold more efficient than **2.18** (R=*m*-tolyl). In addition, **2.23** (R=phenyl) was 3-fold less efficient than **2.27** (R=cyclohexyl), which illustrated that the planar six-member ring, was not as well accommodated by the enzyme active site. Interestingly, **2.21**(R=cyclopropyl), with a smaller three-member ring was also 4-fold less efficient than **2.20** (R=cyclopentyl), which suggested that either the three-member ring was too small to provide effective hydrophobic interactions between enzyme moieties and the side chain of triazole ring, or the flat ring structure of **2.21** (R= cyclopropyl) decreased affinity between enzyme and inactivator.

The compounds having the lowest values of k_i/K_i were **2.19** (R=3-phenyl-propyl) and **2.22** (R=4-hydroxylbutyl) and no particular correlation between the k_i/K_i values and the substituents on

52

2.19 (R=3-phenyl-propyl) and **2.22** (R=4-hydroxylbutyl) was observed, which indicated that compounds with a long side chain on the triazole ring may not be good choices as inactivators due to the limited size of the active site cleft.

Surprisingly, **2.28** (R=(*t*-butoxycarbonylamino)methyl) with a longer side chain on triazole ring (compared to **2.22** (R=4-hydroxylbutyl)) had a 3-fold higher k_i/K_i value, which might be related to the interactions between moieties within the active site and the carbamate functional group of the side chain. The negatively-charged **2.26** (R=carboxyl) and the positively-charged **2.29** (R=aminomethyl) were tested and were found to be less efficient than **2.20** (R=cyclopentyl). Additionally, **2.26** (R=carboxyl) was a much better inactivator than **2.29** (R=aminomethyl), which suggested that electrostatic interactions between the negative charge and binding pocket may contribute to the interaction. The behavior of **2.29** (R=aminomethyl) was consistent with Buchini's demonstration that **2.30** did not inactivate (Figure 2.13).[32] Possibly **2.29** (R=aminomethyl) has some inactivation activity due to the greater distance of the positive charge from C-9 and/or the triazole ring.

2.30
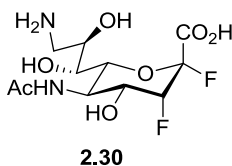
Figure 2.13 Compound **2.30** from Buchini's paper with no inactivation reactivity.

For all of the triazole inactivators in this synthetic library, the k_i/K_i values were lower than those for reference compound **2.12** and full inactivation was not observed. This indicated that the substituted triazole ring at C-9 may be too close to the sugar ring, reducing the affinity for TcTS. In order to gain some insight into the effects of the 9-triazole on reactivation rates, reactivation assays for the reference compound **2.12** ($k_i/K_i = 5.09 \times 10^{-2}$ min^{-1}mM^{-1}) and **2.20** ($k_i/K_i = 4.10 \times 10^{-2}$ min^{-1}mM^{-1}) with the highest efficiency in the small synthetic library were carried out.

2.4　　　　Reactivation Studies of Selected Inactivator with TcTS

　　　　Time-dependent reactivations for clicked inactivators **2.19**, **2.20**, **2.28** and reference compound **2.12** were conducted in the absence and presence of 100 mM lactose. After incubation with 1 mM **2.12** and 9.4 mM clicked inactivators for 2 h in order to reach 90% inactivation, respectively, the unbound inactivators were removed from TcTS by a micro-spin G-25 size exclusion column. The re-isolated TcTS was diluted into 200 µL buffer and incubated in the presence of 1% BSA at 25°C to start the reactivation incubation. Aliquots of incubated TcTS mixture were taken at different time points and added into a 0.5 mM TFMU-SA solution, which was pre-incubated at 25 °C for 10 minutes. Control assays were also conducted without inactivator addition: results showed that the enzyme activity kept constant through the reactivation process. No reactivation by hydrolysis was observed for either clicked inactivators or **2.12**. However, reactivations were observed in the presence of lactose. These reactivation results are presented in Figure 2.14 and fitted to a first-order with offset equation in Grafit 5 to yield the values shown in Table 2.8.
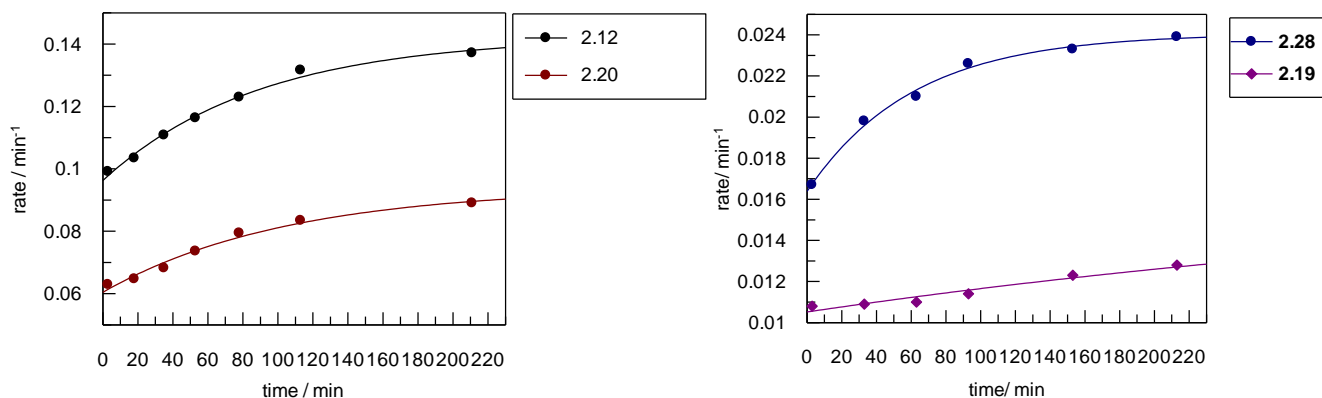
Figure 2.14 Reactivation data.

Table 2.8 Values of $k_{r\ obs}$ in the presence of 100 mM lactose and k_i/K_i obtained previously.

Compound	$k_{r\ obs}$ (min^{-1})	k_i/K_i ($\times 10^3$ min^{-1}mM^{-1})
2.12	0.0112±0.0017	50.9
2.19	0.0019±0.0004	3.5
2.20	0.0081±0.0023	40.9
2.28	0.0163±0.0023	10.2

The reactivation rate constants for clicked inactivators were not significantly lower than for **2.12**. Based on Buchini's observation, the dramatically decreased rate of reactivation (1000-fold) by an aryl attachment at C-9 was due to the reorientation of the substituted glycerol chain, which blocks part of the lactose acceptor binding pocket.[32] In addition, the distance between O-9 and Trp120 is only 3.04 Å(covalent intermediate).[15] The explanation for the slightly reduced reactivation rate might be that the triazole ring (at C-9) forms π-π stacking interactions with nearby Trp120, which restricts the orientation of the R— groups. Consequently, the substituent at C-9 fails to occupy the lactose acceptor binding pocket. Another possibility is that the amide structure is important in the reorientation of the C-9 substituent.

2.5   Conclusion

2,3-Difluoro-9-triazol sialic acid derivatives were proven to be neither efficient nor specific enough to serve as the drug candidate for Chagas disease. However, several insights into the substrate binding pocket of TcTS can be derived from the kinetic results. First, TcTS prefers non-polar substituents close to C-9, especially cyclic aliphatics rather than aromatic moieties. Second, the size of the active site cleft is limited and it can tolerate negative charges better than positive charges. Third, the triazole structure may fail to induce the glycerol side chain reorientation. This suggests that the amide structure may play an important role in the reorientation and consequent

55

affinity increase. One way to evaluate the function of the amide would be to synthesize and test the compounds shown below, which are ether-linked analogues of Buchini's amides.
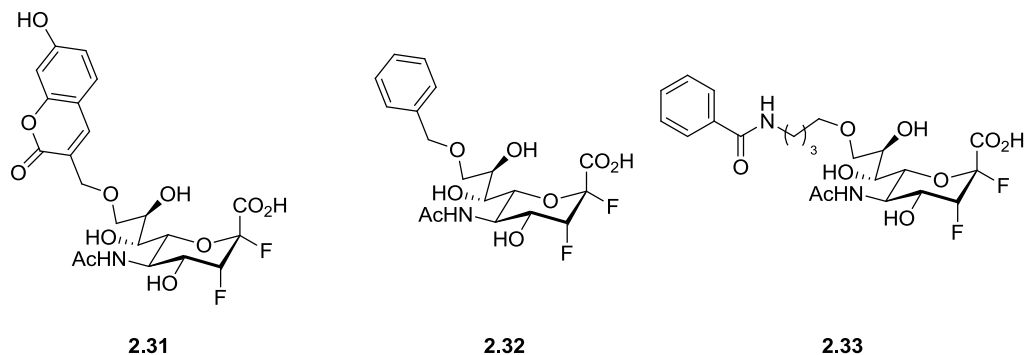
Figure 2.15 Compounds to synthesize in the future work.

In addition, a larger library of 9-amido-2,3-difluoro sialic acid derivatives could be built in order to identify better binding and specific inactivators based on the improved linker.

3 Materials and Methods

3.1   Synthesis

3.1.1 General Materials and Methods

All reagents were purchased from commercial suppliers and were used without further purification, unless otherwise stated. Moisture sensitive reactions were carried out with anhydrous/dry solvents under an atmosphere of argon. DMF was dried over 4 Å molecular sieves. DCM and pyridine were distilled from calcium hydride, while methanol was distilled from magnesium. All aqueous solutions were prepared with deionized water, purified with a Millipore Direct-Q^{TM} 5 Ultrapure Water system filter. All reactions were monitored by analytical techniques, such as TLC, ^{19}F NMR spectrometry and MS. TLC was performed on pre-coated aluminum plates of silica gel 60 F_{254} and detected by applying UV light and/or a solution of 10% ammonium molybdate in 2 M H_2SO_4 followed by charring. Column chromatography was carried out with silica gel (230 - 400 mesh) and/or Waters Sep-Pak C-18 RP cartridges and/or ion exchange (Dowex® 1×8 50-100 mesh formate form). All NMR spectra were acquired on a Bruker AV-300, Bruker AV-400 or Bruker AV-600 and chemical shifts were recorded in parts per million (ppm) as referenced from tetramethylsilane (TMS) for ^{1}H NMR, deuterated chloroform (CDCl$_3$) for ^{13}C NMR or TFA for ^{19}F NMR. Low and high resolution mass spectra were obtained on an electrospray ionization (ESI) equipped PE-Sciex API 300 triple quadrupole mass spectrometer.

3.1.2 Generous Gifts

Dr. Thomas Morley, a past member in Withers group synthesized trifluoromethyl umbelliferyl β-sialoside and anhydrous TBAF, and Dr. Hongming Chen synthesized BTTES, part of the methyl 5-acetamido-4,7,8-tri-*O*-acetyl-9-azido-3,5,9-trideoxy-3-fluoro-D-*erythro*-β-L-*manno*-non-2-ulopyranosonate fluoride was synthesized by Dr. Sabrina Buchini.

3.1.3 5-Acetamido-9-azido-3,5,9-trideoxy-3-fluoro-D-*erythro*-β-L-*manno*-non-2-ulopyranosonic Fluoride (2.12)

2-Acetamido-1,3,4-tri-*O*-acetyl-2,6-dideoxy-6-tosyl-D-mannopyranose(2.2)
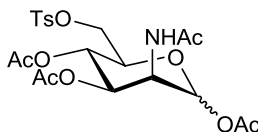
2.2

A solution of tosyl chloride (4.24 g, 22.24 mmol) in pyridine (20 mL) was added dropwise to a solution of *N*-acetyl-D-mannosamine (2 g, 9.04 mmol) in pyridine (28 mL) at 0°C over 1.5 h. The mixture was stirred for 5 h at this temperature, then Ac$_2$O (16 mL) was added and the solution was stirred overnight at room temperature. After evaporation *in vacuo*, the residue was diluted with EA (30 mL) and washed with 1 M HCl (2×10 mL) and then saturated NaHCO$_3$ (2×10 mL). The organic phase was dried over anhydrous MgSO$_4$, filtered and concentrated. The resulting residue was purified by flash column chromatography (EA/Hexanes=1/1 to 5/1) to afford product **2.2** (3.49 g, 77%) as a white solid. **^{1}H NMR** (CDCl$_3$, 300 MHz) δ 7.80 (d, *J*=8.2 Hz, 2 H, Ar), 7.37 (d, *J*=8.0 Hz, 2 H, Ar), 5.98 - 6.10 (m, 2 H, H-1, N*H*), 5.21 - 5.38 (m, 2 H, H-3, H-4), 4.64 (ddd, *J$_{2,NH}$*=9.3 Hz, *J$_{2,3}$*=3.8 Hz, *J$_{2,1}$*=1.7 Hz, 1 H, H-2), 4.31 (dd, *J$_{5,4}$*=11.2 Hz, *J$_{5,6}$*=1.4 Hz, 1 H, H-5), 4.00 - 4.15 (m, 2 H, H-6), 2.46 (s, 3 H, *Me*-Ar), 2.16 (s, 3 H, NH*Ac*), 2.07, 2.03, 2.01 (3 s, 9 H, *Ac*×3). ESI MS *m/z* 524.2 [M+Na]$^+$.

2-Acetamido-1,3,4-tri-*O*-acetyl-6-azido-2,6-dideoxy-D-mannopyranose (2.6)
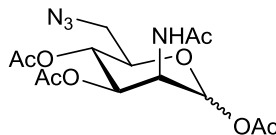
2.6

Sodium azide (0.76 g, 11.69 mmol) and 18-crown-6 (0.2 g, 0.76 mmol) were added to a solution of compound **2.2** (1 g, 2 mmol) in dry DMF (7 mL) under an argon atmosphere at 60 °C.

The mixture was stirred at this temperature for 22 h, then cooled to room temperature, EA (20 mL) added and the solution washed with H_2O (2×10 mL). The organic portion was dried over anhydrous $MgSO_4$, filtered and concentrated. The resulting residue was purified by flash column chromatography (EA/Hexanes=1/1 to 5/1) to yield compound **2.6** as a white foam (0.56 g, 75.7%). **^{1}H NMR** (CDCl$_3$, 300 MHz) δ 6.14 (d, $J_{NH,2}$=9.1 Hz, 1 H, N*H*), 6.03 (d, $J_{1,2}$=1.3 Hz, 1 H, H-1), 5.31 (dd, $J_{3,4}$=10.1 Hz, $J_{3,2}$=4.3 Hz, 1 H, H-3), 5.18 (t, $J_{4,5}$=$J_{4,3}$=10.1 Hz, 1 H, H-4), 4.62 (ddd, $J_{2,NH}$=9.1 Hz, $J_{2,3}$=4.3 Hz, $J_{2,1}$=1.3 Hz, 1 H, H-2), 3.96 (ddd, $J_{5,4}$=10.0 Hz, $J_{5,6b}$=4.9 Hz, $J_{5,6a}$=2.8 Hz, 1 H, H-5), 3.41 (dd, $J_{6a,6b}$=13.2 Hz, $J_{6a,5}$=2.8 Hz, 1 H, H-6a), 3.29 (dd, $J_{6b,6a}$=13.3 Hz, $J_{6b,5}$=5.0 Hz, 1 H, H-6b), 2.18 (s, 3 H, NH*Ac*), 2.03 (3 s, 9 H, 3×*Ac*). ESI MS *m/z* 395.2 [M+Na]$^+$.

2-Acetamido-6-azido-2,6-dideoxy-ᴅ-mannopyranose (2.7)

2.7

Compound **2.6** (1.3 g, 3.49 mmol) was dissolved in dry MeOH (50 mL) and a solution of sodium methylate (30 mL, 0.14 g Na (s) in 30 mL of dry MeOH, 6.09 mmol) was added dropwise at 0°C. The mixture was stirred at this temperature for 2 h. Amberlite IR120-H$^+$ was added until the pH of the solution was neutral. The resin was removed by suction filtration and the filtrate was concentrated. The resulting residue was purified by flash column chromatography (CH_2Cl_2/MeOH=12/1) to obtain compound **2.7** as a white powder (0.59 g, 69%). **^{1}H NMR** (D$_2$O, 300 MHz) the major anomer (α) δ 4.94 (s, 1 H, H-1), 4.14 (dd, $J_{2,3}$= 4.8 Hz, $J_{2,1}$= 1.3 Hz, 1 H, H-2), 3.89 (dd, $J_{3,4}$=9.6 Hz, $J_{3,2}$= 4.8 Hz, 1 H, H-3), 3.82 (ddd, $J_{5,4}$=12.6 Hz, $J_{5,6a}$=6.4 Hz, $J_{5,6b}$=2.7 Hz, 1 H, H-5), 3.35 - 3.46 (m, 3 H, H-4, H-6), 1.92 (s, 3 H, NH*Ac*). ESI MS *m/z* 269.3 [M+Na]$^+$.

Methyl 5-acetamido-2,4,7,8-tetra-*O*-acetyl-9-azido-3,5,9-trideoxy-3-fluoro-D-*erythro*-α-L-*manno*-non-2-ulopyranosonate (2.9a) and *gluco*-non-2-ulopyranosonate (2.9b)

2.9a axial
2.9b equatorial
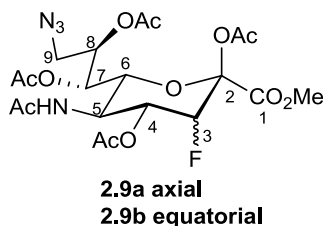
Sodium β-fluoropyruvate (0.16 g, 1.2 mmol) and Neu5Ac aldolase (40 mg, 23 U/mg) were added to a solution of compound **2.7** (1.039 g, 4.22 mmol) in H_2O (24 mL). After 10 h, ^{19}F NMR indicated the full conversion of the sodium β-fluoropyruvate. Another 0.3 eq. of sodium β-fluoropyruvate was added, then two other portions over a period of 3 days. After enzyme filtration (Amicon 30kDa) and ion exchange chromatography (Dowex®, 1×8, 50-100 mesh, formate form, H_2O to 1 M formic acid), the lyophilisation yielded a white foam (1.28 g, 86%). The white foam was dissolved in dry MeOH (120 mL) and TFA (1.2 mL) was added. The reaction mixture was stirred for 3 h at room temperature, the solvent evaporated *in vacuo* and the product used directly in the next reaction. To this residue, pyridine (10 mL) and Ac_2O (20 mL) were added. After stirring overnight under an argon atmosphere, TLC analysis indicated that the acetylation was finished and the mixture was concentrated *in vacuo*. The resulting residue was diluted with 30 mL EA, washed with 1M HCl (2×15 mL) and then saturated $NaHCO_3/H_2O$ (2×10 mL). The organic layer was dried over $MgSO_4$, filtered and evaporated. The product was purified by flash column chromatography (EA/hexanes=4/1 to 6/1) to afford compound **2.9a** as a white foam (0.65 g, 33.6%). **^{1}H NMR** (CDCl$_3$, 300 MHz) δ 5.52 (d, $J_{NH,5}$=10.6 Hz, 1 H, N*H*), 5.32 - 5.46 (m, 2 H, H-4, H-7), 4.80 - 5.05 (m, 2 H, H-3, H-8), 4.13 - 4.36 (m, 2 H, H-5, H-6), 3.77 - 4.01 (m, 4 H, O*Me*, H-9a), 3.43 (dd, $J_{9b,9a}$=13.5 Hz, $J_{9b,8}$= 7.7 Hz, 1 H, H-9b), 2.02 - 2.41 (4 s, 12 H, 4×*Ac*), 1.92 (s, 3 H, NH*Ac*). **^{19}F NMR** (CDCl$_3$, 282 MHz) δ -209.04 (dd, $J_{F3,3}$=47.7 Hz, $J_{F3,4}$=28.1 Hz, 1F, F-3 ax). ESI MS *m/z* 557.5 [M+Na]$^+$.

Methyl 5-acetamido-4,7,8-tri-*O*-acetyl-9-azido-3,5,9-trideoxy-3-fluoro-D-*erythro*-α-L-*manno*-2-non-2-ulopyranosonate (2.10)

2.10
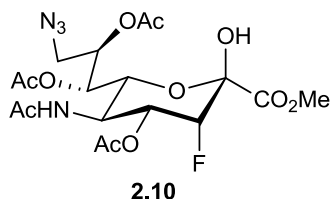
To a solution of **2.9a** (293 mg, 0.55 mmol) in dry DCM (2.5 mL) was added a solution of hydrazine acetate (0.23 g, 2.51 mmol) in dry MeOH (3.8 mL) at 0°C. After stirring for 6 h at this temperature under an argon atmosphere, the mixture was concentrated *in vacuo*. The remaining residue was dissolved in EA (10 mL), washed with H_2O (1×5 mL), 1 M HCl (1×5 mL) and then saturated $NaHCO_3$ (1×5 mL). The organic phase was dried over anhydrous $MgSO_4$, filtered and evaporated. The resulting residue was purified by flash column chromatography (EA/ hexanes=4/1 to 6/1) to afford compound **2.10** as a white solid (198 mg, 73%). **^{1}H NMR** (CDCl$_3$, 300 MHz) δ 5.99 (d, $J_{NH,5}$=9.3 Hz, 1 H, N*H*), 5.58 (ddd, $J_{4,F3}$=28.7 Hz, $J_{4,5}$=10.7 Hz, $J_{4,3}$=1.6 Hz, 1 H, H-4), 5.37 (t, $J_{7,8}$=$J_{7,6}$=2.7 Hz, 1 H, H-7), 5.16 (dt, $J_{8,9b}$=8.9 Hz, $J_{8,9a}$=2.4 Hz, $J_{8,7}$=2.7 Hz, 1 H, H-8), 4.98 (dd, $J_{3,F3}$=49.1 Hz, $J_{3,4}$=1.6 Hz, 1 H, H-3), 4.50 (d, $J_{6,5}$=10.1 Hz, 1 H, H-6), 4.10 - 4.30 (m, 1 H, H-5), 3.93 (dd, $J_{9a,9b}$=13.6 Hz, $J_{9a,8}$=2.4 Hz, 1 H, H-9a), 3.88 (s, 3 H, O*Me*), 3.44 (dd, $J_{9b,9a}$=13.6 Hz, $J_{9b,8}$=8.9 Hz, 1 H, H-9b), 2.11-2.19 (3 s, 9 H, 3× *Ac*), 1.95 (s, 3 H, NH*Ac*). **^{19}F NMR** (CDCl$_3$, 282 MHz) δ -207.08 (dd, $J_{F3,3}$=49.0 Hz, $J_{F3,4}$=28.7 Hz, 1 F, F-3 ax). ESI MS *m/z* 515.3 [M+Na]$^+$.

Methyl 5-acetamido-4,7,8-tri-*O*-acetyl-9-azido-3,5,9-trideoxy-3-fluoro-D-*erythro*-β-L-*manno*-non-2-ulopyranosonate fluoride (2.11a) and -α-L-*manno*-non-2-ulopyranosonate fluoride (2.11b)


2.11a equatorial
2.11b axial
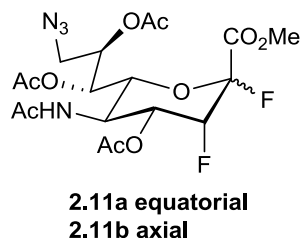
DAST (39.5 µL, 0.3 mmol) was added dropwise to a solution of **2.10** (100 mg, 0.2 mmol) in dry DCM (3.95 mL) at -35°C. The reaction mixture was stirred at this temperature for 15 mins and then 0.1 mL MeOH was added to quench the reaction. After evaporation, the residue was dissolved in DCM (5 mL), washed with H_2O (1×2.5 mL), 1M HCl (1×2.5 mL) and then saturated $NaHCO_3$ (1×2.5 mL). The organic layer was dried over $MgSO_4$ and evaporated. Purification by flash column chromatography (EA/hexanes=1/1 to 6/1) afforded compound **2.11a** as a white powder (50 mg, 50%). **^{1}H NMR** (CDCl$_3$, 300 MHz) δ 5.25 - 5.54 (m, 3 H, N*H*, H-7, H-8), 5.18 (dt, $J_{3,F3}$=50.5 Hz, $J_{3,4}$=$J_{3,F2}$= 2.3 Hz, 1 H, H-3), 4.31 (d, $J_{6,5}$=10.7 Hz, 1 H, H-6), 4.10 - 4.21 (m, 2 H, H-4, H-5), 3.92 (s, 3 H, O*Me*), 3.69 (dd, $J_{9a,9b}$=13.6 Hz, $J_{9a,8}$=2.5 Hz, 1 H, H-9a), 3.35 (dd, $J_{9b,9a}$=13.6 Hz, $J_{9b,8}$=5.7 Hz, 1 H, H-9b), 2.20, 2.15, 2.12 (3 s, 9 H, 3×*Ac*), 1.94 (s, 3 H, NH*Ac*). **^{19}F NMR** (CDCl$_3$, 282 MHz) δ -217.22 (ddd, $J_{F3,3}$=50.5, $J_{F3,4}$=25.8, $J_{F3,F2}$=11.5 Hz, 1 F, F-3 ax) -123.64 (d, $J_{F3,F2}$=11.5 Hz, 1 F, F-2 eq). ESI MS *m/z* 517.3 [M+Na]$^+$.

5-Acetamido-9-azido-3,5,9-trideoxy-3-fluoro-D-*erythro*-β-L-*manno*-non-2-ulopyranosonate fluoride (2.12)

2.12
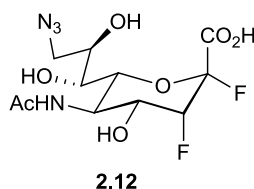
To a solution of **2.11a** (40 mg, 81 µmol) in dry MeOH (5 mL), sodium methylate solution (128 µL, 0.823 M) was added dropwise at 0°C. The mixture was stirred at this temperature for 1 h, then H_2O (0.1 mL) was added and stirred for 0.5 h at room temperature. The reaction mixture was neutralized (ion exchange resin Amberlite IR 120-H$^+$), filtered, and concentrated. The residue was purified by flash column chromatography (EA/MeOH/H$_2$O=10/2/1) and then by reverse phase (C18) column chromatography (eluting with H_2O to MeOH) to yield product **2.12** as a white powder (28 mg, 79%). **^{1}H NMR** (CD$_3$OD, 400 MHz) δ 5.20 (d, $J_{3,F3}$=52.5 Hz, 1 H, H-3), 4.10 - 4.21 (m, 2 H, H-4, H-5), 3.90 - 4.08 (m, 1 H, H-8), 3.64 (d, J=10.5 Hz, 1 H, H-6), 3.46 - 3.56 (m, 2 H, H-7, H-9a), 3.38 (dd, $J_{9b,9a}$=12.8 Hz, $J_{9b,8}$= 6.4 Hz, 1 H, H-9b), 2.04 (s, 3 H, NH*Ac*). **^{13}C NMR** (CD$_3$OD, 75 MHz) δ 174.27 (*Ac*), 169.14 (d, $J_{C1,F2}$=24.7 Hz, C-1), 107.01 (d, $J_{C2,F2}$=216.1 Hz, C-2), 89.47 (dd,

$J_{C3,F3} = 186.2$ Hz, $J_{C3,F2} = 18.4$ Hz, C-3), 73.13 (d, $J_{C6,F2} = 4.0$ Hz, C-6), 70.49 (C-4), 68.83 - 69.67 (C-7, C-8), 53.57 (C-9), 21.43 (NH*Ac*). **¹⁹F NMR** (CD₃OD, 282MHz): δ -221.94 (ddd, $J_{F3,3} = 52.5$ Hz, $J_{F3,4} = 28.1$ Hz, $J_{F3,F2} = 9.2$ Hz, 1 F, F-3 ax), -124.77 (d, $J_{F2,F3} = 9.2$ Hz, 1 F, F-2 eq). ESI MS *m/z* 377.2 [M+Na]⁺.

3.1.4 3-[1-(5-Acetamido-3,5,9-trideoxy-2,3-difluoro-D-*erythro*-β-L-*manno*-non-2-ulopyranosonate-9-yl)-1*H*-1,2,3-triazol-4-yl]-toluene (2.18)

2.18
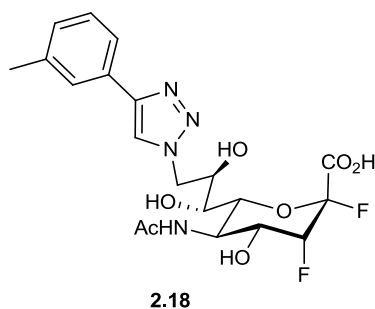
Compound **2.11a** (20 mg, 40.5 μmol) was dissolved in *t*BuOH:H₂O=1:1 mixture (0.8 mL), then BTTES (0.6 mg, 1.21 μmol), CuSO₄ (20 μL, 250 mM, 5 μmol), NaAsc (20 μL, 1 M, 20 μmol), and *m*-tolyl-acetylene (6.5 μL, 50.36 μmol) were added. The reaction mixture was stirred overnight at room temperature. DCM (12 mL) was added to the reaction mixture, which was washed with H₂O (2×2 mL). The organic layer was dried over MgSO₄, filtered and concentrated *in vacuo*. The resulting residue was purified by flash column chromatography (DCM:MeOH=1/0 to 19/1) afford a white powder (20 mg, 81%), which was dissolved in dry MeOH (3.6 mL) and sodium methylate (52 μL, 0.823 M) was added dropwise at 0°C. The mixture was stirred at this temperature for 1 h, then H₂O (0.1 mL) was added and stirred for 0.5 h at room temperature. The reaction mixture was neutralized (ion exchange resin Amberlite IR 120-H⁺), filtered and concentrated. The residue was purified by flash column chromatography (EA/MeOH/H₂O=10/2/1) and then by reverse phase (C18) column chromatography (H₂O to MeOH, gradient increase by 10%) to yield product **2.18** as a white

foam (10 mg, 65%). **^{1}H NMR** (CD$_3$OD, 400 MHz): δ 8.31 (s, 1 H, *triazole*), 7.65 (s, 1 H, *Ar*), 7.60 (d, *J*=7.8 Hz, 1 H, *Ar*), 7.31 (t, *J*=7.7 Hz, 1 H, *Ar*), 7.17 (d, *J*=7.5 Hz, 1 H, *Ar*), 5.20 (d, $J_{3,F3}$=52.5 Hz, 1 H, H-3), 4.83 (dd, $J_{9a,9b}$=14.2 Hz, $J_{9a,8}$=2.1 Hz, 1 H, H-9a), 4.55 (dd, $J_{9b,9a}$=14.3 Hz, $J_{9b,8}$=7.8 Hz, 1 H, H-9b), 4.22 - 4.33 (m, 1 H, H-8), 4.13 - 4.22 (m, 1 H, H-5), 4.01 (dd, $J_{4,F3}$=27.4 Hz, $J_{4,5}$=10.7 Hz, 1 H, H-4), 3.66 (d, *J*=10.5 Hz, 1 H, H-6), 3.43 (d, *J*=9.0 Hz, 1 H, H-7), 2.40 (s, 3 H, *Me*-Ar), 2.00 (s, 3 H, NH*Ac*). **^{13}C NMR** (CD$_3$OD, 100 MHz): δ 174.2 (*Ac*), 147.5 (C=C), 138.5, 130.5, 128.67, 128.60, 126.0, 122.6 (*Ar*), 122.1 (C=C), 88.9 (dd, $J_{C3,F3}$=184.8 Hz, $J_{C3,F2}$=18.4 Hz, C-3), 73.1 (d, $J_{C6,F2}$=3.8 Hz, C-6), 69.8 (C-8), 69.6 (C-7), 69.3 (dd, $J_{C4,F3}$=18.4 Hz, $J_{C4,F2}$=6.9 Hz, C-4), 53.3 (C-9), 21.6 (s, NH*Ac*), 19.9 (s, *Me*). **^{19}F NMR** (CD$_3$OD, 282 MHz): δ -221.02 (ddd, $J_{F3,3}$=52.5 Hz, $J_{F3,4}$=27.5 Hz, $J_{F3,F2}$=9.8 Hz, 1 F, F-3 ax), -124.63 (d, $J_{F2,F3}$=9.8 Hz, 1 F, F-2 eq). ESI MS *m/z* 469.2 [M-H]$^-$.
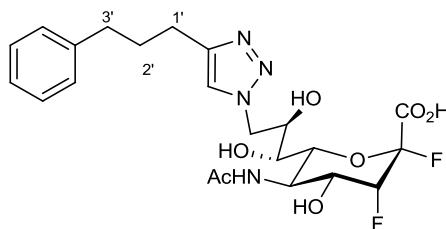
3.1.5　1-[1-(5-Acetamido-3,5,9-trideoxy-2,3-difluoro-D-*erythro*-β-L-*manno*-non-2-ulopyranosonate-9-yl)-1*H*-1,2,3-triazol-4-yl]-3-phenyl-propane (2.19)

2.19

　　Compound **2.11a** (27.6 mg, 55.8 µmol) was dissolved in ^{t}BuOH:H$_2$O=1:1 mixture (1.1 mL), and BTTES (0.74 mg, 1.49 µmol), CuSO$_4$ (25 µL, 250 mM, 6.25 µmol), NaAsc (25 µL, 1 M, 25 µmol), and 5-phenyl-1-pentyne (11 µL, 72.47 µmol) were added. The reaction mixture was stirred overnight at room temperature. DCM (12 mL) was added to the reaction mixture, which was washed with H$_2$O (2×2 mL). The organic layer was dried over MgSO$_4$, filtered and concentrated *in vacuo*. The resulting residue was purified by flash column chromatography (DCM/MeOH=1/0 to

19/1) to afford the product as a white powder (28 mg, 78.5%). The product was dissolved in dry MeOH (4.8 mL) and sodium methylate (70 μL, 0.823 M) was added dropwise at 0 °C. The mixture was stirred at this temperature for 1 h, then H_2O (0.1 mL) was added and stirred for 0.5 h at room temperature. The reaction mixture was neutralized (ion exchange resin Amberlite IR 120-H$^+$), filtered and concentrated. The residue was purified by flash column chromatography (EA/MeOH/H_2O=17/3/1) and then by reverse phase (C18) column chromatography (H_2O to MeOH, gradient increase by 10%) to yield product **2.19** (15.5 mg, 71.2%). **^{1}H NMR** (CD$_3$OD, 400 MHz): δ 7.79 (s, 1 H, *triazole*), 6.93 - 7.43 (m, 5 H, *Ar*), 5.21 (d, $J_{3,F3}$=52.8 Hz, 1 H, H-3), 4.76 (dd, $J_{9a,9b}$=14.0 Hz, $J_{9a,8}$=2.0 Hz, 1 H, H-9a), 4.45 (dd, $J_{9b,9a}$=14.0 Hz, $J_{9b,8}$=7.9 Hz, 1 H, H-9b), 4.13 - 4.25 (m, 2 H, H-5, H-8), 4.02 (dd, $J_{4,F3}$=28.0 Hz, $J_{4,5}$=10.5 Hz, 1 H, H-4), 3.64 (d, *J*=10.4 Hz, 1 H, H-6), 3.39 (d, *J*=9.4 Hz, 1 H, H-7), 2.71 (dt, *J*=15.0, 7.6 Hz, 4 H, H-2`, H-3`), 1.95 - 2.08 (m, 5 H, NH*Ac*, H-1`). **^{13}C NMR** (CD$_3$OD, 100 MHz): δ 173.9 (*Ac*), 147.3 (C=C), 141.9, 128.2, 128.1, 125.6 (*Ar*), 122.9 (C=C), 89.2 (dd, $J_{C3,F3}$=185.6 Hz, $J_{C3,F2}$=18.4 Hz, C-3), 73.0 (d, $J_{C6,F2}$=4.6 Hz, C-6), 69.8 (C-8), 69.7 (C-7), 69.3 (dd, $J_{C4,F3}$=18.4 Hz, $J_{C4,F2}$=5.4 Hz, C-4), 52.6 (C-9), 35.0, 31.1, 24.5 (C-1`, C-2`, C-3`), 21.3 (s, NH*Ac*). **^{19}F NMR** (CD$_3$OD, 282 MHz): δ -220.94 (ddd, $J_{F3,3}$=52.8 Hz, $J_{F3,4}$=28.1 Hz, $J_{F3,F2}$=9.2 Hz, 1 F, F-3 ax), -124.63 (d, $J_{F2,F3}$=9.2 Hz, 1 F, F-2 eq). ESI MS *m/z* 497.6 [M-H]$^-$.

3.1.6   [1-(5-Acetamido-3,5,9-trideoxy-2,3-difluoro-D-*erythro*-β-L-*manno*-non-2-ulopyranosonate-9-yl)-1*H*-1,2,3-triazol-4-yl]-cyclopentane (2.20)
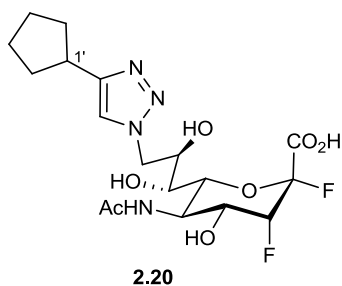

2.20

Compound **2.11a** (24.8 mg, 50.2 μmol) was dissolved in ^{t}BuOH: H_2O=1:1 mixture (1.1 mL), and BTTES (0.82 mg, 1.65 μmol), $CuSO_4$ (28 μL, 250 mM, 7 μmol), NaAsc (28 μL, 1 M, 28 μmol), cyclopentyl acetylene (8.4 μL, 72.4 μmol) were added. The reaction mixture was stirred overnight at room temperature. DCM (12 mL) was added to the reaction mixture, which was washed with H_2O (2×2 mL). The organic layer was dried over $MgSO_4$, filtered and concentrated *in vacuo*. The resulting residue wa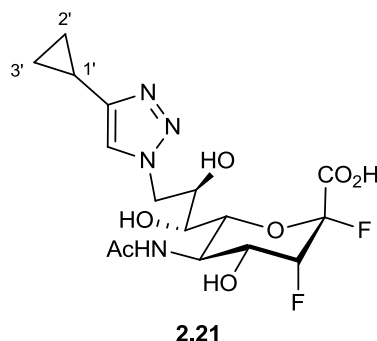s purified by flash column chromatography (DCM/MeOH=1/0 to 19/1) to afford the product as a white powder (27 mg, 91.4%). The product was dissolved in dry MeOH (5 mL) and sodium methylate (73 μL, 0.823 M) was added dropwise at 0 °C. The mixture was stirred at this temperature for 1 h, then H_2O (0.1 mL) was added and stirred for 0.5 h at room temperature. The reaction mixture was neutralized (ion exchange resin Amberlite IR 120-H^+), filtered and concentrated. The residue was purified by flash column chromatography (EA/MeOH/H_2O=13/2/1) and then by reverse phase (C18) column chromatography (H_2O to MeOH, gradient increase by 10%) to yield product **2.20** (17 mg, 82.7%) **^{1}H NMR** (CD$_3$OD, 400 MHz): δ 7.77 (s, 1 H, *triazole*), 5.19 (d, $J_{3,F3}$=52.5 Hz, 1 H, H-3), 4.74 (dd, $J_{9a,9b}$=14.0 Hz, $J_{9a,8}$=2.2 Hz, 1 H, H-9a), 4.43 (dd, $J_{9b,9a}$=14.0 Hz, $J_{9b,8}$=7.9 Hz, 1 H, H-9b), 4.12 - 4.26 (m, 2 H, H-5, H-8), 3.99 (dd, $J_{4,F3}$=27.4 Hz, $J_{4,5}$=10.2 Hz, 1 H, H-4), 3.61 (d, J=10.4 Hz, 1 H, H-6), 3.38 (d, J=9.1 Hz, 1 H, H-7), 3.17 (s, 1 H, H-1`), 2.10 (d, J=4.1 Hz, 2 H, *cyclopentyl*), 2.01 (s, 3 H, NH*Ac*), 1.59 - 1.91 (m, 6 H, *cyclopentyl*). **^{13}C NMR** (CD$_3$OD, 75 MHz): δ 174.1 (*Ac*), 168.9 (C-1), 151.9 (C=C), 122.0 (C=C), 89.4 (dd, $J_{C3,F3}$=185.6 Hz, $J_{C3,F2}$=19.5 Hz, C-3), 73.0 (d, $J_{C6,F2}$=4.6 Hz, C-6), 69.8 (C-8), 69.7 (C-7), 69.3 (dd, $J_{C4,F3}$=17.8 Hz, $J_{C4,F2}$=5.2 Hz, C-4), 53.0 (C-9), 36.6, 33.0, 24.8 (*cyclopentyl*), 21.4 (s, NH*Ac*). **^{13}C NMR** (CD$_3$OD, 151 MHz) δ 49.99 Hz (C-5), 108.06 Hz (C-2) by HMBC. **^{19}F NMR** (CD$_3$OD, 282MHz): δ -220.89 (ddd, $J_{F3,3}$=52.5 Hz, $J_{F3,4}$=27.5 Hz, $J_{F3,F2}$=10.3 Hz, 1 F, F-3 ax), -124.89 (d, $J_{F2,F3}$=10.3 Hz, 1 F, F-2 eq). ESI MS *m/z* 448.7 [M-H]$^-$.

3.1.7 [1-(5-Acetamido-3,5,9-trideoxy-2,3-difluoro-D-*erythro*-β-L-*manno*-non-2-ulopyranosonate-9-yl)-1*H*-1,2,3-triazol-4-yl]-cyclopropane (2.21)

2.21

Compound **2.11a** (29.4 mg, 59.5 μmol) was dissolved in ^{t}BuOH: H_2O=1:1 mixture (1.1 mL), and BTTES (0.88 mg, 1.77 μmol), $CuSO_4$ (30 μL, 250 mM, 7.5 μmol), NaAsc (30 μL, 1 M, 30 μmol), cyclopropyl acetylene (6.5 μL, 76.8 μmol) were added. The reaction mixture was stirred overnight at room temperature. DCM (12 mL) was added to the reaction mixture, which was washed with H_2O (2×2 mL). The organic layer was dried over $MgSO_4$, filtered and concentrated *in vacuo*. The resulting residue was purified by flash column chromatography (DCM/MeOH=1/0 to 19/1) to afford the product as a white powder (25 mg, 75%). The product was dissolved in dry MeOH (5 mL) and sodium methylate (71 μL, 0.823 M) was added dropwise at 0 °C. The mixture was stirred at this temperature for 1 h, then H_2O (0.1 mL) was added and stirred for 0.5 h at room temperature. The reaction mixture was neutralized by addition of AcOH (8.3 μL) and concentrated. The residue was purified by flash column chromatography (EA/MeOH/H_2O=13/2/1) and then by reverse phase (C18) column chromatography (H_2O to MeOH, gradient increase by 10%) to yield product **2.21** (14 mg, 74.7%) **^{1}H NMR** (CD$_3$OD, 400 MHz): δ 7.71 (s, 1 H, *triazole*), 5.19 (d, $J_{3,F3}$=52.7 Hz, 1 H, H-3), 4.72 (dd, $J_{9a,9b}$=13.9 Hz, $J_{9a,8}$=2.3 Hz, 1 H, H-9a), 4.40 (dd, $J_{9b,9a}$=13.9 Hz, $J_{9b,8}$=7.9 Hz, 1 H, H-9b), 4.11 - 4.26 (m, 2 H, H-5, H-8), 4.01 (dd, $J_{4,F3}$=28.0 Hz, $J_{4,5}$=11.9 Hz, 1 H, H-4), 3.62 (d, J=9.9 Hz, 1 H, H-6), 3.37 (d, J=6.9 Hz, 1 H, H-7), 1.88 - 2.15 (m, 4 H, NH*Ac*, H-1`), 0.92 - 1.03 (m, 2 H, H-2`), 0.68 - 0.85 (m, 2 H, H-3`). **^{13}C NMR** (CD$_3$OD, 100 MHz): δ

174.2 (*Ac*), 149.9 (C=C), 121.9 (C=C), 89.4 (dd, $J_{C3,F3}$=185.6 Hz, $J_{C3,F2}$=19.9 Hz, C-3), 73.1 (d, $J_{C6,F2}$=3.8 Hz, C-6), 69.8 (C-8), 69.7 (C-7), 69.4 (dd, $J_{C4,F3}$=19.2 Hz, $J_{C4,F2}$=6.9 Hz, C-4), 52.5 (C-9), 48.6 (C-5) 21.3 (s, NH*Ac*), 6.8, 6.0 (*cyclopropyl*). **^{19}F NMR** (CD$_3$OD, 282 MHz): δ -220.98 (ddd, $J_{F3,3}$=52.8 Hz, $J_{F3,4}$=28.1 Hz, $J_{F3,F2}$=10.3 Hz, 1 F, F-3 ax), -124.76 (d, $J_{F2,F3}$=10.3 Hz, 1 F, F-2 eq). ESI MS *m/z* 420.2 [M-H]$^-$.
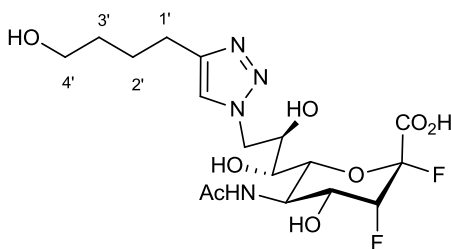
3.1.8   4-[1-(5-Acetamido-3,5,9-trideoxy-2,3-difluoro-D-*erythro*-β-L-*manno*-non-2-ulopyranosonate-9-yl)-1*H*-1,2,3-triazol-4-yl]-butan-1-ol (2.22)

2.22

Compound **2.11a** (27.65 mg, 55.9 µmol) was dissolved in *t*BuOH: H$_2$O=1:1 mixture (1.1 mL), and BTTES (0.82 mg, 1.65 µmol), CuSO$_4$ (28 µL, 250 mM, 7 µmol), NaAsc (28 µL, 1 M, 28 µmol), 5-hexyne-1-ol (7.9 µL, 71.7 µmol) were added. The reaction mixture was stirred overnight at room temperature. DCM (12 mL) was added to the reaction mixture, which was washed with H$_2$O (2×2 mL). The organic layer was dried over MgSO$_4$, filtered and concentrated *in vacuo*. The resulting residue was purified by flash column chromatography (DCM/MeOH=1/0 to 19/1) to afford the product as a white powder (24 mg, 72.3%). The product was dissolved in dry MeOH (5 mL) and sodium methylate (64.5 µL, 0.823 M) was added dropwise at 0 °C. The mixture was stirred at this temperature for 1 h, then H$_2$O (0.1 mL) was added and stirred for 0.5 h at room temperature. The reaction mixture was neutralized by addition of AcOH (7.5 µL) and concentrated. The residue was purified by flash column chromatography (EA/MeOH/H$_2$O=10/2/1) and then by

reverse phase (C18) column chromatography (H$_2$O to MeOH, gradient increase by 10%) to yield product **2.22** (10 mg, 54.6%). **^{1}H NMR** (CD$_3$OD, 400 MHz): δ 7.81 (s, 1 H, *triazole*), 5.20 (d, $J_{3,F3}$=52.2 Hz, 1 H, H-3), 4.75 (dd, $J_{9a,9b}$=13.6 Hz, $J_{9a,8}$=1.7 Hz, 1 H, H-9a), 4.42 (dd, $J_{9b,9a}$=13.7 Hz, $J_{9b,8}$=7.9 Hz, 1 H, H-9b), 4.11 - 4.25 (m, 2 H, H-5, H-8), 3.99 (dd, $J_{4,F3}$=28.1, $J_{4,5}$=10.8 Hz, 1 H, H-4), 3.55 - 3.68 (m, 3 H, H-6, H-4'), 3.38 (d, J=9.1 Hz, 1 H, H-7), 2.75 (t, J=7.5 Hz, 2 H, H-1'), 2.02 (s, 3 H, NH*Ac*), 1.70 - 1.82 (m, 2 H, H-3'), 1.54 - 1.69 (m, 2 H, H-2'). **^{13}C NMR** (CD$_3$OD, 100 MHz): δ 174.9 (*Ac*), 147.5 (C=C), 121.5 (C=C), 89.5 (dd, $J_{C3,F3}$=184.8 Hz, $J_{C3,F2}$=18.4 Hz, C-3), 73.0 (d, $J_{C6,F2}$=4.6 Hz, C-6), 69.8 (C-8), 69.7 (C-7), 69.4 (dd, $J_{C4,F3}$=19.2 Hz, $J_{C4,F2}$=6.1 Hz, C-4), 61.7 (C-4'), 52.5 (C-9), 31.8 (C-1'), 25.6, 24.7 (C-2', C-3'), 21.3 (s, NH*Ac*). **^{19}F NMR** (CD$_3$OD, 282 MHz) δ -220.89 (ddd, $J_{F3,3}$=52.2 Hz, $J_{F3,4}$= 28.1 Hz, $J_{F3,F2}$=9.8 Hz, 1 F, F-3 ax), -124.83 (d, $J_{F2,F3}$=9.8 Hz, 1 F, F-2 eq). ESI MS *m/z* 452.2 [M-H]$^-$.

3.1.9 [1-(5-Acetamido-3,5,9-trideoxy-2,3-difluoro-D-*erythro*-β-L-*manno*-non-2-ulopyranosonate-9-yl)-1*H*-1,2,3-triazol-4-yl]-benzene (2.23)
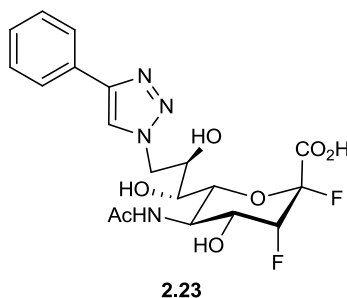

2.23

Compound **2.11a** (27.53 mg, 55.7 µmol) was dissolved in ^{t}BuOH: H$_2$O=1:1 mixture (1.1 mL), and BTTES (0.82 mg, 1.65 µmol), CuSO$_4$ (28 µL, 250 mM, 7 µmol), NaAsc (28 µL, 1 M, 28 µmol), phenyl acetylene (7.8 µL, 71.0 µmol) were added. The reaction mixture was stirred overnight at room temperature. DCM (12 mL) was added to the reaction mixture, which was washed with H$_2$O (2×2 mL). The organic layer was dried over MgSO$_4$, filtered and concentrated *in vacuo*. The resulting residue could be purified by flash column chromatography (DCM/MeOH=1/0 to 19/1) to afford the product as a white powder (33 mg, 99.3 %). The product was dissolved in dry

MeOH (5 mL) and sodium methylate (88 μL, 0.823 M) was added dropwise at 0 °C. The mixture was stirred at this temperature for 1 h, then H_2O (0.1 mL) was added and stirred for 0.5 h at room temperature. The reaction mixture was neutralized by addition of AcOH (10.3 μL) and concentrated. The residue was purified by flash column chromatography (EA/MeOH/H_2O=10/2/1) and then by reverse phase (C18) column chromatography (H_2O to MeOH, gradient increase by 10%) to yield product **2.23** (19 mg, 75.2 %). **^{1}H NMR** (CD$_3$OD, 400 MHz): δ 8.34 (s, 1 H, *triazole*), 7.82 (d, *J*=7.5 Hz, 2 H, *Ar*), 7.38 - 7.49 (m, 2 H, *Ar*), 7.35 (d, *J*=7.3 Hz, 1 H, *Ar*), 5.20 (d, $J_{3,F3}$=52.8 Hz, 1 H, H-3), 4.82 (dd, $J_{9a,9b}$=14.3 Hz, $J_{9a,8}$=1.7 Hz, 1 H, H-9a), 4.55 (dd, $J_{9b,9a}$=14.3 Hz, $J_{9b,8}$=6.7 Hz, 1 H, H-9b), 4.13 - 4.37 (m, 2 H, H-5, H-8) 3.99 (dd, $J_{4,F3}$=28.0 Hz, $J_{4,5}$=11.6 Hz, 1 H, H-4), 3.61 (d, *J*=10.7 Hz, 1 H, H-6), 3.42 (d, *J*=9.3 Hz, 1 H, H-7), 1.99 (s, 3 H, NH*Ac*). **^{13}C NMR** (CD$_3$OD, 100 MHz): δ 174.2 (*Ac*), 168.7 (d, $J_{C1,F2}$=26.1 Hz, C-1), 147.3 (C=C), 130.6, 128.7, 127.9, 125.4 (*Ar*), 122.2 (C=C), 89.4 (dd, $J_{C3,F3}$=185.6 Hz, $J_{C3,F2}$=18.4 Hz, C-3), 73.1 (d, $J_{C6,F2}$=4.6 Hz, C-6), 69.8 (C-8), 69.7 (C-7), 69.6 (dd, $J_{C4,F3}$=19.2 Hz, $J_{C4,F2}$=6.1 Hz, C-4), 53.2 (C-9), 21.3 (s, NH*Ac*). **^{19}F NMR** (CD$_3$OD, 282 MHz): δ -220.85 (ddd, $J_{F3,3}$=52.8 Hz, $J_{F3,4}$=28.1 Hz, $J_{F3,F2}$=9.2 Hz, 1 F, F-3 ax), -124.78 (d, $J_{F2,F3}$=9.2 Hz, 1 F, F-2 eq). ESI MS *m/z* 455.3 [M-H]⁻.
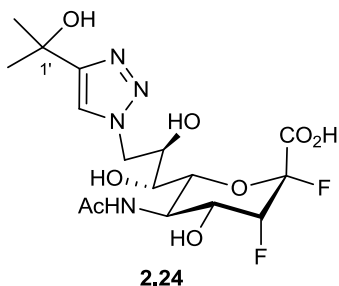
3.1.10 2-[1-(5-Acetamido-3,5,9-trideoxy-2,3-difluoro-D-*erythro*-β-L-*manno*-non-2-ulopyranosonate-9-yl)-1*H*-1,2,3-triazol-4-yl]-propan-2-ol (2.24)

2.24

Compound **2.11a** (28.72 mg, 58.1 μmol) was dissolved in ^{t}BuOH: H_2O=1:1 mixture (1.1 mL), and BTTES (0.85 mg, 1.71 μmol), $CuSO_4$ (29 μL, 250 mM, 7.3 μmol), NaAsc (29 μL, 1 M, 29 μmol), 2-methyl-3-butyn-2-ol (7.2 μL, 73.7 μmol) were added. The reaction mixture was stirred overnight at room temperature. DCM (12 mL) was added to the reaction mixture, which was washed with H_2O (2×2 mL). The organic layer was dried over $MgSO_4$, filtered and concentrated *in vacuo*. The resulting residue could be purified by flash column chromatography (DCM/MeOH=1/0 to 19/1) to afford the product as a white powder (32 mg, 95.2 %). The product was dissolved in dry MeOH (5 mL) and sodium methylate (88 μL, 0.823 M) was added dropwise at 0 °C. The mixture was stirred at this temperature for 1 h, then H_2O (0.1 mL) was added and stirred for 0.5 h at room temperature. The reaction mixture was neutralized by addition of AcOH (10.3 μL) and concentrated. The residue was purified by flash column chromatography (EA/MeOH/H_2O=10/2/1) and then by reverse phase (C18) column chromatography (H_2O to MeOH, gradient increase by 10%) to yield product **2.24** (18 mg, 56.3 %). **^{1}H NMR** (CD$_3$OD, 400 MHz): δ 7.90 (s, 1 H, *triazole*), 5.19 (d, $J_{3,F3}$=52.4 Hz, 1 H, H-3), 4.78 (dd, $J_{9a,9b}$=14.2 Hz, $J_{9a,8}$=2.0 Hz, 1 H, H-9a), 4.45 (dd, $J_{9b,9a}$=14.2 Hz, $J_{9b,8}$=7.9 Hz, 1 H, H-9b), 4.12 - 4.27 (m, 2 H, H-5, H-8), 3.98 (dd, $J_{4,F3}$=28.0 Hz, $J_{4,5}$=10.8 Hz, 1 H, H-4), 3.60 (d, J=10.1 Hz, 1 H, H-6), 3.40 (d, J=9.4 Hz, 1 H, H-7), 2.01 (s, 3 H, NH*Ac*), 1.59 (s, 6 H, 2×*Me*). **^{13}C NMR** (CD$_3$OD, 100 MHz): δ 174.2 (*Ac*), 169.1 (d, $J_{C1,F2}$=25.9 Hz, C-1), 155.4 (C=C), 121.7 (C=C), 89.1 (dd, $J_{C3,F3}$=186.2 Hz, $J_{C3,F2}$=19.0 Hz, C-3), 73.1 (d, $J_{C6,F2}$=4.0 Hz, C-6), 69.9 (C-8), 69.8 (C-7), 69.4 (dd, $J_{C4,F3}$=17.8 Hz, $J_{C4,F2}$=5.7 Hz, C-4), 67.8 (C-1'), 53.1 (C-9), 29.4 (s, 2×*Me*), 21.4 (s, NH*Ac*). **^{19}F NMR** (CD$_3$OD, 282 MHz): δ -220.85 (ddd, $J_{F3,3}$=52.5 Hz, $J_{F3,4}$=28.1 Hz, $J_{F3,F2}$=10.3 Hz, 1 F, F-3 ax), -124.96 (d, $J_{F2,F3}$=10.3 Hz, 1 F, F-2 eq). ESI MS *m/z* 437.3 [M-H]$^-$.

3.1.11 2-[1-(5-Acetamido-3,5,9-trideoxy-2,3-difluoro-D-*erythro*-β-L-*manno*-non-2-ulopyranosonate-9-yl)-1*H*-1,2,3-triazol-4-yl]-2-methyl-propane (2.25)

2.25
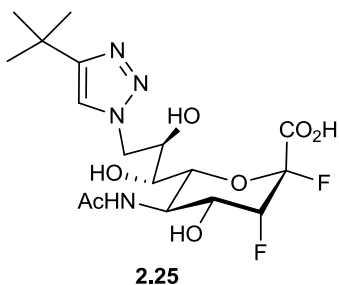
Compound **2.11a** (28.46 mg, 57.6 µmol) was dissolved in ^{t}BuOH: H_2O=1:1 mixture (1.1 mL), and BTTES (0.85 mg, 1.71 µmol), $CuSO_4$ (29 µL, 250 mM, 7.3 µmol), NaAsc (29 µL, 1 M, 29 µmol), 3,3-dimethyl-1-butyne (9.6 µL, 77.9 µmol) were added . The reaction mixture was stirred overnight at room temperature. DCM (12 mL) was added to the reaction mixture, which was washed with H_2O (2×2 mL). The organic layer was dried over $MgSO_4$, filtered and concentrated *in vacuo*. The resulting residue could be purified by flash column chromatography (DCM/MeOH=1/0 to 19/1) to afford the product as a white powder (26 mg, 78.3 %). The product was dissolved in dry MeOH (5 mL) and sodium methylate (71.7 µL, 0.823 M) was added dropwise at 0 °C. The mixture was stirred at this temperature for 1 h, then H_2O (0.1 mL) was added and stirred for 0.5 h at room temperature. The reaction mixture was neutralized by addition of AcOH (8.4 µL) and concentrated. The residue was purified by flash column chromatography (EA/MeOH/H_2O=14/2/1) and then by reverse phase (C18) column chromatography (H_2O to MeOH, gradient increase by 10%) to yield product **2.25** (15 mg, 76.2 %). **^{1}H NMR** (CD$_3$OD, 400 MHz): δ 7.78 (s, 1 H, *triazole*), 5.21 (d, $J_{3,F3}$=52.4 Hz, 1 H, H-3), 4.76 (dd, $J_{9a,9b}$=14.0 Hz, $J_{9a,8}$=2.3 Hz, 1 H, H-9a), 4.44 (dd, $J_{9b,9a}$=14.0 Hz, $J_{9b,8}$=7.9 Hz, 1 H, H-9b), 4.13 - 4.28 (m, 2 H, H-5, H-8), 4.00 (dd, $J_{4,F3}$=28.0 Hz, $J_{4,5}$=10.7 Hz, 1 H, H-4), 3.64 (d, J=10.5 Hz, 1 H, H-6), 3.39 (d, J=9.1 Hz, 1 H, H-7), 2.01 (s, 3 H, NH*Ac*), 1.34 - 1.39 (3 s, 9 H, 3×*Me*). **^{13}C NMR** (CD$_3$OD, 100 MHz): δ 174.0 (*Ac*), 168.6 (d, $J_{C1,F2}$=26.8 Hz, C-1) 156.8 (C=C), 120.9 (C=C), 89.4 (dd, $J_{C3,F3}$=185.6 Hz, $J_{C3,F2}$=18.4 Hz, C-3), 73.0 (d, $J_{C6,F2}$=4.6 Hz, C-6), 69.8 (C-8), 69.7 (C-7), 69.4 (dd, $J_{C4,F3}$=18.4 Hz, $J_{C4,F2}$=6.1 Hz, C-4), 53.0 (C-9), 30.3 (*t-butyl*),

29.4 (3×*Me*), 21.3 (s, NH*Ac*). **^{13}C NMR** (CD$_3$OD, 151 MHz) δ 49.99 Hz (C-5), 107.55 Hz (C-2) by HMBC. **^{19}F NMR** (CD$_3$OD, 282 MHz): δ -220.91 (ddd, $J_{F3,3}$=52.5 Hz, $J_{F3,4}$=28.1 Hz, $J_{F3,F2}$=10.3 Hz, 1 F, F-3 ax), -124.73 (d, $J_{F2,F3}$=10.3 Hz, 1 F, F-2 eq). ESI MS *m/z* 435.3 [M-H]⁻.

3.1.12 [1-(5-Acetamido-3,5,9-trideoxy-2,3-difluoro-D-*erythro*-β-L-*manno*-non-2-ulopyranosonate-9-yl)-1*H*-1,2,3-triazol-4-yl]-cyclohexane (2.27)

2.27
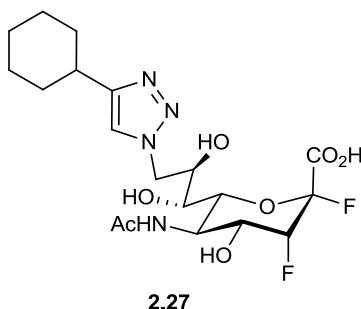
Compound **2.11a** (25.92 mg, 52.4 μmol) was dissolved in ^{t}BuOH: H$_2$O=1:1 mixture (1.1 mL), and BTTES (0.83 mg, 1.67 μmol), CuSO$_4$ (29 μL, 250 mM, 7.3 μmol), NaAsc (29 μL, 1 M, 29 μmol), cyclohexyl acetylene (9.1 μL, 69.7 μmol) were added. The reaction mixture was stirred overnight at room temperature. DCM (12 mL) was added to the reaction mixture, which was washed with H$_2$O (2×2 mL). The organic layer was dried over MgSO$_4$, filtered and concentrated *in vacuo*. The resulting residue could be purified by flash column chromatography (DCM/MeOH=1/0 to 19/1) to afford the product as a white powder (26.4 mg, 85.7 %). The product was dissolved in dry MeOH (5 mL) and sodium methylate (382 μL, 0.153 M) was added dropwise at 0 °C. The mixture was stirred at this temperature for 1 h, then H$_2$O (0.1 mL) was added and stirred for 0.5 h at room temperature. The reaction mixture was neutralized by addition of AcOH (8.3 μL) and concentrated. The residue was purified by flash column chromatography (EA/MeOH/H$_2$O=10/2/1) and then by reverse phase (C18) column chromatography (H$_2$O to MeOH, gradient increase by 10%) to yield product **2.27** (17 mg, 81.9 %). **^{1}H NMR** (CD$_3$OD, 400 MHz): δ 7.79 (s, 1 H, *triazole*), 5.24

(d, $J_{3,F3}$=52.5 Hz, 1 H, H-3), 4.76 (d, $J_{9a,9b}$=13.9 Hz, 1 H, H-9a), 4.44 (dd, $J_{9b,9a}$=13.9 Hz, $J_{9b,8}$= 8.2 Hz, 1 H, H-9b), 4.12 - 4.25 (m, 2 H, H-8, H-5), 4.02 (dd, $J_{4,F3}$=27.7 Hz, $J_{4,5}$=9.6 Hz, 1 H, H-4), 3.65 (d, J=9.9 Hz, 1 H, H-6), 3.39 (d, J=8.8 Hz, 1 H, H-7), 2.75 (s, 1 H, *cyclohexyl*), 1.98 - 2.14 (m, 5 H, *cyclohexyl*, NH*Ac*), 1.71 - 1.90 (m, 3 H, cyclohexyl), 1.39 - 1.54 (m, 4 H, *cyclohexyl*), 1.26 - 1.38 (m, 1 H, *cyclohexyl*). [13]**C NMR** (CD$_3$OD, 100 MHz): δ 173.7 (*Ac*), 124.3 (C=C), 89.9 (dd, $J_{C3,F3}$=184.8 Hz, $J_{C3,F2}$=17.6 Hz, C-3), 72.8 (d, $J_{C6,F2}$=3.1 Hz, C-6), 69.8 (C-8), 69.7 (C-7), 69.3 (dd, $J_{C4,F3}$=18.4 Hz, $J_{C4,F2}$=6.1 Hz, C-4), 53.1 (C-9), 35.0, 32.87, 26.0, 25.8 (*cyclohexyl*), 21.4 (NH*Ac*). [19]**F NMR** (CD$_3$OD, 282 MHz): δ -221.02 (dd, $J_{F3,3}$=52.5 Hz, $J_{F3,4}$=27.6 Hz, 1 F, F-3 ax), -124.63 (s, 1 F, F-2 eq). ESI MS *m/z* 461.3 [M-H]⁻.

3.1.13   [1-(5-Acetamido-3,5,9-trideoxy-2,3-difluoro-D-*erythro*-β-L-*manno*-non-2-ulopyranosonate-9-yl)-1*H*-1,2,3-triazol-4-yl]-formic acid (2.26)

2.26
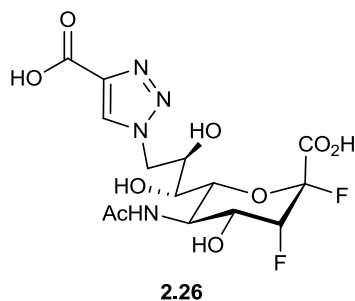
Compound **2.11a** (30.44 mg, 61.6 μmol) was dissolved in *t*BuOH: H$_2$O=1:1 mixture (1.1 mL), and BTTES (0.92 mg, 1.85 μmol), CuSO$_4$ (33 μL, 250 mM, 8.3 μmol), NaAsc (33 μL, 1 M, 33 μmol), methyl propiolate (8.0 μL, 89.9 μmol) were added. The reaction mixture was stirred for 24 h at room temperature. DCM (12 mL) was added to the reaction mixture, which was washed with H$_2$O (2×2 mL). The organic layer was dried over MgSO$_4$, filtered and concentrated *in vacuo*. The resulting residue could be purified by flash column chromatography (DCM/MeOH=1/0 to 19/1) to afford the product as a white powder (30 mg, 84.3 %). The product was dissolved in dry MeOH

(5 mL) and sodium methylate (1022 μL, 0.153 M) was added dropwise at 0° C. The mixture was stirred at this temperature for 1 h, then 0.1 M NaOH (0.2 mL) was added and the stirred for overnight at room temperature. AcOH (10 μL) was added to the reaction mixture and then added dropwise until neutral. The residue was purified by flash column chromatography (EA/MeOH/H$_2$O=5/2/1) and then by reverse phase (C18) column chromatography (H$_2$O to MeOH, gradient increase by 10%) to yield product **2.26** (18 mg, 81.8%). **^{1}H NMR** (D$_2$O, 400 MHz): δ 8.16 (s, 1 H, *triazole*), 5.15 (d, $J_{3,F3}$=51.6 Hz, 1 H, H-3), 4.81 (dd, $J_{9a,9b}$=14.3 Hz, $J_{9a,8}$=2.1 Hz, 1 H, H-9a), 4.53 (dd, $J_{9b,9a}$=14.3 Hz, $J_{9b,8}$= 7.5 Hz, 1 H, H-9b), 4.04 - 4.31 (m, 3 H, H-8, H-5, H-4), 3.78 (d, J=10.4 Hz, 1 H, H-6), 3.37 (d, J=9.1 Hz, 1 H, H-7), 1.98 (s, 3 H, NH*Ac*). **^{13}C NMR** (D$_2$O,101 MHz) δ 181.3 (*C*OOH), 175.2 (*Ac*), 171.1 (C=C), 169.6 (dd, $J_{C1,F2}$ =26.8 Hz, $J_{C1,F3}$ = 3.8 Hz, C-1), 128.2 (C=C), 106.8 (dd, $J_{C2,F2}$=220.8 Hz, $J_{C2,F3}$= 14.6 Hz, C-2), 89.1 (dd, $J_{C3,F3}$=184.0 Hz, $J_{C3,F2}$=18.4 Hz, C-3), 72.4 (d, $J_{C6,F2}$=4.6 Hz, C-6), 69.2 (dd, $J_{C4,F3}$=18.0 Hz, $J_{C4,F2}$=5.8 Hz, C-4), 68.9 (C-8), 68.8 (C-7), 53.6 (C-9), 47.0 (d, $J_{C5,F3}$=3.1 Hz, C-5), 22.1 (s, NH*Ac*). **^{19}F NMR** (D$_2$O, 282 MHz) δ -220.9 (ddd, $J_{F3,3}$=51.6 Hz, $J_{F3,4}$=27.5 Hz, $J_{F3,F2}$=10.3 Hz, 1 F, F-3 ax), -124.8 (d, $J_{F2,F3}$=10.3 Hz, 1 F, F-2 eq). ESI MS *m/z* 445.2 [M-2H+Na]$^-$.

3.1.14   [1-(5-Acetamido-3,5,9-trideoxy-2,3-difluoro-D-*erythro*-β-L-*manno*-non-2-ulopyranosonate-9-yl)-1*H*-1,2,3-triazol-4-yl]-methanamine (2.29)
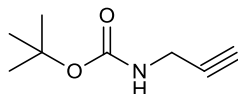
tert-Butyl prop-2-ynylcarbamate

Di-*tert*-butyl dicarbonate (0.874 g, 4.0 mmol) was added dropwise to a solution of prop-2-yn-1-amine (0.274 mL, 4.0 mmol) in DCM (10 mL) at 0 °C and stirred for 1 h at room temperature. The reaction mixture was concentrated under vacuum yielding a light yellow solid (0.458 g, 81.2%). No further purification applied. . **^{1}H NMR** (CDCl$_3$, 400 MHz) δ 4.72 (s, 1 H, N*H*), 3.93 (s, 2 H, *CH$_2$*), 2.22 (t, *J*=2.4 Hz, 1 H, *CH*), 1.46 (s, 9 H, 3×*Me*).

tert-Butyl-{[1-(5-Acetamido-3,5,9-trideoxy-2,3-difluoro-D-_erythro_-β-L-_manno_-non-2-ulopyranosonate-9-yl)-1_H_-1,2,3-triazol-4-yl]methyl}-carbamate (2.28)
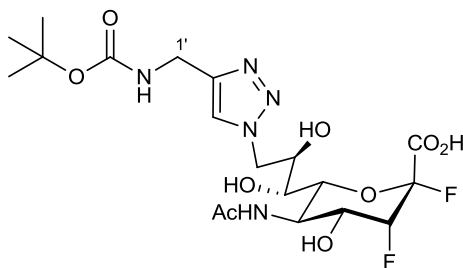
2.28

Compound **2.11a** (33.44 mg, 67.6 μmol) was dissolved in ^{t}BuOH: H_2O=1:1 mixture (1.1 mL), and BTTES (0.90 mg, 1.81 μmol), $CuSO_4$ (36.3 μL, 250 mM, 9.1 μmol), NaAsc (36.3 μL, 1 M, 36.3 μmol), _tert_-butyl prop-2-ynylcarbamate (12.4 mg, 87.9 μmol) were added. The reaction mixture was stirred overnight at room temperature. DCM (12 mL) was added to the reaction mixture, which was washed with H_2O (2×2 mL). The organic layer was dried over $MgSO_4$, filtered and concentrated _in vacuo_. The resulting residue could be purified by flash column chromatography (DCM/MeOH=1/0 to 19/1) to afford the product as a white powder (37 mg, 57.0 μmol, 84.3 %). The product was dissolved in dry MeOH (5 mL) and sodium methylate (497 μL, 0.153 M) was added dropwise at 0 °C. The mixture was stirred at this temperature for 1 h, then H_2O (0.1 mL) was added and stirred for 0.5 h at room temperature. The reaction mixture was neutralized by addition of AcOH (10.8 μL) and concentrated. The residue was purified by flash column chromatography (EA/MeOH/H_2O=10/2/1) to yield product **2.28** (28 mg, 96.4 %). **^{1}H NMR** (CD$_3$OD, 300 MHz) δ 7.82 (s, 1 H, _triazole_), 5.16 (d, $J_{3,F3}$=50.5 Hz, 1 H, H-3), 4.48 (dd, $J_{9a,9b}$=14.0 Hz, $J_{9a,8}$=7.7 Hz, 1 H, H-9a), 4.29 (s, 2 H, H-1'), 4.03-4.25 (m, 3 H, H-4, H-5, H-8), 3.76 (d, J=10.1 Hz, 1 H, H-6), 3.36 (d, J=8.9 Hz, 1 H, H-7), 2.02 (s, 3 H, NH_Ac_), 1.37 (s, 9 H, 3×_Me_). **^{13}C NMR** (CD$_3$OD, 101 MHz) δ 174.6 (O_C_ON), 174.2 (_Ac_), 169.5 (C-1), 156.4 (C=C), 124.2 (C=C), 89.4 (dd, $J_{C3,F3}$=186.3 Hz, $J_{C3,F2}$=19.2 Hz, C-3), 78.7 (^{t}Bu), 73.0 (d, $J_{C6,F2}$=3.8 Hz, C-6), 69.9 (C-8), 69.8 (C-7), 69.2 (dd, $J_{C4,F3}$=19.2 Hz, $J_{C4,F2}$=6.1 Hz, C-4), 53.3 (C-9), 34.3 (C-1'), 27.5 (3×_Me_), 21.4 (s, NH_Ac_). **^{19}F NMR** (D$_2$O, 282 MHz) δ -218.23 (ddd, $J_{F3,3}$=50.5 Hz, $J_{F3,4}$=28.1 Hz, $J_{F3,F2}$=8.0 Hz, 1 F, F-3 ax), -121.52 (d, $J_{F2,F3}$=8.0 Hz, 1 F, F-2 eq). ESI MS _m/z_ 508.4 [M-H]$^-$.
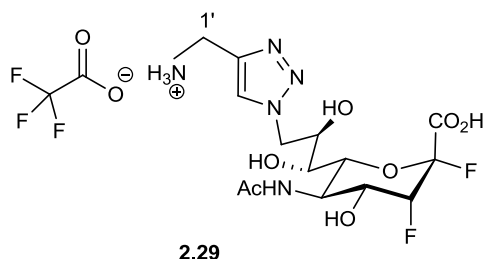
[1-(5-Acetamido-3,5,9-trideoxy-2,3-difluoro-D-*erythro*-β-L-*manno*-non-2-ulopyranosonate-9-yl)-1*H*-1,2,3-triazol-4-yl]- methanamine (2.29)

2.29

Compound **2.28** (10.72 mg, 21.0 μmol) was dissolved in TFA (1 mL) and the mixture was stirred for 4 h at room temperature. The extra TFA residue was removed by evaporation *in vacuo* followed by precipitation and lyophilisation. After lyophilisation, **2.29** and TFA complex was formed (8 mg, 90.3%). No further purification was applied. **^{1}H NMR** (D$_2$O, 300 MHz) δ 8.08 (s, 1 H, *triazole*), 5.12 (d, $J_{3,F3}$=51.5 Hz, 1 H, H-3), 4.39 - 4.51 (m, 2 H, H-9), 4.28 (s, 2 H, H-1'), 4.03 - 4.23 (m, 3 H, H-4, H-5, H-8), 3.73 (d, J=11.0 Hz, 1 H, H-6), 3.39 (d, J=8.1 Hz, 1 H, H-7), 1.95 (s, 3 H, NH*Ac*). **^{13}C NMR** (D$_2$O, 101 MHz) δ 175.2 (*Ac*), 169.6 (d, $J_{C1,F2}$=23.8 Hz, C-1), 139.8 (C=C), 126.2 (C=C), 89.0 (dd, $J_{C3,F3}$=184.8 Hz, $J_{C3,F2}$=18.4 Hz, C-3), 72.5 (d, $J_{C6,F2}$=4.6 Hz, C-6), 69.1 - 69.2 (m, C-7, C-8), 69.2 (dd, $J_{C4,F3}$=18.4 Hz, $J_{C4,F2}$=5.4 Hz, C-4), 53.6 (C-9), 47.0 (d, $J_{C5,F3}$=3.8 Hz, C-5), 34.1 (C-1'), 22.1 (s, NH*Ac*). **^{19}F NMR** (D$_2$O, 282 MHz) δ -218.23 (ddd, $J_{F3,3}$=51.5 Hz, $J_{F3,4}$=29.8 Hz, $J_{F3,F2}$=11.5 Hz, 1 F, F-3 ax), -121.48 (d, $J_{F2,F3}$=11.5 Hz, 1 F, F-2 eq), -76.00 (s, *TFA*). ESI MS *m/z* 408.3 [M-H]$^-$.

3.2   Enzymology

3.2.1 Enzyme Preparation

Wild-type TcTS was expressed in *Escherichia coli*. A single colony was inoculated into LB medium (30 mL) containing 0.1 mg/mL ampicillin and grown overnight at 25 °C. This culture (5 mL for each) was inoculated into four×500 mL of LB medium containing 0.1 mg/mL ampicillin

and grown for 4 h at 37°C. TcTS was expressed by induction with 0.5 mM isopropyl β-D-1-thiogalactopyranoside (IPTG) and incubated at 30 °C with constant agitation at 200 rpm overnight. Cells were centrifuged at 5000 g for 30 min and the cell pellets were re-suspended in 25 mL of lysis buffer A (20 mM Tris-HCl at pH 8, 0.5 M NaCl) and lysed by French press followed by addition of EDTA-free protease inhibitor. The lysed cell mixture was centrifuged at 15000 rpm for 30 minutes. The supernatant was subjected to a 1.0 mL HisTrapFF column and eluted using a gradient of imidazole (from 0.5 mM to 100 mM). Unbound proteins were washed using buffer A and the elution of the desired protein was monitored by UV at 280 nm. Fractions containing TcTS were run on SDS-PAGE gels to measure purity and the approximate molecular weights were determined by comparing with pre-stained molecular weight markers (Bio-Rad). Those fractions with 95% or more purity were combined. By using a 30 K molecular weight cut-off centrifugal filter (Amicon Ultra), the enzyme was concentrated and the buffer storing the enzyme was exchanged into stock buffer (pH 7.48 tris-HCl buffer with 20 mM NaCl). The resulting enzyme was stored at 4°C. The enzyme concentration was determined by UV at 280 nm based on the following equation (The extinction coeffient constant ε of wild-type TcTS is 1.699 mL/mg, A_{280} stands for the absorbance at 280 nm):

$$[E] = (A_{280} \times \text{diluted factor})/\varepsilon \qquad \textbf{Equation 3.1}$$

3.2.2 *Trypanosoma cruzi* **Trans-Sialidase Kinetics**

All kinetics experiments were performed in an assay buffer (20 mM Tris-HCl/20 mM NaCl with a pH of 7.48) at 25°C on a Varian Cary 4000 or Varian Cary 300 UV-Vis spectrophotometer at 385 nm using a continuous UV spectrophotometric assay. 5-Acetamido-3,5-dideoxy-2-(4-trifluoromethylumberliferyl)-D-*glycero*-α-D-*galacto*-non-2-ulopyranosonic acid (TFMU-SA) was used as the substrate for all kinetic assays and the release of 4-trifluoromethylumbellifery alcohol was measured at 385 nm, the extinction coefficient of TFMU in this buffer system is 6.565 mM^{-1}cm^{-1}.[16] Quartz cuvettes with a path length of 1 cm were used.

3.2.2.1   pH Stability of TcTS

To determine the stability of TcTS at a series of pH values, the following buffers were used: 30 mM phosphate-citrate incubation buffer was used for pH 3-6, 20 mM Tris-HCl /30 mM NaCl buffer for pH 7-9, 10 mM HCl-sodium citrate buffer for pH 2 and glycine-NaOH buffer for pH 10. TcTS was incubated in different pH buffers in the presence of 1% BSA and added aliquots removed at time intervals for assaying. The assays were conducted by the addition of 20 µL incubated enzyme into 180 µL assay buffer containing a substrate concentration of 1.28 mM.

3.2.2.2   pH Profile of TcTS

The substrate depletion method was used to measure k_{cat}/K_M at each pH value. From the substrate depletion assay, we accessed the pH profile by incubating TcTS in different pH buffers (30 mM phosphate-citrate buffer for pH 4-8 and 50 mM sodium carbonate/bicarbonate buffer for pH 8-9). The assays were conducted by the addition of 20 µL incubated enzyme into 180 µL assay buffer containing TFMU-SA, with initial concentration of 7.5 µM. Reaction was monitored continuously at 385 nm.

3.2.2.3   Inactivation Studies of TcTS

For all the inactivation studies, the initial rates of the reactions were measured in the assay buffer at 25 °C with a fixed concentration of TFMU-SA (0.5 mM) and incubated TcTS (1.4 µM for incubation and 0.07 µM for final assays) while varying the inactivator concentration (incubation concentrations generally from 10 mM to 0.1 mM). The data collected at different time points were plotted as a function of time and fitted according to the equation below using Grafit 5.

$$v_t = v_{t=0} . e^{-k_{iobs}t} + \text{offset} \qquad \textbf{Equation 3.2}$$

The equation with offset was applied since the rates did not decrease to zero.

According to the following equation, the inactivation rate constant (k_i) and the reversible dissociation constant for the inactivator (K_i) were obtained by fitting $k_{i\ obs}$ as a function of inactivator concentration to the Michaelis-Menton equation.

$$k_{i\ obs} = k_i[I]/(K_i+[I]) \qquad\qquad \textbf{Equation 3.3}$$

Consequently, the specificity constants of inactivators (k_i/K_i) were calculated. In the case of **2.12**, $[I]<<K_i$, the above equation becomes

$$k_{i\ obs} = k_i[I]/K_i \qquad\qquad \textbf{Equation 3.4}$$

All the k_i/K_i values are shown in Section 2.3. The graphic representations of inactivation data are presented in Section A.3.

3.2.2.4   Reactivation Studies of TcTS

After incubation with 1 mM **2.12** and 9.4 mM **2.20** for 2 h, the excess inactivator was removed by applying the inactivated TcTS solution (80 µL) to a micro-spin G-25 size exclusion column (Amersham Biosciences) at 0°C. The resin was washed with the same volume of buffer and then diluted into 200 µL and incubated in the presence of 1% BSA at 25°C to start the reactivation incubation. Time-dependent reactivations were conducted by adding an aliquot of eluted enzyme in the assay buffer at 25 °C with a fixed concentration of TFMU-SA (0.5 mM). Control assays were also conducted without inactivator additions. For the reactivation studies with lactose as trans-sialylation acceptor, a concentration of 100 mM was applied. The data collected at different time point were plotted as a function of time and fitted to the first order equation. First-order rate constants for reactivation ($k_{r\ obs}$) were obtained and shown in Section 2.4.

References

(1) Vimr, E. R.; Kalivoda, K. A.; Deszo, E. L.; Steenbergen, S. M. *Microbio Mol Bio R* **2004**, *68*, 132.

(2) Varki, N. M.; Varki, A. *Lab Invest* **2007**, *87*, 851.

(3) Schauer, R. *Trends Bio Sci* **1985**, *10*, 357.

(4) Wang, B.; Brand-Miller, J. *Eur J Clin Nutr* **2003**, *57*, 1351.

(5) Varki A, C. R., Esko J, et al., editors.; 2nd ed.; Cold Spring Harbor Laboratory Press: Cold Spring Harbor (NY), 1999; Vol. Chapter 15, Sialic Acids

(6) Schauer, R.; Kamerling, J. P. *ChemBioChem* **2011**, *12*, 2246.

(7) Buschiazzo, A.; Alzari, P. M. *Curr Opin Chem Bio* **2008**, *12*, 565.

(8) Morley, T. J.; Willis, L. M.; Whitfield, C.; Wakarchuk, W. W.; Withers, S. G. *J Bio Chem* **2009**, *284*, 17404.

(9) Wilson, J. C.; Angus, D. I.; Von Itzstein, M. *J Am Chem Soc* **1995**, *117*, 4214.

(10) Kao, Y. H.; Lerner, L.; Warner, T. G. *Glycobiology* **1997**, *7*, 559.

(11) Todeschini, A. R.; Mendonca-Previato, L.; Previato, J. O.; Varki, A.; van Halbeek, H. *Glycobiology* **2000**, *10*, 213.

(12) Newstead, S. L.; Potter, J. A.; Wilson, J. C.; Xu, G. G.; Chien, C. H.; Watts, A. G.; Withers, S. G.; Taylor, G. L. *J Bio Chem* **2008**, *283*, 9080.

(13) Manzoni, M.; Colombi, P.; Papini, N.; Rubaga, L.; Tiso, N.; Preti, A.; Venerando, B.; Tettamanti, G.; Bresciani, R.; Argenton, F.; Borsani, G.; Monti, E. *Biochem J* **2007**, *408*, 395.

(14) Kobayashi, T.; Ito, M.; Ikeda, K.; Tanaka, K.; Saito, M. *J BioChem* **2000**, *127*, 569.

(15) Amaya, M. F.; Watts, A. G.; Damager, I.; Wehenkel, A.; Nguyen, T.; Buschiazzo, A.; Paris, G.; Frasch, A. C.; Withers, S. G.; Alzari, P. M. *Structure* **2004**, *12*, 775.

(16) Damager, I.; Buchini, S.; Amaya, M. F.; Buschiazzo, A.; Alzari, P.; Frasch, A. C.; Watts, A.; Withers, S. G. *Biochemistry* **2008**, *47*, 3507.

(17) Watts, A. G.; Damager, I.; Amaya, M. L.; Buschiazzo, A.; Alzari, P.; Frasch, A. C.; Withers, S. G. *J Am Chem Soc* **2003**, *125*, 7532.

(18) Watts, A. G.; Oppezzo, P.; Withers, S. G.; Alzari, P. M.; Buschiazzo, A. *J Bio Chem* **2006**, *281*, 4149.

(19) Zechel, D. L.; Withers, S. G. *Acc Chem Res* **2000**, *33*, 11.

(20) Watson, J. N.; Newstead, S.; Narine, A. A.; Taylor, G.; Bennet, A. J. *ChemBioChem* **2005**, *6*, 1999.

(21) Kim, S.; Oh, D. B.; Kang, H. A.; Kwon, O. *Appl Microbiol and Biot* **2011**, *91*, 1.

(22) Dowle, M. D.; Howes, P. D. *Expert Opin Ther Pat* **1998**, *8*, 1461.

(23) Meindl, P.; Tuppy, H. *Monatsh Chem* **1969**, *100*, 1295.

(24) Meindl, P.; Bodo, G.; Palese, P.; Schulman, J.; Tuppy, H. *Virology* **1974**, *58*, 457.

(25) Azuma, Y.; Taniguchi, A.; Matsumoto, K. *Glycoconjugate J* **2000**, *17*, 301.

(26) Beau, J. M.; Schauer, R.; Haverkamp, J.; Kamerling, J. P.; Dorland, L.; Vliegenthart, J. F. G. *Eur Biochem* **1984**, *140*, 203.

(27) Saito, M.; Rosenberg, A. *Biochemistry* **1984**, *23*, 3784.

(28) Von Itzstein, M.; Wu, W. Y.; Kok, G. B.; Pegg, M. S.; Dyason, J. C.; Jin, B.; Phan, T. V.; Smythe, M. L.; White, H. F.; Oliver, S. W.; Colman, P. M.; Varghese, J. N.; Ryan, D. M.; Woods, J. M.; Bethell, R. C.; Hotham, V. J.; Cameron, J. M.; Penn, C. R. *Nature* **1993**, *363*, 418.

(29) Von Itzstein, M.; Dyason, J. C.; Oliver, S. W.; White, H. F.; Wu, W. Y.; Kok, G. B.; Pegg, M. S. *J Med Chem* **1996**, *39*, 388.

(30) Withers, S. G.; Street, I. P.; Bird, P.; Dolphin, D. H. *J Am Chem Soc* **1987**, *109*, 7530.

(31) Withers, S. G., Watts, A. G., Kim, J. H., Wennekes, T. WO/2011/006237 **2011**.

(32) Buchini, S.; Buschiazzo, A.; Withers, S. G. *Angew Chem Int Edit* **2008**, *47*, 2700.

(33) Pierdominici-Sottile, G.; Horenstein, N. A.; Roitberg, A. E. *Biochemistry* **2011**, *50*, 10150.

(34) Chagas, C. *Mern. Inst. Oswaldo Cruz* **1909**, *1*, 11.

(35) Rabinovich, J. E.; Wisniveskycolli, C.; Solarz, N. D.; Gurtler, R. E. *B World Health Organ* **1990**, *68*, 737.

(36) http://pathmicro.med.sc.edu/lecture/trypanosomiasis.htm, 15/03/10, **2010**.

(37) Pereira, K. S.; Sciimidt, F. L.; Guaraldo, A. M. A.; Franco, R. M. B.; Dias, V. L.; Passos, L. A. C. *J Food Protect* **2009**, *72*, 441.

(38) Coura, J. R.; Vinas, P. A. *Nature* **2010**, *465*, S6.

(39) Punukollu, G.; Gowda, R. A.; Khan, I. A.; Navarro, V. S.; Vasavada, B. C. *Int J Cardiol* **2007**, *115*, 279.

(40) Bern, C.; Montgomery, S. P.; Herwaldt, B. L.; Rassi, A.; Marin, J. A.; Dantas, R. O.; Maguire, J. H.; Acquatella, H.; Morillo, C.; Kirchhoff, L. V.; Gilman, R. H.; Reyes, P. A.; Salvatella, R.; Moore, A. C. *Jama-J Am Med Assoc* **2007**, *298*, 2171.

(41) Duffy, T.; Bisio, M.; Altcheh, J.; Burgos, J. M.; Diez, M.; Levin, M. J.; Favaloro, R. R.; Freilij, H.; Schijman, A. G. *PLOS Neglect Trop Dis* **2009**, *3*.

(42) Urbina, J. A. *Acta Tropica* **2010**, *115*, 55.

(43) Apt, W. *Drug Des Dev Ther* **2010**, *4*, 243.

(44) Maya, J. D.; Cassels, B. K.; Iturriaga-Vasquez, P.; Ferreira, J.; Faundez, M.; Galanti, N.; Ferreira, A.; Morello, A. *Comp Biochem Physiol A Mol Integr Physiol* **2007**, *146*, 601.

(45) Le Loup, G.; Pialoux, G.; Lescure, F. X. *Curr Opin Infect Dis* **2011**, *24*, 428.

(46) Salomon, C. J. *J Pharm Sci* **2012**, *101*, 888.

(47) Rassi, A.; Rassi, A.; Marin-Neto, J. A. *Lancet* **2010**, *375*, 1388.

(48) Mckerrow, J. H.; Mcgrath, M. E.; Engel, J. C. *Parasitol Today* **1995**, *11*, 279.

(49) Cazzulo, J. J.; Stoka, V.; Turk, V. *Curr Pharm Des* **2001**, *7*, 1143.

(50) Guedes, P. M. M.; Silva, G. K.; Gutierrez, F. R. S.; Silva, J. S. *Expert Rev Anti-Infect Ther* **2011**, *9*, 609.

(51) Molina, J.; Martins-Filho, O. A.; Brener, Z.; Romanha, A. J.; Loebenberg, D.; Urbina, J. A. *Antimicrob Agents Chemother* **2000**, *44*, 150.

(52) Pereira, M. E.; Loures, M. A.; Villalta, F.; Andrade, A. F. *J Exp Med* **1980**, *152*, 1375.

(53) Engstler, M.; Reuter, G.; Schauer, R. *Mol Biochem Parasitol* **1992**, *54*, 21.

(54) Engstler, M.; Reuter, G.; Schauer, R. *Mol Biochem Parasitol* **1993**, *61*, 1.

(55) Schenkman, S.; Decarvalho, L. P.; Nussenzweig, V. *J Exp Med* **1992**, *175*, 567.

(56) Schenkman, S.; Yoshida, N.; Dealmeida, M. L. C. *Mol Biochem Parasitol* **1988**, *29*, 141.

(57) Rosenberg, I.; Prioli, R. P.; Ortegabarria, E.; Pereira, M. E. A. *Mol Biochem Parasitol* **1991**, *46*, 303.

(58) Jazin, E. E.; Luquetti, A. O.; Rassi, A.; Frasch, A. C. C. *Infect Immun* **1991**, *59*, 2189.

(59) Vandekerckhove, F.; Schenkman, S.; Decarvalho, L. P.; Tomlinson, S.; Kiso, M.; Yoshida, M.; Hasegawa, A.; Nussenzweig, V. *Glycobiology* **1992**, *2*, 541.

(60) Harrison, J. A.; Kartha, K. P. R.; Fournier, E. J. L.; Lowary, T. L.; Malet, C.; Nilsson, U. J.; Hindsgaul, O.; Schenkman, S.; Naismith, J. H.; Field, R. A. *Org Biomol Chem* **2011**, *9*, 1653.

(61) Buschiazzo, A.; Amaya, M. F.; Cremona, M. L.; Frasch, A. C.; Alzari, P. M. *Mol Cell* **2002**, *10*, 757.

(62) Demir, O.; Roitberg, A. E. *Biochemistry* **2009**, *48*, 3398.

(63) Mitchell, F. L.; Miles, S. M.; Neres, J.; Bichenkova, E. V.; Bryce, R. A. *Biophys J* **2010**, *98*, L38.

(64) Schenkman, S.; Eichinger, D.; Pereira, M. E. A.; Nussenzweig, V. *Annu Rev Microbiol* **1994**, *48*, 499.

(65) Arner, E.; Kindlund, E.; Nilsson, D.; Farzana, F.; Ferella, M.; Tammi, M. T.; Andersson, B. *BMC Genomics* **2007**, *8*.

(66) Tonelli, R. R.; Giordano, R. J.; Barbu, E. M.; Torrecilhas, A. C.; Kobayashi, G. S.; Langley, R. R.; Arap, W.; Pasqualini, R.; Colli, W.; Alves, M. J. M. *PLOS Neglect Trop Dis* **2010**, *4*.

(67) Docampo, R.; Moreno, S. N. J. *Parasitol Today* **1996**, *12*, 61.

(68) Tribulatti, M. V.; Mucci, J.; Van Rooijen, N.; Leguizamon, M. S.; Campetella, O. *Infect Immun* **2005**, *73*, 201.

(69) Yoshida, N.; Dorta, M. L.; Ferreira, A. T.; Oshiro, M. E. M.; Mortara, R. A.; AcostaSerrano, A.; Favoreto, S. *Mol Biochem Parasitol* **1997**, *84*, 57.

(70) Leguizamon, M. S.; Mocetti, E.; Rivello, H. G.; Argibay, P.; Campetella, O. *J Infect Dis* **1999**, *180*, 1398.

(71) Paris, G.; Ratier, L.; Amaya, M. F.; Nguyen, T.; Alzari, P. M.; Frasch, A. C. C. *J Mol Biol* **2005**, *345*, 923.

(72) Neres, J.; Brewer, M. L.; Ratier, L.; Botti, H.; Buschiazzo, A.; Edwards, P. N.; Mortenson, P. N.; Charlton, M. H.; Alzari, P. M.; Frasch, A. C.; Bryce, R. A.; Douglas, K. T. *Bioorg Med Chem Lett* **2009**, *19*, 589.

(73) Arioka, S.; Sakagami, M.; Uematsu, R.; Yamaguchi, H.; Togame, H.; Takemoto, H.; Hinou, H.; Nishimura, S. *Bioorg Med Chem* **2010**, *18*, 1633.

(74) Lima, A. H.; Lameira, J.; Alves, C. N. *Struct Chem* **2012**, *23*, 147.

(75) Buschiazzo, A.; Muia, R.; Larrieux, N.; Pitcovsky, T.; Mucci, J.; Campetella, O. *PLOS Pathogens* **2012**, *8*.

(76) Agusti, R.; Paris, G.; Ratier, L.; Frasch, A. C. C.; de Lederkremer, R. M. *Glycobiology* **2004**, *14*, 659.

(77) Carvalho, I.; Andrade, P.; Campo, V. L.; Guedes, P. M. M.; Sesti-Costa, R.; Silva, J. S.; Schenkman, S.; Dedola, S.; Hill, L.; Rejzek, M.; Nepogodiev, S. A.; Field, R. A. *Bioorg Med Chem* **2010**, *18*, 2412.

(78) Giorgi, M. E.; Ratier, L.; Agusti, R.; Frasch, A. C. C.; de Lederkremer, R. M. *Glycoconjugate J* **2010**, *27*, 549.

(79) Carvalho, S. T.; Sola-Penna, M.; Oliveira, I. A.; Pita, S.; Goncalves, A. S.; Neves, B. C.; Sousa, F. R.; Freire-de-Lima, L.; Kurogochi, M.; Hinou, H.; Nishimura, S. I.; Mendonca-Previato, L.; Previato, J. O.; Todeschini, A. R. *Glycobiology* **2010**, *20*, 1034.

(80) Meinke, S.; Schroven, A.; Thiem, J. *Org Biomol Chem* **2011**, *9*, 4487.

(81) Campo, V. L.; Sesti-Costa, R.; Carneiro, Z. A.; Silva, J. S.; Schenkman, S.; Carvalho, I. *Bioorg Med Chem* **2012**, *20*, 145.

(82) Lieke, T.; Grobe, D.; Blanchard, V.; Grunow, D.; Tauber, R.; Zimmermann-Kordmann, M.; Jacobs, T.; Reutter, W. *Glycoconjugate J* **2011**, *28*, 31.

(83) Kolb, H. C.; Finn, M. G.; Sharpless, K. B. *Angew ChemInt Edit* **2001**, *40*, 2004.

(84) Hein, J. E.; Fokin, V. V. *Chem Soc Rev* **2010**, *39*, 1302.

(85) Rasmussen, L. K.; Boren, B. C.; Fokin, V. V. *Org Lett* **2007**, *9*, 5337.

(86) Chan, T. R.; Hilgraf, R.; Sharpless, K. B.; Fokin, V. V. *Org Lett* **2004**, *6*, 2853.

(87) Beliczey, J.; Liese, A.; Wandrey, C.; Hamacher, K.; Coenen, H.H.; Tierling, T.; Forschungszentrum Julich GmbH US 6,355,453 **2002**.

(88) Watts, A. G.; Withers, S. G. *Can J Chem-Rev* **2004**, *82*, 1581.

(89) Perrin, D. D. a. A., W. L. F. *Purification Laboratory Chemicals*; Pergamon Press: Oxford, 1988.

(90) Sharma, R. K.; Fry, J. L. *J Org Chem* **1983**, *48*, 2112.

(91) Cox, D. P.; Terpinski, J.; Lawrynowicz, W. *J Org Chem* **1984**, *49*, 3216.

(92) Braun, P.; Nagele, B.; Wittmann, V.; Drescher, M. *Angew Chem Int Edit* **2011**, *50*, 8428.

(93) Ercegovic, T.; Magnusson, G. *J Org Chem* **1996**, *61*, 179.

(94) Gantt, R.; Millner, S.; Binkley, S. B. *Biochem* **1964**, *3*, 1952.

(95) Besanceney-Webler, C.; Jiang, H.; Zheng, T. Q.; Feng, L.; del Amo, D. S.; Wang, W.; Klivansky, L. M.; Marlow, F. L.; Liu, Y.; Wu, P. *Angew Chem Int Edit* **2011**, *50*, 8051.

(96) Weiwer, M.; Chen, C. C.; Kemp, M. M.; Linhardt, R. J. *Eur J Org Chem* **2009**, 2611.

(97) Lu, Y.; Gervay-Hague, J. *Carbohyd Res* **2007**, *342*, 1636.

(98) He, W. Y.; Du, F. P.; Wu, Y.; Wang, Y. H.; Liu, X.; Liu, H. Y.; Zhao, X. D. *J Fluorine Chem* **2006**, *127*, 809.

(99) Paris, G.; Cremona, M. L.; Amaya, M. F.; Buschiazzo, A.; Giambiagi, S.; Frasch, A. C. C.; Alzari, P. M. *Glycobiology* **2001**, *11*, 305.

(100) Schenkman, S.; Eichinger, D.; Pereira, M. E.; Nussenzweig, V. *Annu Rev Microbiol* **1994**, *48*, 499.

Appendices

A.1   Michaelis-Menten Kinetics

Michaelis-Menten equation, where a single substrate (S) is converted to a single product (P) by enzyme (E), is shown below:

$$E \quad + \quad S \quad \underset{k_{-1}}{\overset{k_1}{\rightleftharpoons}} \quad ES \quad \xrightarrow{k_{cat}} \quad E \quad + \quad P$$
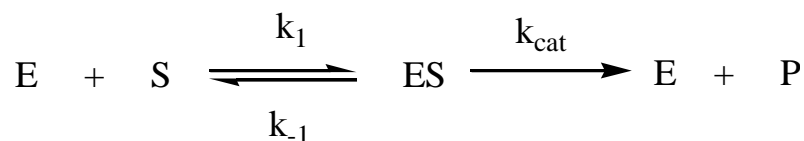
Scheme A. 1 General scheme for enzyme-catalyzed conversion of a single substrate into a single product.

The main concept in the above scheme is the existence of an enzyme-substrate complex (ES), before the enzyme turns over the substrate to generate the product (P). This ES complex sometimes is referred as Michaelis complex. In most of the cases, the rate of the chemical reaction is much slower than the rate for E, S and ES to reach equilibrium, an assumption can be made to greatly simplify the calculations, which is that under steady state conditions, [ES] can be regarded as constant:

$$\frac{d[ES]}{dt} = k_1[E]_{free}[S] - k_{-1}[ES] - k_{cat}[ES] = 0 \qquad \text{\textbf{Equation A. 1}}$$

Therefore,

$$[ES] = (k_1[E]_{free}[S]) / (k_{-1} + k_{cat}) \qquad \text{\textbf{Equation A. 2}}$$

Since $[E]_{free} = [E]_{total} - [ES]$ and K_m is defined as: $K_m = \dfrac{k_{-1} + k_{cat}}{k_1}$,

$$[ES] = ([E]_{total} - [ES])[S] / K_m \qquad \text{\textbf{Equation A. 3}}$$

Solving for [ES] in Equation A.3,

$$[ES] = \frac{[E]_{total}[S]}{K_m + [S]} \qquad \text{\textbf{Equation A. 4}}$$

Therefore, the overall rate:

$$v = \frac{d[ES]}{dt} = -\frac{d[P]}{dt} = \frac{k_{cat}[E]_{total}[S]}{K_m + [S]}$$

Equation 0.1

   This is the Michaelis Menten equation and in most of the cases, it satisfyingly rationalizes the relationship between enzymatic rate and the substrate concentration. There are two important kinetic parameters in this equation, namely, k_{cat} and K_m. K_m is roughly equivalent to the dissociation constant of ES complex and the smaller it is, the substrate binds tighter with the enzyme. Mathematically, it equals to the substrate concentration when 50% of the enzyme in bound with the substrate. k_{cat} is the amount of substrate which can be turned over by the enzyme in a specified unit of time and the bigger it is, the better the enzyme catalyzes the reaction. v_{max} is defined as the product of k_{cat} and $[E]_{total}$:

$$v_{max} = k_{cat}[E]_{total}$$

Equation A. 5

   It represents the maximum kinetic rate for a fixed amount of enzyme. When $[S] \gg K_m$,

$$v = \frac{k_{cat}[E]_{total}[S]}{K_m + [S]} \approx \frac{k_{cat}[E]_{total}[S]}{[S]} = v_{max}$$

Equation A. 6

When $[S] \ll K_m$,

$$v = \frac{k_{cat}[E]_{total}[S]}{K_m + [S]} \approx \frac{k_{cat}[E]_{total}[S]}{K_m} = \frac{k_{cat}}{K_m}[E]_{total}[S]$$

Equation 2.2

   Therefore, the kinetic rate v is directly proportional to $[S]$ and this reaction becomes a first-order reaction. The constant, $\frac{k_{cat}}{K_m}$, is a very useful index for comparing the relative specificity of one enzyme acting on different substrates and is referred to as specificity constant.

   In terms of sialidases which are the main focus of this thesis, the k_{cat} value is actually the overall reaction rate of a two -step reaction, which includes sialylation (k_2) and desialylation (k_3) steps, as shown in the following scheme:

$$E + S \underset{k_{-1}}{\overset{k_1}{\rightleftharpoons}} ES \xrightarrow{k_2} E\text{-}S \xrightarrow{k_3} E + P$$
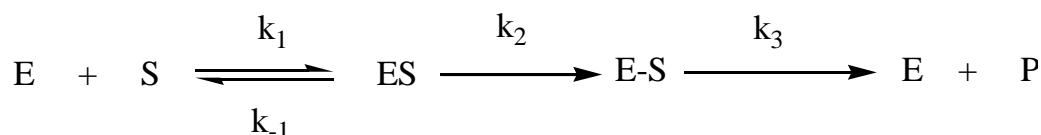
Scheme A. 2 General scheme for the two-step enzyme-catalyzed conversion of a single substrate into a single product.

There are many ways to derive the relationship between the overall rate k_{cat} and the individual rate k_2, k_3. Since k_{cat} is defined as the amount of substrate which can be turned over by the enzyme in a specified unit of time, its reciprocal, $1/k_{cat}$ can be regarded as the average time the enzyme needs to turn over one substrate molecule. Likewise, $1/k_2$ and $1/k_3$ can be interpreted as the average time which is spent by one substrate molecule on the sialylation step and desialylation step, respectively. Therefore, the following relationship is very obvious:

$$\frac{1}{k_{cat}} = \frac{1}{k_2} + \frac{1}{k_3}$$

Equation A. 7

$$k_{cat} = \frac{k_2 k_3}{k_2 + k_3}$$

Equation A. 8

When $k_2 \gg k_3$ (desialylation step is the rate-limiting step):

$$k_{cat} = \frac{k_2 k_3}{k_2 + k_3} \approx \frac{k_2 k_3}{k_2} = k_3$$

Equation A. 9

When $k_3 \gg k_2$ (sialylation step is the rate-limiting step):

$$k_{cat} = \frac{k_2 k_3}{k_2 + k_3} \approx \frac{k_2 k_3}{k_3} = k_2$$

Equation A. 10

Interestingly, from the above equations, specially designed substrates which has either sialylation or desialylation step rate-limiting can be used for enzyme kinetics. The overall rates measured experimentally will correspond to the rate of the slower step.

A.2   Mechanism-based Inactivation Kinetics of Sialidases

A significant part of this thesis focused on developing mechanism-based inactivators of retaining sialidases. Therefore the kinetics involved is discussed below. For a covalent mechanism-based inactivator, the following scheme is applied:

$$\text{E} \quad + \quad \text{I} \quad \underset{k_{-1}}{\overset{k_1}{\rightleftharpoons}} \quad \text{EI} \quad \overset{k_i}{\longrightarrow} \quad \text{E-I} \quad \overset{k_{\text{reactivation}}}{\longrightarrow} \quad \text{E} \quad + \quad \text{P}$$
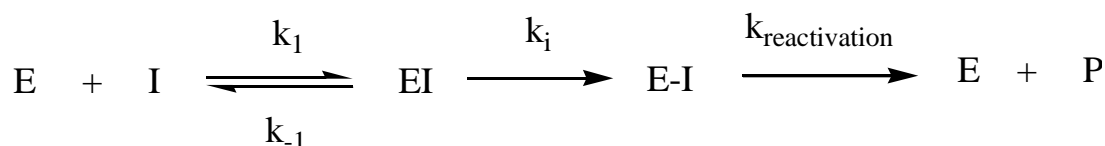
Scheme A. 3 General scheme for mechanism-based inactivators of retaining sialidases.

Since the $k_{\text{reactivation}}$ is negligible compared with the inactivation rate k_i, this scheme can be simplified into:
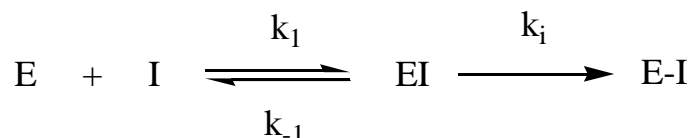
$$\text{E} \quad + \quad \text{I} \quad \underset{k_{-1}}{\overset{k_1}{\rightleftharpoons}} \quad \text{EI} \quad \overset{k_i}{\longrightarrow} \quad \text{E-I}$$

Scheme 1.3 Simplified scheme for mechanism-based inactivators of retaining sialidases.

In most of the cases, [I] >>[E]. Therefore, the kinetic equation is very similar to that of Michaelis-Menten kinetics:

$$v = \frac{k_i[E][I]}{K_i + [I]} = k_{\text{obs}}[E] \qquad\qquad \textbf{Equation A. 11}$$

$$k_{\text{obs}} = \frac{k_i[I]}{K_i + [I]} \qquad\qquad \textbf{Equation A. 12}$$

Since k_{obs} is only dependent on the following values: the inactivation rate constant (k_i), the apparent dissociation constant of enzyme with the inactivator (K_i) and the inactivator concentration ([I]), the above process can be regarded as a pseudo first-order reaction for the enzyme. This explains why exponential decay of enzymatic activity can be observed when enzyme is incubated with mechanism-based inactivators. By plotting the k_{obs} against different inactivator concentrations [I], the values of k_i and K_i can also be extrapolated. Sometimes the K_i value of certain inactivator can be much larger than the inactivator concentration which can be experimentally achieved (due to the availability and the solubility of the compound). In these cases when $K_i >> [I]$:

$$k_{\text{obs}} = \frac{k_i[I]}{K_i + [I]} = \frac{k_i}{K_i}[I] \qquad\qquad \textbf{Equation A. 13}$$

Instead of obtaining individual values of k_i and K_i, only the second-order inactivation constant k_i/K_i can be accurately determined.

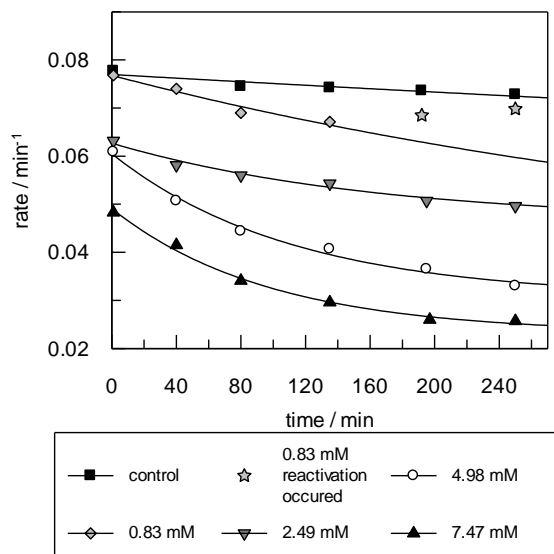# A.3   Graphical Representation of Inactivation Data

3-[1-(5-Acetamido-3,5,9-trideoxy-2,3-difluoro-D-*erythro*-β-L-*manno*-non-2-ulopyranosonate-9-yl)-1*H*-1,2,3-triazol-4-yl]-toluene (2.18)
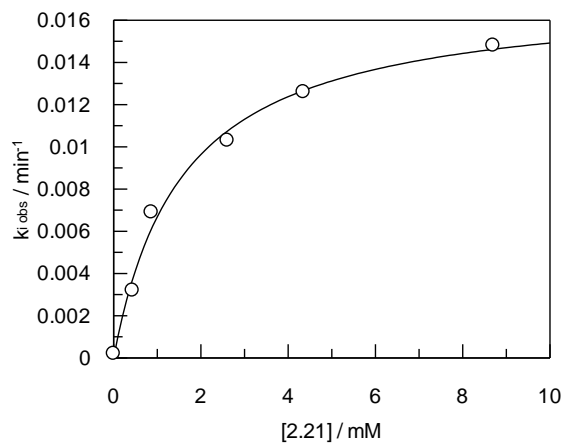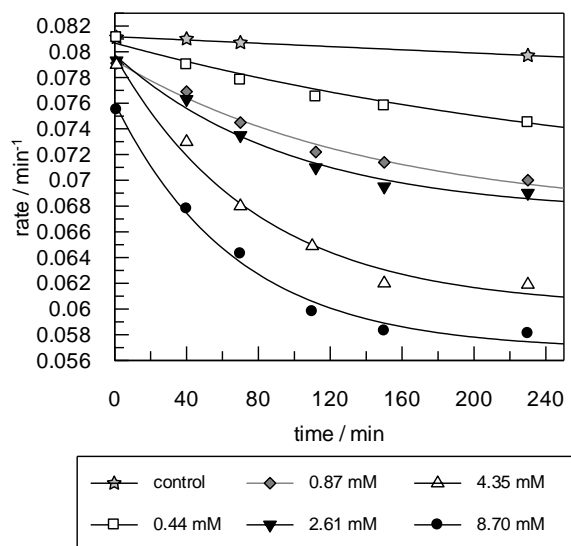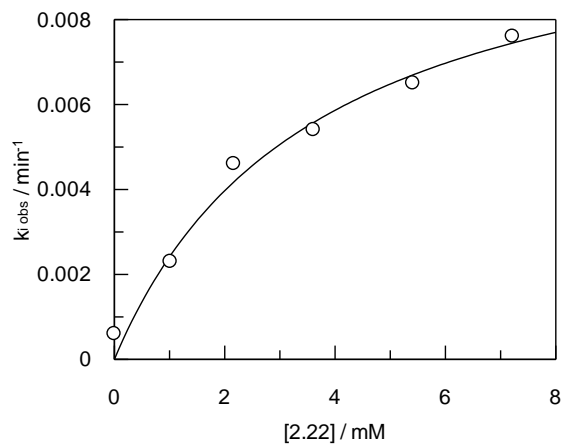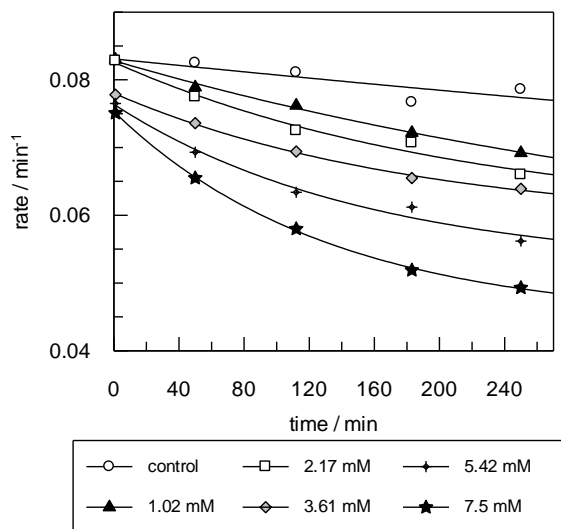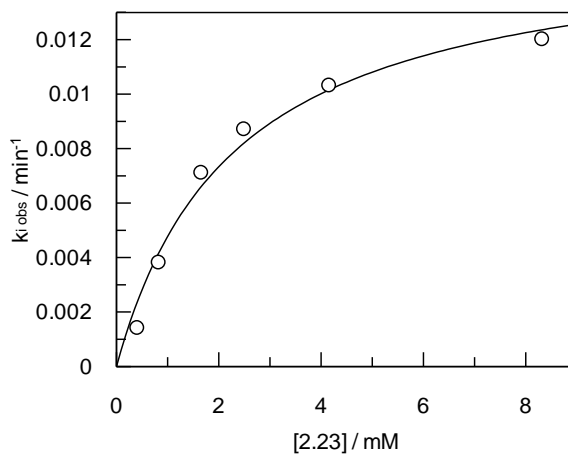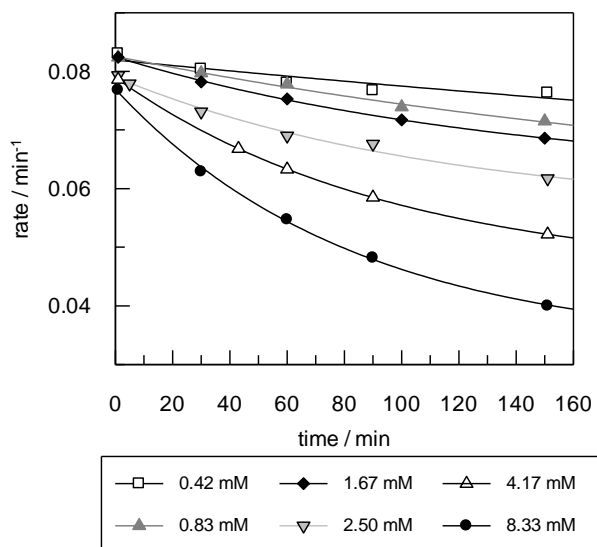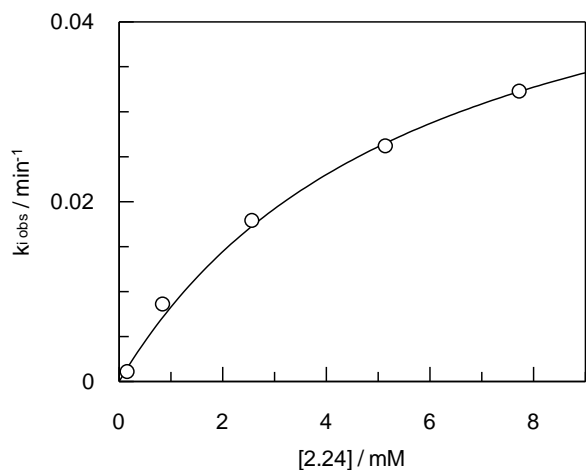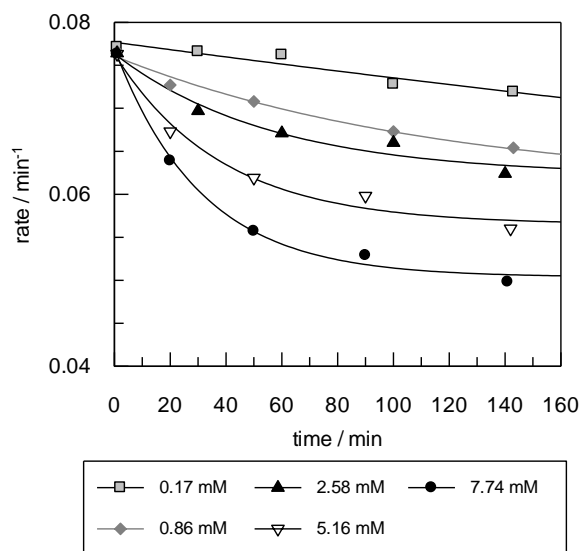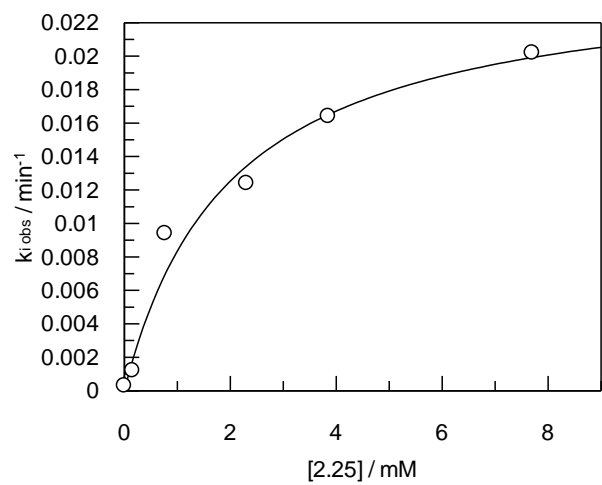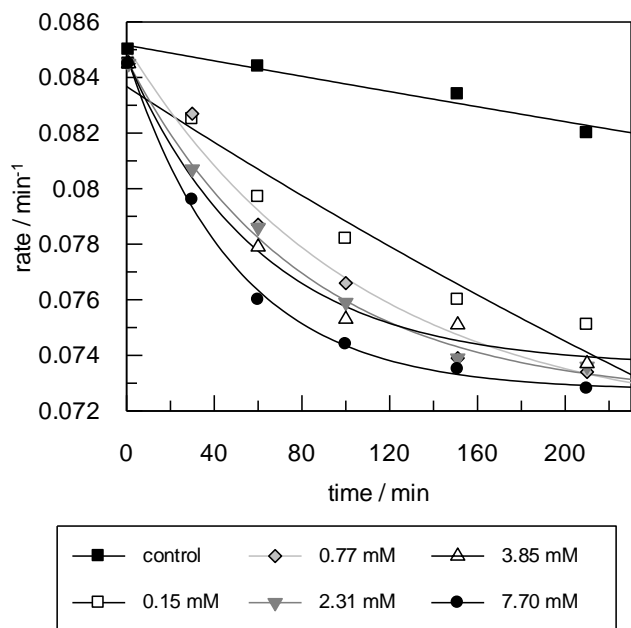
Inactivation
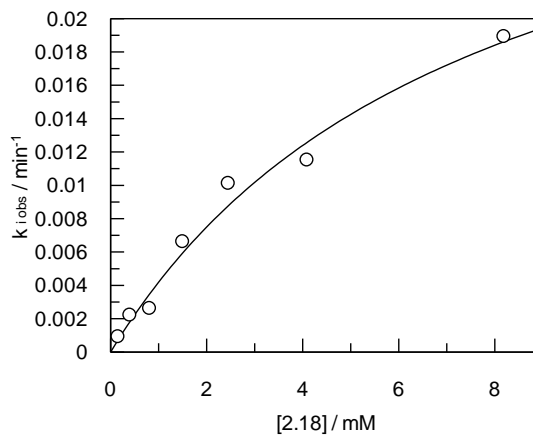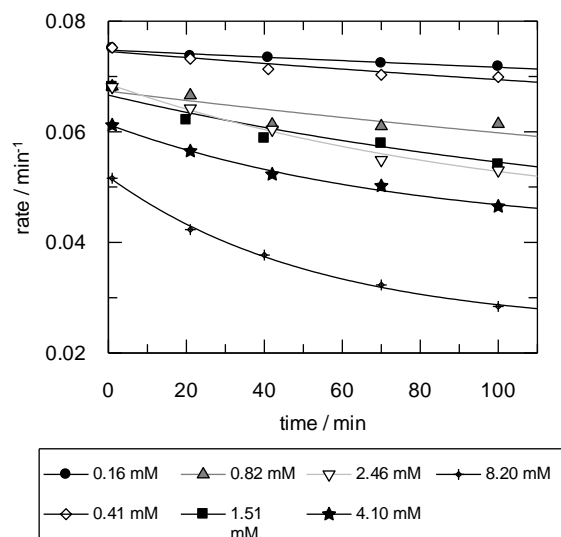
1-[1-(5-Acetamido-3,5,9-trideoxy-2,3-difluoro-D-*erythro*-β-L-*manno*-non-2-ulopyranosonate-9-yl)-1*H*-1,2,3-triazol-4-yl]-3-phenyl-propane (2.19)
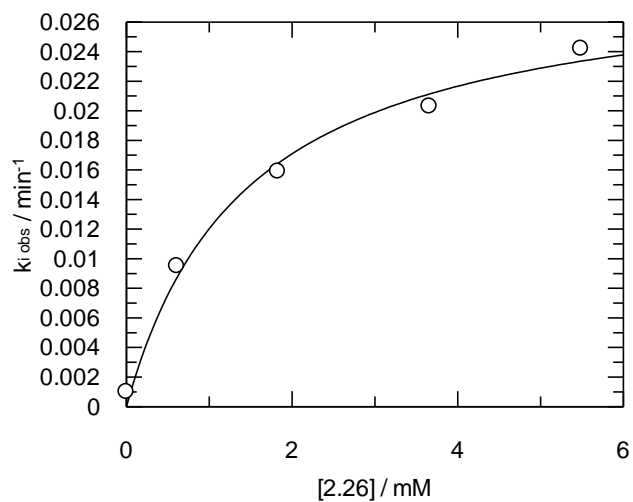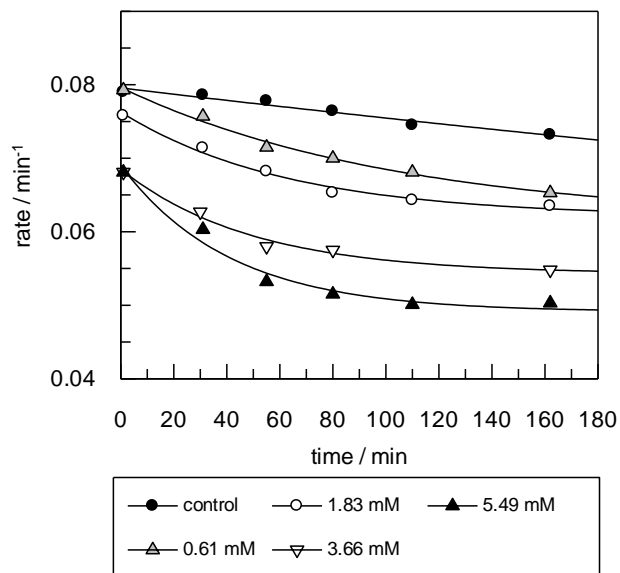
Inactivation
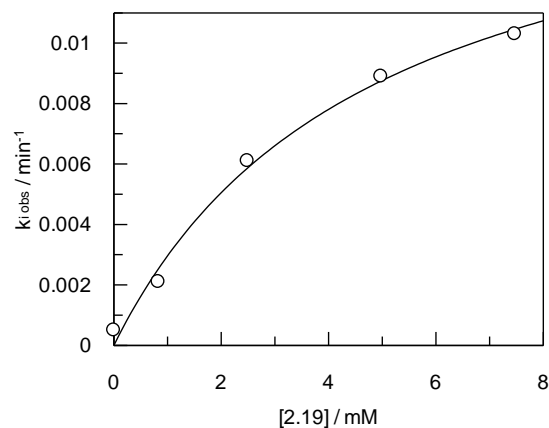
[1-(5-Acetamido-3,5,9-trideoxy-2,3-difluoro-D-*erythro*-β-L-*manno*-non-2-ulopyranosonate-9-yl)-1*H*-1,2,3-triazol-4-yl]-cyclopropane (2.21)

Inactivation

4-[1-(5-Acetamido-3,5,9-trideoxy-2,3-difluoro-D-*erythro*-β-L-*manno*-non-2-ulopyranosonate-9-yl)-1*H*-1,2,3-triazol-4-yl]-butan-1-ol (2.22)

Inactivation

[1-(5-Acetamido-3,5,9-trideoxy-2,3-difluoro-D-*erythro*-β-L-*manno*-non-2-ulopyranosonate-9-yl)-1*H*-1,2,3-triazol-4-yl]-benzene (2.23)

Inactivation

2-[1-(5-Acetamido-3,5,9-trideoxy-2,3-difluoro-D-*erythro*-β-L-*manno*-non-2-ulopyranosonate-9-yl)-1*H*-1,2,3-triazol-4-yl]-propan-2-ol (2.24)

Inactivation

2-[1-(5-Acetamido-3,5,9-trideoxy-2,3-difluoro-D-*erythro*-β-L-*manno*-non-2-ulopyranosonate-9-yl)-1*H*-1,2,3-triazol-4-yl]-2-methyl-propane (2.25)
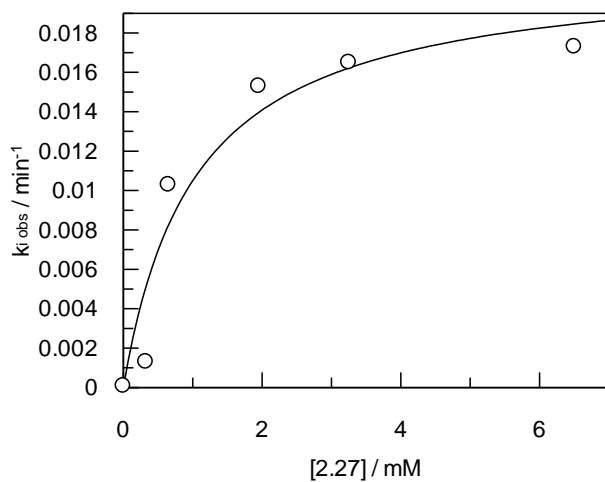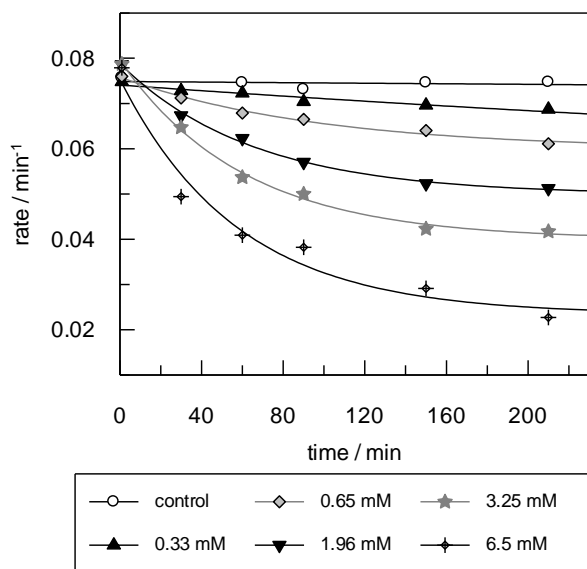
Inactivation

[1-(5-Acetamido-3,5,9-trideoxy-2,3-difluoro-D-*erythro*-β-L-*manno*-non-2-ulopyranosonate-9-yl)-1*H*-1,2,3-triazol-4-yl]-formic acid (2.26)
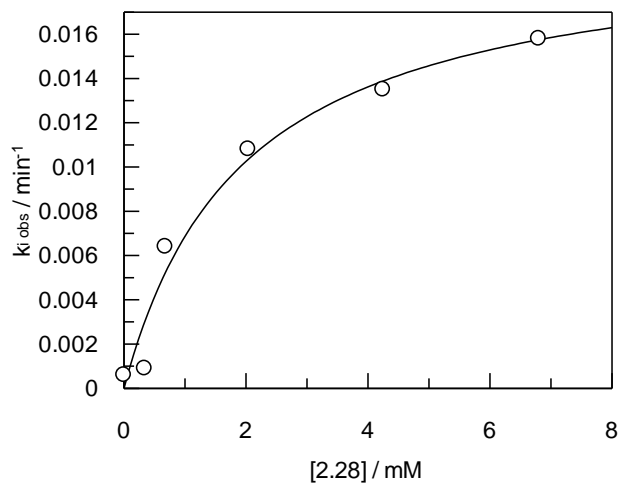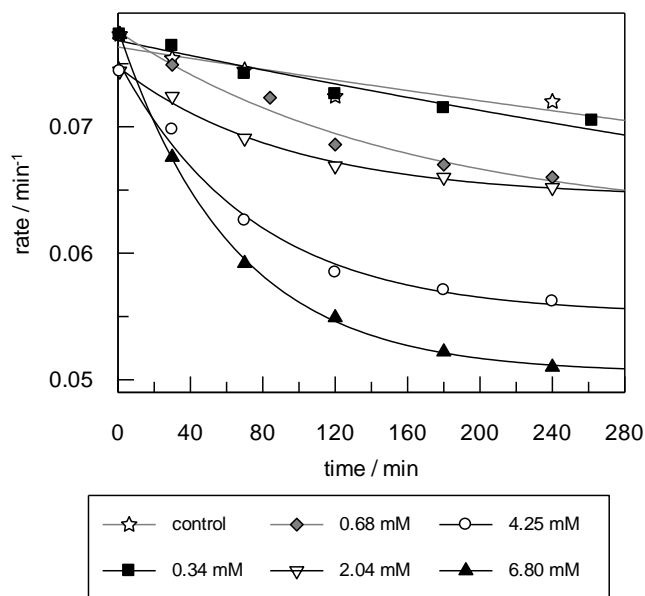
Inactivation

[1-(5-Acetamido-3,5,9-trideoxy-2,3-difluoro-D-*erythro*-β-L-*manno*-non-2-ulopyranosonate-9-yl)-1*H*-1,2,3-triazol-4-yl]-cyclohexane (2.27)

Inactivation

Tert-butyl-{[1-(5-Acetamido-3,5,9-trideoxy-2,3-difluoro-D-*erythro*-β-L-*manno*-non-2-ulopyranosonate-9-yl)-1*H*-1,2,3-triazol-4-yl]methyl}-carbamate (2.28)

Inactivation

[1-(5-Acetamido-3,5,9-trideoxy-2,3-difluoro-D-*erythro*-β-L-*manno*-non-2-ulopyranosonate-9-yl)-1*H*-1,2,3-triazol-4-yl]- methanamine (2.29)

Inactivation